



# Electrochemical oxidation of azo dyes in water: a review

Abdulgalim B. Isaev<sup>1</sup> · Nabi S. Shabanov<sup>2</sup> · Asiyat G. Magomedova<sup>1</sup> · P. V. Nidheesh<sup>3</sup> · Mehmet A. Oturan<sup>4</sup>

Received: 20 February 2023 / Accepted: 6 May 2023 / Published online: 7 June 2023  
© The Author(s), under exclusive licence to Springer Nature Switzerland AG 2023

## Abstract

Pollution of waters by azo dyes is a major global issue because some azo dyes have carcinogenic and mutagenic effects. Therefore, advanced methods are required to remove those pollutants from wastewater. For instance, electrochemical oxidation processes have been developed using various approaches to remove azo dyes from wastewater. Here, we review electrochemical processes for the oxidative degradation of azo dyes. Processes include anodic oxidation, electro-Fenton, photo-electro-Fenton, and solar photo-electro-Fenton. The influence of various parameters including process design, design of reactors, and the characteristic degradation products and their toxicity, are discussed. Low molecular weight carboxylic acids are mainly formed as by-products.

**Keywords** Advanced oxidation processes · Electrochemical oxidation · Azo dye · Wastewater treatment · Toxicity

## Abbreviations

BDD Boron-doped diamond  
·OH Hydroxyl radical

## Introduction

Rapid population growth and urbanization in the twentieth century and early twenty-first century contributed greatly to the environmental pollution problems. Among the problems associated with environmental pollution, water pollution with persistent organic pollutants is the most critical one. The discharge of industrial wastewater containing organic compounds has led to the pollution of aquatic ecosystems.

The problem of water pollution with various toxic/persistent organic pollutants such as pesticides, pharmaceutical and human care products, dyes, and chlorinated phenols has been the subject of a large number of studies (Nidheesh et al. 2013; Bokare and Choi 2014; Asghar et al. 2015; Elkacmi and Bennajah 2019; Paździor et al. 2019; Wang et al. 2021; Brillas 2022).

Among the classes of organic pollutants, synthetic dyes are widely used in various industries such as textile, pharmaceutical, food and cosmetics. The most considerable contribution to wastewater containing synthetic dyes comes from the textile industry (Nidheesh et al. 2022b). Dyes are organic compounds with a complex structure that give color to various products. Dyes and their degradation products have a direct toxicological effect on different living organisms and humans (Copaciu et al. 2013). Currently, there are a large number of dyes used worldwide and their production reaches more than 900,000 tons per year. Azo dyes are the most widely dyes used in various industries. More than 60% of the dyes produced in the world are azo dyes (Gürses et al. 2016), and over 70% of the dyes used in industries are also azo dyes (Berradi et al. 2019). According to various sources, about 4–12% azo dyes are released into the environment along with the industrial wastewater generated during their production and dyeing processes (Pearce et al. 2003; Srivastava et al. 2022). As a result, about 280,000 tons of dyes per year are released globally with wastewater (Jin et al. 2007).

To date, various physicochemical methods such as adsorption (Ayati et al. 2016; Raval et al. 2016), coagulation

✉ Abdulgalim B. Isaev  
abdul-77@yandex.ru

✉ Mehmet A. Oturan  
mehmet.oturan@univ-eiffel.fr

<sup>1</sup> Department of Inorganic Chemistry and Chemical Ecology, Dagestan State University, 43a M. Gadjeva Street, Makhachkala, Russia 367001

<sup>2</sup> Analytical Center for Collective Use, Dagestan Federal Research Center, Russian Academy of Sciences, 45 M. Gadjeva Street, Makhachkala, Russia

<sup>3</sup> CSIR-National Environmental Engineering Research Institute, Nagpur, Maharashtra 440020, India

<sup>4</sup> Laboratoire Géomatériaux et Environnement, EA 4508, Université Gustave Eiffel, 77454 Marne-la-Vallée, Cedex 2, France

(Luo et al. 2019), chemical oxidation and reduction (Selvaraj et al. 2021), non-thermal plasma treatment (Tarkwa et al. 2019b) and membrane filtration (Katuri et al. 2009) are used to treat wastewater containing azo dyes. Many studies are devoted to the use of biological methods for treating wastewater containing azo dyes (Solanki et al. 2013; Bhatia et al. 2017; Shah 2019). Most of the existing methods have severe limitations for practical use, such as the high cost of the technology, low removal efficacy, formation of secondary waste to be further treated, and formation of more toxic products than the parent pollutant.

Among advanced oxidation processes, electrochemical advanced oxidation processes for the removal of azo dyes from wastewater received great interest (Sirés et al. 2014; Brillas and Martínez-Huitle 2015; Moreira et al. 2017; Garcia-Segura et al. 2018; Ghime and Ghosh 2019; Selvaraj et al. 2021; Rodríguez-Narváez et al. 2021). Electrochemical methods are quite easy to operate and can be referred as “green technologies”; since wastewater treatment does not require additional chemical compounds and does not generate harmful organic intermediate products, because organic pollutants can be oxidized until the mineralization stage (transformation to CO<sub>2</sub>) before being released into the environment (Nidheesh and Gandhimathi 2012; Titchou et al. 2021a).

One of the most used electrochemical methods for azo dye removal is anodic oxidation process (Panizza and Cerisola 2009; Jiang et al. 2021; Martínez-Huitle 2021). This process is based on the direct oxidation of azo dyes on the surface of an appropriate anode via hydroxyl radical (·OH)-mediated oxidation. In this case, the anode material plays a crucial role (Peralta-Hernández et al. 2012; El Aggadi et al. 2021; Cornejo et al. 2021; Clematis and Panizza 2021; Karim et al. 2021; Ganzoury et al. 2022). During electrochemical oxidation, azo dyes can be partially oxidized with the formation of intermediate organic products that are generally biodegradable (Cornejo et al. 2021; Nidheesh et al. 2022a), or they can be completely mineralized with the formation of carbon dioxide, water, and other inorganic ions (Garcia-Segura et al. 2018; Nidheesh et al. 2019; Titchou et al. 2021a). Electrochemical processes for dye removal are based on the generation of various oxidants such as hydroxyl radical, hydrogen peroxide, and hypochlorite ion (Titchou et al. 2021a; Ganzoury et al. 2022) during electrolysis for the indirect oxidation of dyes (Särkkä et al. 2015; Nidheesh et al. 2018).

In contrast, the indirect electrochemical oxidation of azo dyes includes the generation of homogeneous reactive oxygen species in the bulk solution. Production of ·OH through electrochemically generated Fenton's reagent via electro-Fenton process is the best example for indirect electrochemical oxidation process (Lahkimi et al. 2007; Brillas et al. 2009; Oturan and Oturan 2018; Nidheesh et al. 2023a,b).

Photo-electro-Fenton, sono-electro-Fenton, electro-peroxone, peroxicoagulation and bioelectro-Fenton are the other examples of indirect electrochemical oxidation process. Recently, electrochemical generation of sulfate radical via decomposition of persulfate or peroxydisulfate and direct conversion of sulfate ions are also received much attention (Srivastava et al. 2021; Syam Babu and Nidheesh 2022; Araújo et al. 2022). At the same time, combined methods are used to increase the efficiency of electrochemical processes. A large number of papers on the use of combined methods for the removal of azo dyes from real and simulated wastewater have been published. Combined methods include the combination of electrochemical oxidation with adsorption, ultrasonic treatment, UV light irradiation, photo-catalysis, biological oxidation and ozonation (Ganzenko et al. 2014; Martínez-Huitle et al. 2015; Patidar et al. 2020; Qiao and Xiong 2021; Koulini et al. 2022).

This review considers the most important aspects of electrochemical oxidation of azo dyes, which comprise one of the largest groups of dyes used in various industries. Characteristics, classification and toxicity of azo dyes and their intermediates are briefly discussed to understand how to prevent water pollution. The main directions of research in the field of electrochemical oxidation are given, and the prospects for the development of electrochemical methods, which are considered as the most environmentally friendly methods of wastewater treatment, are outlined.

## Characteristics of azo dyes

Azo dyes constitute the largest group of synthetic dyes and are widely used due to ease of use, various properties, and a wide range of colors from yellow to black. They are highly light-resistant and used in multiple industries such as textile, printing, paint and varnish to dye various products. Azo dyes can color most natural, artificial and synthetic materials, including leather, plastic, and rubber products. Most of the azo dyes are water soluble, and the coloration of various materials is associated with their physical adsorption, absorption, or mechanical fixation (Bafana et al. 2011).

Azo dyes are characterized by the presence of the functional azo group (–N=N–) included in two or more symmetrical or asymmetrical aromatic groups (Bafana et al. 2011). The azo group can be linked to benzene rings, naphthalene, aromatic heterocycles, or aliphatic groups, which give color with various shades and intensities to the dye (Benkhaya et al. 2020b). In terms of the number of azo bonds in the molecule, azo dyes can be classified into monoazo, diazo, and polyazo dyes. In accordance with the international classification of dyes, azo dyes have color index (C.I.) numbers from 11,000 to 39,000 (Selvaraj et al. 2021). The color index number is indicated after the name of the dye, which reflects

the dye technical classification and color (Kiernan 2001). For example, Reactive Black 5 (C.I. 20,505) is a black dye belonging to the group of reactive azo dyes.

The most water-soluble azo dyes, which can subsequently get into the environment with wastewater, are acid, direct, reactive, basic (cationic) and mordant ones. Acid and reactive azo dyes, mainly mono- and diazo ones, make up more than half of the currently used azo dyes (Benkhaya et al. 2017). Acid dye molecules contain sulfonic groups, which define the solubility and acidic properties of the dye. Protein fibers are colored using acid azo dyes, and the colors are characterized by brightness and purity of the hue. As a rule, acid dyes are sodium salts, which form colored anions in the solution (Benkhaya et al. 2020a). The class of reactive azo dyes includes the dyes that form a covalent bond with cellulose, protein and similar fibers during their dyeing. As a result, the dye becomes a fiber component, providing high color fastness.

Currently, there is a rapid introduction of reactive dyes into the technologies for the textile industry due to their valuable dyeing properties including high color fastness to wet treatment comparable to the color fastness of vat dyes as well as more excellent brightness of colors compared to direct, acid, and basic dyes (Alsantali et al. 2022). Direct azo dyes are mainly belong to diazo and polyazo compounds. They contain many hydroxylamino groups and nitrogen heterocycles. As a result, they form hydrogen bonds between the dye groups and are used for dyeing cellulose fibers (Bafana et al. 2011). The basic azo dyes are cationic in nature, which can color fibers containing acid groups. The molecules of these dyes have free or alkylated amino groups and do not contain either sulfonic or carboxyl groups (Kiernan 2001).

Reactive azo dyes are mainly used for dyeing cellulose fibers. The mechanism of dyeing materials with reactive dyes involves the formation of covalent bonds between the dye molecules and the fibers, which are more resistant to various conditions of use. Reactive substituents of these azo dyes can also react with the hydroxyl groups present in the dye bath due to the alkaline environment, and as a result, part of the hydrolyzed dyes can no longer react with the fiber. Thus, from 10 to 50% of the initial dye charge will be present in the dye bath effluent, resulting in a strongly colored effluent (Al-Degs et al. 2000). It should be noted that reactive dyes have a toxicological effect on living organisms (Salazar and Ureta-Zañartu 2012). They reduce the amount of ammonium-oxidizing bacteria in the soil, which may limit the efficiency of using nitrogen by plants, thereby decreasing the productivity of land ecosystems (Topaç et al. 2009).

Direct azo dyes are the cheapest and easiest to use. Most direct azo dyes are diazo and polyazo compounds. The disadvantage of direct azo dyes is their poor recovery from the dye bath, and therefore, about 30–60% of the dye enters the wastewater. Direct azo dyes are mainly used to dye cellulose

fibers, and they link with the fibers by hydrogen bonding and van der Waals interactions. Therefore, direct azo dyes have low color fastness to wet treatment, and they are currently less used (Bafana et al. 2011). It should be noted that direct azo dyes, like other groups of azo dyes, have a pronounced toxicological effect on populations of living organisms in ecosystems (Hernández-Zamora and Martínez-Jerónimo 2019a, 2019b).

Azo dyes have mutagenic properties (Hashemi and Kaykhahi 2022), and they are difficult to oxidize under aerobic conditions at biological treatment plants (Senthil Rathi and Senthil Kumar 2022). Under certain conditions, their degradation can result in toxic products (Gottlieb et al. 2003; Rawat et al. 2016). In addition, mammal microbiota, including skin or intestinal microflora, can turn the azo dyes into carcinogenic metabolites (Feng et al. 2012). The toxicological effect of selected azo dyes is presented in Table 1.

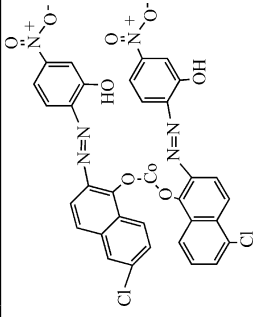
Many of the azo dyes, products of their reductive splitting as well as chemically related aromatic amines are reported to affect human health by causing allergies and other human diseases. Some azo dyes exhibit toxic effects. For example, Acid Orange 10 or Orange G is a monoazo dye used mainly for dyeing silk and woolen products, paper and industrial ink, and is also used in the manufacture of pencils and dyeing cell structures in biochemical research. Acid Orange 10 has shown genotoxicity and may also be hazardous to human health (Jović-Jovičić et al. 2010). Monoazo dye Acid Red 14 is used for dyeing woolen fabrics, silk and polyamide fibers (see the structural formula in Table 2). Acid Red 14 is also used in the food industry and is known as carmoisine or food additive E122. According to the European Food Safety Agency, the hyperactive-child syndrome may be associated with the ingestion of carmoisine (Thiam et al. 2015c). Acid Red 27 or amaranth food color is a water-soluble monoazo dye. Acid Red 27 is added during the manufacture of various food products, giving them a distinctive red color (Rovina et al. 2017). Some countries have banned the use of Acid Red 27 in food and beverages because its toxicological effect was scientifically proven (Barros et al. 2014; Rovina et al. 2017). Therefore, Acid Red 27 removal from aqueous solutions by various methods, including electrochemical oxidation, was reported (Fan et al. 2008).

To date, most dyes are not controlled for toxicity and are considered nontoxic. However, supposedly nontoxic azo dyes have functional groups that can impart mutagenic and carcinogenic properties upon degradation. For example, they can lead to the formation of degradation products such as  $\beta$ -naphthylamine, aniline, triazine, p-phenylenediamine, and  $\beta$ -amino- $\alpha$ -naphthol, which are well-known genotoxicants (Brüschweiler et al. 2014; Rawat et al. 2016). It should also be noted that diazo, triazo and polyazo dyes are the most toxic among azo dyes (Golka et al. 2004). When assessing toxicity of azo dyes, attention is focused only on a laboratory study.

**Table 1** Selected azo dyes and their toxicological effect on the environment. Adapted from Chung (2016)

| Name  | IUPAC name   | CAS number | Toxicological effect | Structural formula |
|---|--|------------|----------------------|--------------------|
| Aniline Yellow  | 4-Aminoazobenzene  | 60-09-3    | Carcinogenic         |                    |
| C.I. Solvent Yellow 3   | o-Aminoazotoluene  | 97-56-3    | Carcinogenic         |                    |
| Methyl Yellow   | 4-(Dimethylamino)azobenzene  | 97-56-3    | Carcinogenic         |                    |
| Sudan 1 (CI Solvent Yellow 14, Solvent Orange R)                          | 1-phenylazo-2-naphthol   | 842-07-9   | Carcinogenic         |                    |
| Solvent Orange 7 (Sudan II)   | {1-[(2, 4-dimethylphenyl)azo]-2-naphthalenol} or [1-(2, 4-xylyazo)-2-naphthol] | 3118-97-6  | Carcinogenic         |                    |
| Solvent Red 23 (Sudan III, Cerasin Red, C.I. 26,100, Scarlet B, Tony Red) | [1-(4-(phenyldiazenyl)phenyl)azonaphthalen-2-ol]                               | 85-96-9    | Carcinogenic         |                    |
| C.I. Solvent Red 24 (Sudan IV, Sudan R, Fat Red B, Scarlet Red)           | [1-{2-methyl-4-(2-methylphenyldiazenyl)phenyl}azonaphthalen-2-ol]              | 85-83-6    | Carcinogenic         |                    |
| Para Red (Paranitraniline Red, Pigment Red 1, and C.I. 12,070)            | {1-[(E)-(4-nitrophenyl)diazenyl]-2-naphthol}                                   | 6410-10-2  | Carcinogenic         |                    |

Table 1 (continued)

| Name                                       | IUPAC name   | CAS number  | Toxicological effect | Structural formula  |
|--|--|-------------|----------------------|---|
| C.I. Solvent Blue 53 (Orasol Navy Blue 2R) | Cobalt(2+) bis{2-[(2E)-2-(5-chloro-1-oxonaphthalen-2(1H)-ylidene)hydrazinyl]-5-nitrophenolate} | 61,969-42-4 | Mutagenic            |  |

C.I.-color index

Their possible degradation under the influence of various environmental factors, including biological oxidation at biological treatment plants or in natural water, is not taken into account. The formation of toxic degradation products of azo dyes has been shown in many works (Brüschweiler et al. 2014). In particular, the formation of carcinogenic 3,3'-dimethoxybenzidine during the degradation of Direct Blue 15 azo dye is reported (Golka et al. 2004). Degradation of Acid Orange 7 and Reactive Black 5 dyes, which are considered to be non-toxic, also leads to the formation of hazardous aromatic amines (Gottlieb et al. 2003).

The concentration of azo dyes in dyeing wastewater can widely range from 5 to 1500 mg/L, depending on the material to be dyed. The resistance of azo dyes to biodegradation requires their pre-treatment using various physicochemical methods. Physicochemical and biological methods for treating wastewater containing azo dyes are primarily used to remove the color of solutions. Each of the method for color removal has its own advantages and disadvantages, including factors such as the nature of the dye, the composition of wastewater, concentration, toxicity, the cost of used chemicals, as well as the cost of processing of unit volume of wastewater and the equipment. These factors determine the economic feasibility of each method for wastewater treatment of azo dyes effluents (Selvaraj et al. 2021). The oxidation or reduction by-products play a significant role in evaluating the effectiveness of the method for treating wastewater containing azo dyes. It should be noted that using a single method for removing azo dye might be insufficient. In view of this, the study of the processes of azo dye removal has become an urgent task, and the search for environmentally sound methods of dye removal in order to reduce an anthropogenic load on ecosystems associated with the discharge of wastewater containing azo dyes is currently ongoing.

In this context, the interest of researchers in developing methods for azo dye removal from wastewater is increasing (Salazar and Ureta-Zañartu 2012; Jáger et al. 2019). In recent years, many studies have been carried out on developing electrochemical methods for removing azo dyes of different colors (Almomani and Baranova 2012, 2013). Among azo dyes, acid, reactive, and direct dyes are of the greatest interest to researchers. Table 2 lists different azo dyes and their removal by electrochemical approach. Most of the studied azo dyes belong to mono-azo and diazo compounds, and they are characterized by the formation of various aromatic fragments during electrochemical oxidation (Bafana et al. 2011). Electrochemical oxidation has been used to remove azo dyes from solutions due to their toxic properties. In particular, much attention has recently been paid for the removal of various food colors from wastewater because of their effects on human, especially on the child (Parsa et al. 2014; Thiam

**Table 2** Commercial, chemical name and structural formula of some azo dyes, whose degradation has been studied by electrochemical methods

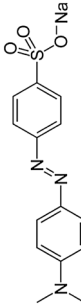
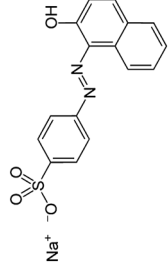
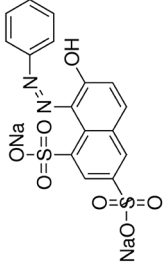
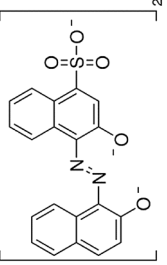
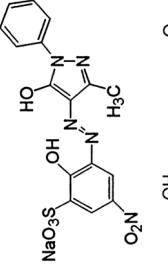
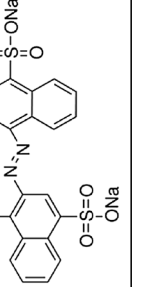
| Name  | IUPAC name  | CAS         | Color index | Structural formula  | Type of process   | References                           |
|---|---|-------------|-------------|---|---|--------------------------------------|
| <i>Acid dyes</i>                              |   |             |             |   |   |                                      |
| Methyl orange                                 | Sodium 4-[[4-(dimethylamino)phenyl]diazanyl]benzene-1-sulfonate   | 547-58-0    | 13,025      |    | Anodic oxidation  | Ramirez et al. 2013                  |
| Acid orange 7 ( <i>Orange ii</i> )            | Sodium 4-[(2E)-2-(2-oxonaphthalen-1-ylidene)hydrazinyl]benzenesulfonate   | 633-96-5    | 15,510      |    | Anodic oxidation  | Wu et al. 2016                       |
| Acid orange 10 ( <i>Orange G</i> )            | 7-Hydroxy-8-phenylazo-1,3-naphthalenedisulfonic acid disodium salt, 1-Phenylazo-2-naphthol-6,8-disulfonic acid disodium salt                            | 1936-15-8   | 16,230      |    | Photo-electrochemical and photo-electro-Fenton oxidation        | Tarkwa et al. 2019a, Liu et al. 2019 |
| Acid blue 161                                 | Disodium; chromium(3+); 1-(2-oxidonaphthalen-1-yl)diazonyl-4-sulfonaphthalen-2-olate; 3-oxido-4-(2-oxidonaphthalen-1-yl)diazonylnaphthalene-1-sulfonate | 12,392-64-2 | 15,706      |    | Electrochemical oxidation combined with microbiological systems | de Almeida et al. 2019               |
| Acid orange 74                                | Sodium;chromium(3+);3-[(3-methyl-5-oxido-1-phenylpyrazol-4-yl)diazonyl]-5-nitro-2-oxidobenzenesulfonate hydroxide                                       | 10,127-27-2 | 18,745      |   | Direct and indirect electrochemical oxidation                   | Li et al. 2021                       |
| Acid red 14 ( <i>Carmoisine, Acid Red B</i> ) | Disodium 4-hydroxy-3-[(4-sulfo-1-naphthalenyl)azo]-1-naphthalenesulfonate   | 3567-69-9   | 14,720      |  | Electro-Fenton  | Wang et al. 2010a                    |

Table 2 (continued)

| Name                        | IUPAC name   | CAS       | Color index | Structural formula | Type of process                                    | References                  |
|-----------------------------|--|-----------|-------------|--------------------|--|-----------------------------|
| Acid blue 92                | 2,7-naphthalenedisulfonicacid,4-((4-aminino-5-sulfo-1-naphthyl)azo)-5-hydroxy  | 3861-73-2 | 13,390      |                    | Photo-stimulated electrochemical oxidation         | Khataee et al. 2013         |
| Acid violet 1               | (6E)-6-imino-5-[2-(4-nitro-2-sulphophenyl)hydrazino]-4-oxo-4,6-dihydronaphthalene-2-sulfonic acid disodium (6E)-6-imino-5-[2-(4-nitro-2-sulfonato-phenyl)hydrazino]-4-oxo-4,6-dihydronaphthalene-2-sulfonate | 6441-91-4 | 17,025      |                    | Electrochemical and photo-electro-Fenton oxidation | Socha et al. 2007           |
| Acid violet 7               | 5-(Acetylamino)-3-[[4-(acetylamino)phenyl]azo]-4-hydroxy-2,7-Naphthalenedisulfonic Acid Disodium salt  | 4321-69-1 | 18,055      |                    | Direct oxidation                                   | Brito et al. 2018b, 2018a   |
| Acid yellow 23 (Tartrazine) | Trisodium 5-hydroxy-1-(4-sulfonatophenyl)-4-[(E)-(4-sulfonato-phenyl)diazenyl]-1H-pyrazole-3-carboxylate   | 1934-21-0 | 19,140      |                    | Electrochemical oxidation                          | Zhang et al. 2019a, b       |
| Eriochrome black T          | Sodium 4-[2-(1-hydroxynaphthalen-2-yl)hydrazin-1-ylidene]-7-nitro-3-oxo-3,4-dihydronaphthalene-1-sulfonate   | 1787-61-7 | 14,645      |                    | Electrochemical oxidation                          | Pacheco-Álvarez et al. 2019 |

Table 2 (continued)

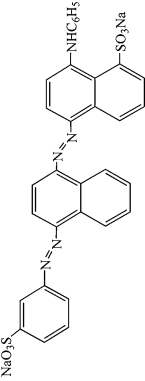
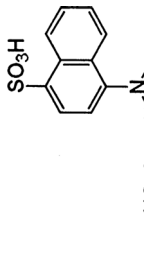
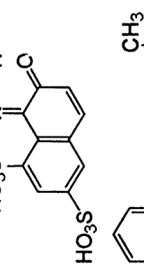
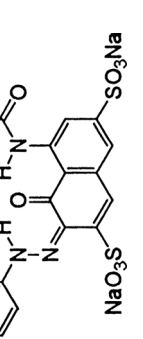
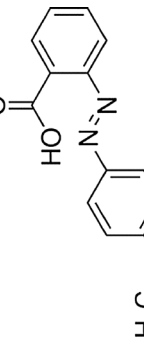
| Name                              | IUPAC name   | CAS       | Color index | Structural formula   | Type of process                  | References                        |
|-----------------------------------|--|-----------|-------------|--|----------------------------------|-----------------------------------|
| Acid blue 113                     | 1-naphthalenesulfonicacid,8-(phenylamino)-5-[4-[(3-sulphonyl)azo]-1-naphthyl;1-naphthalenesulfonicacid,8-(phenylamino)-5-[4-[(3-sulphonyl)azo]-1-naphthalenyl]azo]-,disodiumsalt | 3351-05-1 | 26,360      |   | Electrochemical oxidation        | Rahmani et al. 2016               |
| Acid red 18 ( <i>Ponceau 4R</i> ) | Trisodium 1-(1-naphthylazo)-2-hydroxynaphthalene-4',6,8-trisulphonate  | 2611-82-7 | 16,255      |   | Direct oxidation                 | Rahmani et al. 2015               |
| Acid red 1, ( <i>Acid red G</i> ) | Sodium 4-(2-hydroxy-1-naphthalenylazo)-naphthalenesulfonate  | 3734-67-6 | 118,050     |   | Pulsed electrochemical oxidation | Jiani et al. 2020                 |
| Methyl red                        | 2-(4-Dimethylaminophenylazo)benzoic acid   | 493-52-7  | 13,020      |   | Electro-Fenton                   | Santos et al. 2020b, <sup>a</sup> |
| Acid blue 29                      | Disodium 4-amino-5-hydroxy-3-((3-nitrophenyl)azo)-6-(phenylazo)naphthalene-2,7-disulphonate  | 5850-35-1 | 20,460      |  | Bioelectrodegradation            | Khan et al. 2021a, 2021b          |



Table 2 (continued)

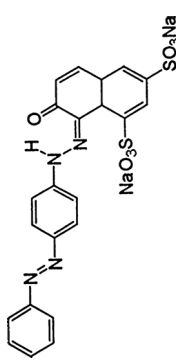
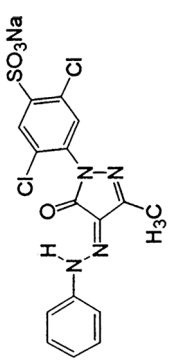
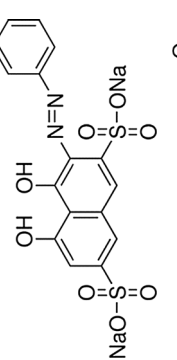
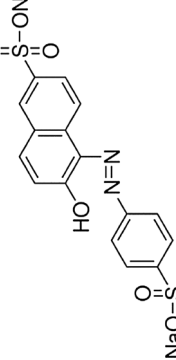
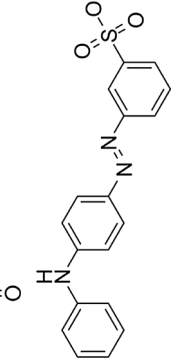
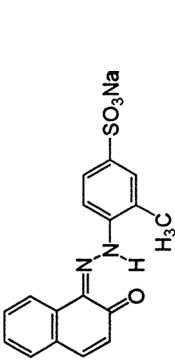
| Name              | IUPAC name   | CAS       | Color index | Structural formula  | Type of process                                | References             |
|-------------------|--|-----------|-------------|---|--|------------------------|
| Acid red 73       | 7-hydroxy-8-[[4-(phenyldiazenyl)phenyl]diazenyl]naphthalene-1,3-disulfonic acid                            | 5413-75-2 | 27,290      |    | Anodic oxidation                               | Xu et al. 2013b, 2015  |
| Acid brown 14     | sodium 2,5-dichloro-4-[(3-methyl-5-oxo-4-[(E)-phenyldiazenyl]-4,5-dihydro-1H-pyrazol-1-yl)benzenesulfonate | 6359-97-3 | 18,960      |    | Anodic oxidation                               | Bassyoumi et al. 2017  |
| Acid Red 29       | 2-(Phenylazo)chromotropic acid disodium salt   | 4197-07-3 | 16,570      |    | Indirect oxidation                             | Oliveira et al. 2007   |
| Sunset yellow FCF | 2-naphthalenesulfonic acid, 6-hydroxy-5-[(4-sulfonyl)azo]-, disodium salt                                  | 2783-94-0 | 15,985      |    | Photo-electro-Fenton with sunlight irradiation | Moreira et al. 2013    |
| Acid yellow 36    | 3-[4-(Phenylamino)phenylazo]benzenesulfonic acid monosodium salt   | 587-98-4  | 13,065      |   | Electrocatalytic oxidation                     | Aguilar et al. 2017    |
| Acid orange 8     | 3-methyl-4-[(2Z)-2-(2-oxonaphthalen-1(2H)-ylidene)hydrazino]benzenesulfonic acid                           | 5850-86-2 | 15,575      |  | Anodic oxidation                               | Abdessamad et al. 2014 |

Table 2 (continued)

| Name  | IUPAC name   | CAS         | Color index | Structural formula | Type of process  | References                              |
|---|--|-------------|-------------|--------------------|--|---|
| Acid red 150 ( <i>Ponceau 5S</i> )                        | Disodium 3-hydroxy-4-[[4-(phenyldiazenyl)phenyl]diazenyl]-2,7-naphthalenedisulfonate   | 6226-78-4   | 27,190      |                    | Photo-electro-Fenton   | dos Santos et al. 2018                  |
| Acid red 112 ( <i>Ponceau S</i> )                         | Tetrasodium;(4Z)-3-oxo-4-[[2-sulfonato-4-[(4-sulfonatophenyl)diazenyl]phenyl]hydrazinylidene]naphthalene-2,7-disulfonate                         | 6226-79-5   | 27,195      |                    | Electro-Fenton   | El-Desoky et al. 2010b                  |
| Allura red AC   | Disodium 6-hydroxy-5-((2-methoxy-5-methyl-4-sulfonatophenyl)diazenyl)naphthalene-2-sulfonate   | 25,956-17-6 | 16,035      |                    | Electrogenerated H <sub>2</sub> O <sub>2</sub> , electro-Fenton and photo-electro-Fenton | Thiam et al. 2015b                      |
| Acid red 33   | 5-Amino-4-hydroxy-3-phenylazo-2,7-naphthalenedisulfonic acid disodium salt, Disodium 5-amino-4-hydroxy-3-(phenylazo)-naphthalene-2,7-disulfonate | 3567-66-6   | 17,200      |                    | Electrochemical oxidation with ozonation   | Nabizadeh Chianeh and Basiri Parsa 2015 |
| Acid black 1, ( <i>Naphthol blue black, Amido black</i> ) | Sodium 4-amino-5-hydroxy-3-((E)-(4-nitrophenyl)diazenyl)-6-((E)-phenyldiazenyl)naphthalene-2,7-disulfonate                                       | 1064-48-8   | 20,470      |                    | Anodic oxidation   | Akrout and Bous-selmi 2013              |
| Acid red 27, ( <i>Amaranth</i> )                          | Trisodium (4E)-3-oxo-4-[[4-sulfonato-1-naphthyl]hydrazono]naphthalene-2,7-disulfonate  | 915-67-3    | 16,185      |                    | Electrochemical and sonoelectrochemical oxidation  | Steter et al. 2014                      |

Table 2 (continued)

| Name                               | IUPAC name   | CAS         | Color index | Structural formula | Type of process           | References               |
|------------------------------------|--|-------------|-------------|--------------------|---------------------------|--------------------------|
| Acid black 210                     | 2,7-Naphthalenedisulfonic acid, 4-amino-6-((4-((4-(2,4-diaminophenyl)azo)phenyl)amino)sulfonyl)phenyl)azo)-5-hydroxy-3-((4-nitrophenyl)azo)-, dipotassium salt | 99,576-15-5 | 300,285     |                    | Electro-oxidation         | Costa et al. 2009        |
| Mordant blue 13, (Acid blue BB)    | Disodium 3-2-5-chloro-2-hydroxyphenyl diazen-1-yl-4,5-dihydroxynaphthalene-2,7-disulfonate   | 1058-92-0   | 16,680      |                    | Electrochemical oxidation | Kenova et al. 2018       |
| <i>Reactive dyes</i>               |  |             |             |                    |                           |                          |
| Reactive black 5 (Remazol black B) | 2-7-naphthalenedisulfonic acid, 4-amino-5-hydroxy-3,6-bis(2-(4-(2-(sulfooxy)ethyl)sulfonyl)phenyl)diazenyl)-, tetra sodium salt                                | 17,095-24-8 | 20,505      |                    | Electrochemical oxidation | Jager et al. 2018        |
| Reactive orange 7                  | 2-Naphthalenesulfonic acid, 6-(acetylamino)-4-hydroxy-3-(3-(2-(sulfooxy)ethyl)sulfonyl)phenyl)azo)-, disodium salt   | 12,225-83-1 | 17,756      |                    | Electrochemical oxidation | Basiri Parsa et al. 2013 |
| Reactive orange 107                | 4-Acetylamino-6-amino-3-[p-[2-(sodiooxysulfonyloxy)ethylsulfonyl]phenyl]azo]benzenesulfonic acid sodium salt   | 12,220-08-5 |             |                    | Electrochemical oxidation | Rajkumar et al. 2015     |
| Reactive orange 16                 | 2-Naphthalenesulfonic acid, 6-(acetylamino)-4-hydroxy-3-[[4-[[2-(sulfooxy)ethyl]sulfonyl]phenyl]azo]-, disodium salt   | 12,225-83-1 | 17,757      |                    | Electrochemical oxidation | Aggadi et al. 2021       |

Table 2 (continued)

| Name   | IUPAC name   | CAS         | Color index | Structural formula | Type of process                                | References                        |
|--|--|-------------|-------------|--------------------|--|-----------------------------------|
| Reactive orange 122  | 2-((6-((4-chloro-6-((4-(2-(sulfoxy)ethyl)sulfonyl)phenyl)amino)-1,3,5-triazin-2-yl)amino)-1-hydroxy-3-sulfo-2-naphthalenyl)azo)-, tetrasodium salt;                  | 12,220-12-1 |             |                    | Oxidation by electrochemically generated ozone | Santana et al. 2009               |
| Reactive orange 4  | 1,5-Naphthalenedisulfonic acid, 2-((6-((4,6-dichloro-1,3,5-triazin-2-yl)methylamino)-1-hydroxy-3-sulfo-2-naphthalenyl)azo)-, trisodium salt                          | 12,225-82-0 | 18,260      |                    | Electrochemical Oxidation                      | Nordin et al. 2015                |
| Reactive orange 1<br>( <i>Reactive brilliant orange X-GN</i> ) | 7-[[4,6-dichloro-1,3,5-triazin-2-yl)amino]-4-hydroxy-3-[(2-sulphophenyl)azo]naphthalene-2-sulphonic acid   | 6522-74-3   | 17,907      |                    | Electrochemical Oxidation                      | Chen et al. 2020                  |
| Reactive yellow 1<br>( <i>Brilliant yellow X-6G</i> )          | Benzenesulfonic acid, 2,5-dichloro-4-(4-((5-((4,6-dichloro-1,3,5-triazin-2-yl)amino)-2-sulfo)phenyl)azo)-4,5-dihydro-3-methyl-5-oxo-1H-pyrazol-1-yl)-, disodium salt | 5089-16-7   | 18,971      |                    | Electrochemical Oxidation                      | Bedolla-Guzman et al. 2016        |
| Reactive red 2 ( <i>Reactive red X-3B</i> )                    | 2,7-Naphthalenedisulfonic acid,5-[[4,6-dichloro-1,3,5-triazin-2-yl)amino]-4-hydroxy-3-(phenylazo)-, disodium salt  | 12,226-03-8 | 18,200      |                    | Bioelectrodegradation                          | Ruan et al. 2010, Cao et al. 2021 |

Table 2 (continued)

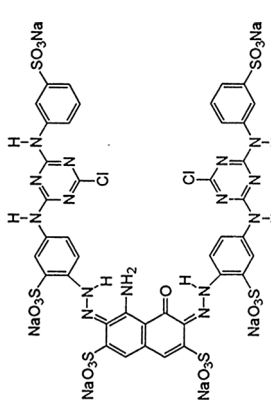
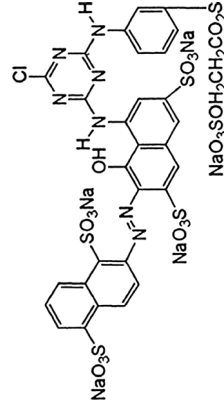
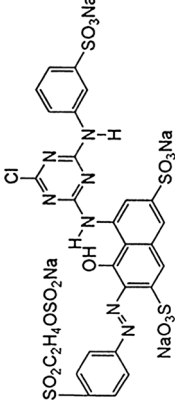
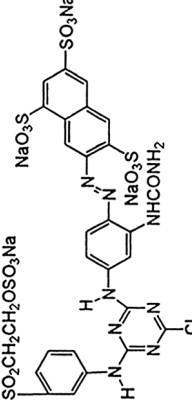
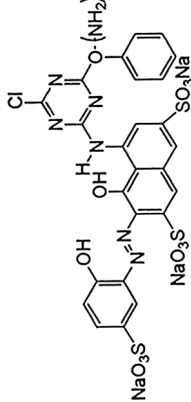
| Name  | IUPAC name   | CAS          | Color index | Structural formula  | Type of process             | References                               |
|---|--|--------------|-------------|---|-----------------------------|--|
| Reactive green 19<br>( <i>Reactive green HE4BD</i> )  | Hexasodium,4-amino-3-[[4-[4-chloro-6-(3-sulfonatoamino)-1,3,5-triazin-2-yl]amino]-2-sulfonatophenyl]diazonyl]-6-[[4-[4-chloro-6-(3-sulfonatoamino)-1,3,5-triazin-2-yl]amino]-2-sulfonatophenyl]hydrazinylidene]-5-oxonaphthalene-2,7-disulfonate | 61,931-49-5  | 205,075     |    | Anodic oxidation            | Petrucci et al. 2015a, 2015b             |
| Reactive red 195                                      | Pentasodium;5-[[6-chloro-4-[3-(2-sulfonatoxyethylsulfonyl)phenyl]imino-1H-1,3,5-triazin-2-ylidene]amino]-4-oxido-3-[(5-sulfonatoxy-1-sulfooxynaphthalen-2-yl)diazonyl]naphthalene-2,7-disulfonate  | 93,050-79-4  |             |    | Electrochemical oxidation   | Song et al. 2010                         |
| Reactive red 198<br>( <i>Remazol red RB</i> )         | 5-[[4-Chloro-6-[(3-sulfoxy)amino]-1,3,5-triazin-2-yl]amino]-4-hydroxy-3-[[4-[[2-(sulfooxy)ethyl]sulfonyl]phenyl]azo]-2,7-naphthalenedisulfonic Acid Tetrasodium Salt   | 145,017-98-7 | 18,221      |    | Electrochemical oxidation   | Khosravi et al. 2015, Araújo et al. 2014 |
| Reactive yellow 145<br>( <i>Reactive yellow F3R</i> ) | Tetrasodium;7-[[3-[[amino(oxido)methylidene]amino]-4-[[4-chloro-6-(2-sulfooxyethylsulfonyl)amino]-1,3,5-triazin-2-yl]amino]phenyl]diazonyl]naphthalene-1,3,6-trisulfonate  | 93,050-80-7  |             |   | Photo-electro-oxone process | Joy et al. 2020                          |
| Reactive violet 2                                     | 5-[[4-amino-6-chloro-1,3,5-triazin-2-yl]amino]-4-hydroxy-3-[[2-(hydroxy-5-sulfoxyphenyl)diazonyl]naphthalene-2,7-disulfonic acid   | 8063-57-8    | 18,157      |  | Anodic oxidation            | El-Ashtoukhy et al. 2017                 |

Table 2 (continued)

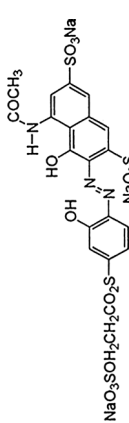
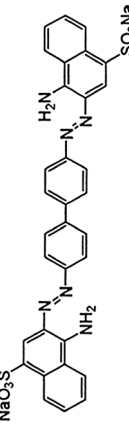
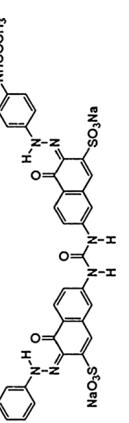
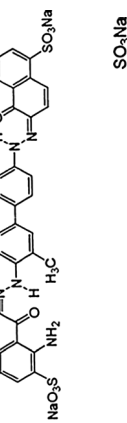
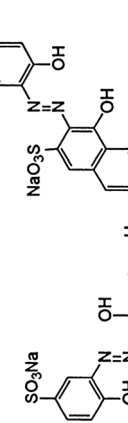
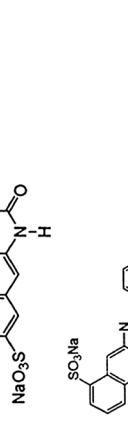
| Name                                 | IUPAC name  | CAS         | Color index | Structural formula  | Type of process  | References                |
|--------------------------------------|---|-------------|-------------|---|------------------|---------------------------|
| Reactive violet 5                    | Trisodium;5-acetamido-4-hydroxy-3-[[2-hydroxy-5-(2-sulfonatoxyethyl)sulfonyl]phenyl]diazenyl]naphthalene-2,7-disulfonate  | 12,226-38-9 | 18,097      |    | Anodic oxidation | Fidaleo et al. 2016       |
| <i>Direct dyes</i>                   |   |             |             |   |                  |                           |
| Congo red ( <i>Direct red 28</i> )   | Disodium 4-amino-3-[[4-[[4-(1-amino-4-sulfonato-2-naphthyl)azo]phenyl]phenyl]azo-naphthalene-1-sulfonate  | 573-58-0    | 22,120      |    | Anodic oxidation | Jalife-Jacobo et al. 2016 |
| Direct red 23                        | Disodium 3-[[4-(4-acetamidophenyl)diazenyl]-4-hydroxy-7-[[5-hydroxy-6-(phenyl diazenyl)-7-sulfonato-2-naphthyl]carbonyl]amino]-2-naphthalenesulfonate                           | 3441-14-3   | 29,160      |    | Electro-Fenton   | Titchou et al. 2021b      |
| Evans blue ( <i>Direct blue 53</i> ) | Tetrasodium (6E,6'E)-6,6'-[[3,3'-dimethylbiphenyl-4,4'-diyl]di(1E)hydrazin-2-yl]-1-ylidene]bis(4-amino-5-oxo-5,6-dihydronaphthalene-1,3-disulfonate)                            | 314-13-6    | 23,860      |    | Electro-Fenton   | Vijayakumar et al. 2016   |
| Direct red 83                        | Tetrasodium;4-oxido-7-[[5-oxido-6-[[2-oxido-5-sulfonatophenyl]diazenyl]-7-sulfonatophthalen-2-yl]carbonyl]amino]-3-[[2-oxido-5-sulfonatophenyl]diazenyl]naphthalene-2-sulfonate | 15,418-16-3 | 29,225      |   | Electro-Fenton   | Kupferle et al. 2006      |
| Direct blue 71                       | Tetrasodium;3-[[4-[[4-[(6-amino-1-hydroxy-3-sulfonatophthalen-2-yl)diazenyl]-6-sulfonatophthalen-1-yl]diazenyl]naphthalen-1-yl]diazenyl]naphthalene-1,5-disulfonate             | 4399-55-7   | 34,140      |  | Anodic oxidation | Xu et al. 2022            |

Table 2 (continued)

| Name             | IUPAC name   | CAS                  | Color index | Structural formula | Type of process                           | References                |
|------------------|--|----------------------|-------------|--------------------|---|---------------------------|
| Direct red 81    | Disodium 7-benzamido-4-hydroxy-3-((4-(4-sulphonatophenyl)azo)phenyl)azo)naphthalene-2-sulphonate   | 2610-11-9/12237-71-7 | 28,160      |                    | Electrochemical and photoelectrochemical  | Socha et al. 2006         |
| Direct black 36  | Disodium 4-amino-3-[(E)-[4'-(E)-(2,4-diaminophenyl)diazonyl]biphenyl-4-yl]diazonyl]-5-hydroxy-6-(E)-phenyldiazonyl]naphthalene-2,7-disulfonate   | 6360-26-5            | 31,665      |                    | Electrochemical and photo-electrochemical | Socha et al. 2006         |
| Direct black 22  | Trisodium;6-[(2,4-diaminophenyl)diazonyl]-3-[[4-[4-[[7-[(2,4-diaminophenyl)diazonyl]-1-hydroxy-3-sulfonatophthalen-2-yl]diazonyl]-2-sulfonatoanilino]phenyl]diazonyl]-4-hydroxynaphthalene-2-sulfonate | 6473-13-8            | 35,435      |                    | Electrochemical oxidation                 | Kharlamova and Aliev 2016 |
| Direct blue 129  | Copper, [tetrahydrogen-3,3'-[(3,3'-dihydroxy-4,4'-biphenylene)bis(azo)]bis[5-amino-4-hydroxy-2,7-naphthalenedisulfonato](4-)]di-, tetrasodium salt   | 8004-65-7            | 27,095      |                    | Photoassisted electrochemical oxidation   | Khataee et al. 2014       |
| Direct blue 15   | Tetrasodium;5-amino-3-[[4-[4-[(8-amino-1-hydroxy-3,6-disulfonatophthalen-2-yl)diazonyl]-3-methoxyphenyl]-2-methoxyphenyl]diazonyl]-4-hydroxynaphthalene-2,7-disulfonate                                | 2429-74-5            | 24,400      |                    | Indirect electro-oxidation                | Yang et al. 2018          |
| Direct orange 26 | 2-Naphthalenesulfonic acid, 7'-(carbonyldiimino)bis[4-hydroxy-3-(phenylazo)-, disodium salt  | 3626-36-6            | 29,150      |                    | Electro-oxidation                         | Zayed et al. 2021         |

et al. 2015a, 2016; Rahmani et al. 2015; Malakootian and Moridi 2017; Ben Hafaiedh et al. 2020).

## Electrochemical oxidation of azo dyes

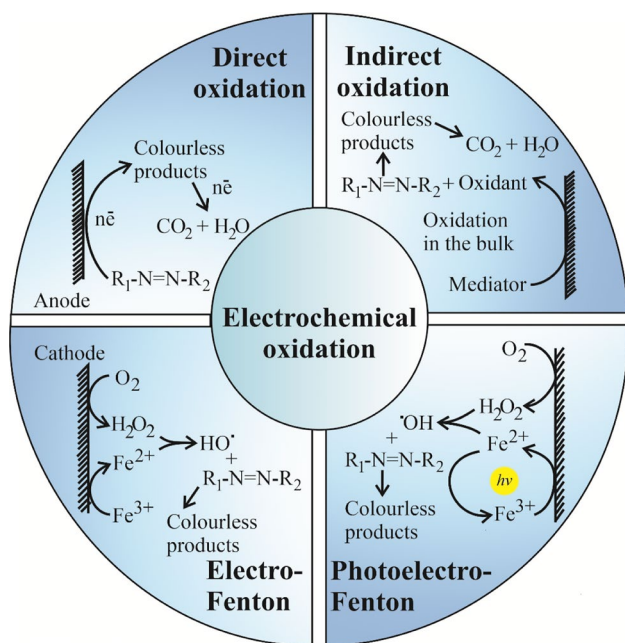
Electrochemical methods for azo dye removal attract much attention as they are environmentally friendly since the leading reagent that oxidizes azo dyes is an electron transferred from the surface of various electrode materials (Shukla and Oturan 2015). Oxidation of azo dyes during electrolysis is also associated with the generation of  $\cdot\text{OH}$  on the surface of the electrodes during oxidation of water (anodic oxidation) and in the bulk of the electrolyte upon adding a catalyst and in situ generation of hydrogen peroxide during electrolysis (electro-Fenton). Electrochemical oxidation removes azo dyes with high chemical oxygen demand ranging from 0.1 to 100 g/L from wastewater (Sirés et al. 2014). On the other hand, electrochemical advanced oxidation processes can be used as a pre-treatment process to increase the biodegradability of azo dyes containing wastewater for a biological post-treatment (Ganzenko et al. 2014).

Other oxidation processes for removing azo dyes have limitations and disadvantages compared to electrochemical advanced oxidation processes. The chemical oxidation processes, such as ozone oxidation and hypochlorite ion oxidation, and advanced oxidation processes such as Fenton's reagent, photo-Fenton, and photo-catalytic oxidation also lead to decolorization of azo dye solutions (Deng et al. 2020). However, applying these methods for wastewater treatment and azo dyes removal is limited due to some disadvantages. For example, the main disadvantage of the Fenton's reagent and related advanced oxidation processes is the formation of an iron-containing sludge and the process is effective only at acidic pH (Oturan and Aaron 2014; Deng and Brillas 2023). Oxidation processes based on ozone have the disadvantage of a short half-life of ozone molecules (Javaid and Qazi 2019). The use of hypochlorite ions as oxidants leads to incomplete destruction of azo dyes with the formation of aromatic amines (Isaev and Magomedova 2022), which can be more toxic than the original azo dyes (Gottlieb et al. 2003). Photo-catalytic methods also have limited application due to high rates of recombination of the photo-generated electrons and holes (Ge et al. 2016). However, the use of advanced oxidation processes for removing azo dyes compared to other physicochemical methods such as adsorption or coagulation does not lead to the secondary pollution associated with the transfer of azo dyes from one phase to another (Ma et al. 2021).

Electrochemical oxidation of azo dyes has advantages over other physical and chemical methods. For example, electrochemical removal of azo dyes can be carried out under relatively mild conditions at ambient temperature and pressure without additional chemicals. Electrochemical methods are highly efficient, do not produce secondary waste, are easily automated, and can be supplemented by other methods for dye removal (Särkkä et al. 2015; El-Kacemi et al. 2017; Cui et al. 2021). The disadvantages of a typical electrochemical process implemented by anodic oxidation include high energy consumption for the treatment of wastewater with a low concentration of organic pollutants, heterogeneous nature of the electrochemical process (mass transfer limitation), and a decrease in the activity of the electrode surface due to adsorption of azo dye degradation products (Garcia-Segura et al. 2018). To compensate disadvantages of this process, various approaches including indirect electrochemical oxidation with the generation of oxidizing agents such as active chlorine species, persulfate (called mediated oxidation) (Panizza and Cerisola 2009), and photo-electrochemical oxidation were developed. On the other hand, the electro-Fenton process and related techniques such as heterogeneous electro-Fenton, photo-electro-catalysis, photo-electro-Fenton and solar photo-electro-Fenton take the advantages to generate hydroxyl radicals homogeneously in the bulk solution, in addition of heterogeneous hydroxyl radical formed on the anode surface, to increase the process efficiency (Titchou et al. 2021a). Figure 1 summarizes the main electrochemical methods used for the removal of azo dyes from wastewater. The main parameters affecting the efficiency of electrochemical oxidation of azo dyes are the electrode material, current density, initial concentration of dyes, nature of the dye and the electrolyte, fluid hydrodynamics, pH, and temperature (Qiao and Xiong 2021).

The electrochemical oxidation of azo dyes has been the subject of a large number of studies. Most of the publications are devoted to electrochemical oxidation of acid and reactive azo dyes using various electrochemical methods, which is due to the wide use of both azo dyes for dyeing various materials. The efficiency of electrochemical oxidation of azo dyes can also be affected by the molecular structure of dyes. Research results show that functional groups, which reduce nucleophilicity of the azo dye, inhibit electrophilic attack of the electro-generated  $\cdot\text{OH}$  and, thus, reduce overall effectiveness and decolorization rate. In addition, the presence of an additional chromophore azo bond in the molecule leads to the formation of a more stable conjugated  $\pi$ -system, which increases the activation energy required for electrophilic attack and enhances the persistent nature of azo dyes (da Costa Soares et al. 2017).



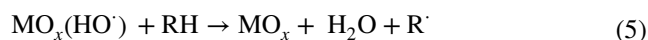
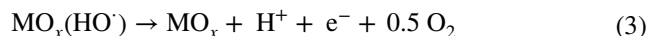
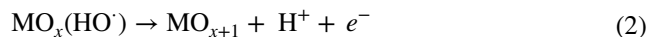
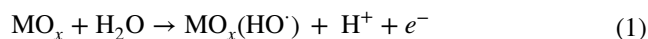


**Fig. 1** Electrochemical oxidation processes for removal of azo dyes. Direct oxidation—oxidation directly on the anode surface due to electron transfer and formation of  $\cdot\text{OH}$  on the anode surface (Panizza and Cerisola 2009; Moreira et al. 2017); indirect oxidation—oxidation due generation of various oxidants such as  $\text{H}_2\text{O}_2$ , hypochlorite, and persulfate (Scialdone 2009); electro-Fenton—oxidation due homogeneous  $\cdot\text{OH}$  via electrochemical generated Fenton's reagent (Oturán and Oturan 2018; Vasudevan and Oturan 2014; Nidhesh et al. 2018); photo-electro-Fenton—oxidation due electrochemical generated Fenton's reagent with simultaneous ultraviolet or sunlight irradiation (Brillas 2020; Ganiyu et al. 2018)

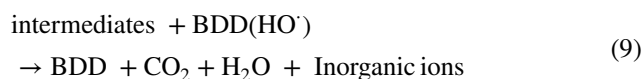
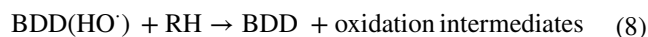
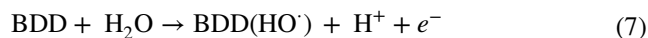
## Anodic oxidation

Anodic oxidation of organics can occur by a direct electron transfer to the anode surface and by hydroxyl radicals formed on the anode surface during water oxidation. The efficiency of producing hydroxyl radicals and, consequently, oxidation of azo dyes are depending on the anode material used in anodic oxidation process. Since the formation of  $\cdot\text{OH}$  is a heterogeneous process, in the case of using active metal and metal oxide anodes (so-called active anodes), chemisorption occurs on the electrode surface and the mineralization of organics is not much high (Panizza and Cerisola 2009). The formation of hydroxyl radicals is facilitated by anodes with high oxygen over-potential (called non-active anodes), such as boron-doped diamond (BDD),  $\text{PbO}_2$ , and sub-stoichiometric titanium oxide (Peralta-Hernández et al. 2012; He et al. 2019; Trellu et al. 2020; Karim et al. 2021; Srivastava et al. 2021). The mechanism of oxidation of organic compounds with the formation of hydroxyl radicals has been studied in sufficient detail by many researchers (Comninellis 1994; Panizza and Cerisola 2009). In the case of active anode, heterogeneous hydroxyl radicals  $\text{MO}_x(\text{HO}\cdot)$

form mainly during water oxidation [Eq. (1)] is strongly adsorbed to the anode surface. Adsorbed radicals lead to the formation of chemisorbed oxygen [Eq. (2)] or oxygen release [Eq. (3)]. Chemisorbed oxygen can then release as gaseous oxygen [Eq. (4)].  $\text{MO}_x(\text{HO}\cdot)$  and oxygen oxidize organic substances (noted RH), followed by catalytic regeneration of the anode surface according to Eqs. (3)–(6).



The proposed mechanism is different in the case of a non-active anode, such as BDD. The  $\text{BDD}(\text{HO}\cdot)$  is very slightly adsorbed on the anode surface and behaves as quasi-free hydroxyl radicals. Therefore, the oxidation of organic pollutants leading to their mineralization can be summarized as follows:



Anodic oxidation of azo dyes results in the formation of low molecular weight organic compounds, such as carboxylic acids, available for biological oxidation or complete mineralization occurring with the formation of  $\text{CO}_2$ ,  $\text{H}_2\text{O}$ , and other inorganic compounds (Alcocer et al. 2018). The efficiency of direct anodic oxidation of dyes depends on several functional groups (for example, azo bonds) in their molecules, making them electro-active for direct electron transfer (Alagesan et al. 2021).

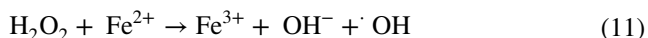
## Indirect electro-oxidation

During indirect oxidation, the reaction of anodic oxidation or cathodic reduction (of water or species present in the medium) results in the formation of intermediate products or oxidizing agents such as ozone, hydrogen peroxide, and other active species on the electrode surface under the action

of external current (Nidheesh et al. 2018). In the presence of  $\text{SO}_4^{2-}$ ,  $\text{Cl}^-$  and  $\text{PO}_4^{3-}$  ions as electrolytes, oxidizing agents such as  $\text{S}_2\text{O}_8^{2-}$ ,  $\text{Cl}_2$ ,  $\text{HClO}$  and  $\text{P}_2\text{O}_8^{4-}$  can also form (El Aggadi et al. 2021; Divyapriya and Nidheesh 2021). Oxidizing agents or active species thus formed can react with organic pollutants leading to their oxidation with the formation of various intermediate compounds (Martínez-Huitle and Brillas 2009; Martínez-Huitle et al. 2015). The initial oxidation reaction occurs on the electrode surface, and the subsequent degradation of pollutants occurs in the bulk electrolyte (Qiao and Xiong 2021).

## Electro-Fenton

The electro-Fenton is one of the most popular electrochemical advanced oxidation processes along and is based on electrochemically assisted Fenton reaction. In contrast to the classical Fenton system in which Fenton's reagent (mixture of  $\text{H}_2\text{O}_2$  and  $\text{Fe}^{2+}$ ) is externally added to the solution to be treated, the electro-Fenton process does not use chemicals except a catalytic amount of ferrous iron (Oturán et al. 2000; Brillas et al. 2009).  $\text{H}_2\text{O}_2$  is formed by a two-electron reduction of  $\text{O}_2$  [Eq. (10)] on a suitable cathode. Formed  $\text{H}_2\text{O}_2$  reacts with externally added catalyst ( $\text{Fe}^{2+}$ ) to form  $\cdot\text{OH}$  homogeneously via Fenton reaction [Eq. (11)].



Continuous generation of  $\cdot\text{OH}$  is then ensured by the electro-regeneration of  $\text{Fe}^{2+}$  [Eq. (12)] from the reduction of  $\text{Fe}^{3+}$  formed in Fenton reaction [Eq. (11)].  $\cdot\text{OH}$  further reacts with organic pollutants leading to their oxidation to biodegradable species, which can be further removed by a biological post-treatment (Olvera-Vargas et al. 2016). Alternatively, organic pollutants can be mineralized to  $\text{CO}_2$  and inorganic ions as in anodic oxidation (Eqs. (9) and (10)). However, the latter option needs longer treatment time and more energy.



The most widely used cathode materials for the efficient production of  $\text{H}_2\text{O}_2$  are based on carbon materials (carbon felt, reticulated vitreous carbon (RVC), carbon sponge, carbon nanotubes (CNT) or graphite) (He and Zhou 2017; Ganiyu et al. 2018; Divyapriya and Nidheesh 2020; Sopaj et al. 2020). The performance of the electro-Fenton process was strongly improved with the use of non-active anodes, mainly BDD anode. The use of BDD as an anode in the electro-Fenton process allows for the simultaneous production of homogeneous  $\cdot\text{OH}$  in the bulk solution [Eq. 11] and

heterogeneous BDD(OH) on the anode surface (Oturán et al. 2012).

The electro-Fenton process is optimal at acidic pH of about 3. To overcome this pH dependency and to recover the catalyst used in the process, several modifications were recently done by developing heterogeneous electro-Fenton process including various solid catalysts, and catalyst loaded on cathode surface. The various advancements in electro-Fenton process are explained in detail in previous research and review articles (Barhoumi et al. 2017; Heidari et al. 2021; Mejjide et al. 2021; Gopinath et al. 2022; Krishnan et al. 2022; Nidheesh et al. 2022c; Nidheesh et al. 2023a, b).

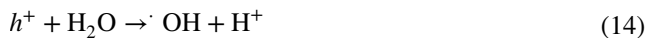
## Photo-electro-catalysis

Photo-electro-catalysis is a rapidly developing method for removing azo dyes from aqueous solutions (García-Segura and Brillas 2017; Brillas and García-Segura 2023). This is due to the increased efficiency of organic dye removal through the synergistic effect of photo-catalysis and electro-catalysis (Laghrib et al. 2020). The main advantage of photo-electro-catalytic oxidation of azo dyes is the high rate of charge separation compared to photo-catalysis and low energy consumption compared to electrochemical oxidation of azo dyes, especially when using sunlight as an energy source (Zhang et al. 2023; Brillas 2023). In this case, the main disadvantage of photo-catalytic oxidation of azo dyes, rapid recombination of photo-generated electrons and holes ( $e^-/h^+$ ), can be eliminated by applying an external potential during photo-electro-catalytic oxidation of azo dyes (Ma et al. 2020). For photo-electro-catalytic oxidation of azo dyes, semiconductor electrodes, that capable of reacting to UV or sunlight, are used and applied onto various substrates. The absorption of a photon by the semiconductor photo-electrode with energy exceeding its band gap results in charge separation, generating electrons ( $e^-$ ) in the conduction band and holes in the valence band [Eq. 13] (Rajput et al. 2021).



Under the influence of an external applied potential, the photo-generated  $e^-$  can move towards the counter electrode, leading to redox reactions on the electrode surfaces (Cao et al. 2017). Simultaneously with the electrolysis process, direct azo dyes oxidation reactions occur on the photo-catalyst surface, forming highly active oxygen-containing particles (Feng et al. 2021). The combination of electro-catalytic and photo-catalytic processes reduces the rate of electron-hole pair recombination and increases the lifetime of holes (Zarei and Ojani 2016). The resulting  $h^+$  has a strong oxidizing ability and can migrate to the surface for direct interaction with azo dyes or react with  $\text{H}_2\text{O}/\text{OH}^-$  to

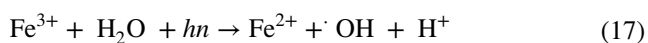
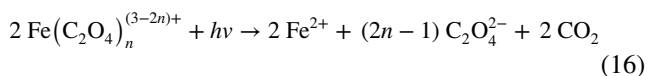
form hydroxyl radicals, which also oxidize organic pollutants [Eq. 14]. Photo-generated electrons can react with dissolved oxygen to form active oxygen-containing particles according to Eq. 15 (Garcia-Segura and Brillas 2017).



In addition to photo-catalytic processes, electrochemical oxidation of azo dye can also occur on oxide–metal semiconductors. Anodic oxidation of azo dye can occur by direct electron transfer to the surface of the anode and  $\cdot\text{OH}$  formed on the surface of the anode during water oxidation. The efficiency of hydroxyl radical formation and thus the oxidation of azo dyes depend on the anode material. Since the formation of  $\cdot\text{OH}$  is a heterogeneous process, the use of active metal and metal oxide anodes leads to chemisorption of oxidation products of azo dyes on the electrode surface and their low activity in the oxidation process (Panizza and Cerisola 2009). Anodes with high oxygen evolution overpotential, such as BDD,  $\text{PbO}_2$ , and others, promote the formation of hydroxyl radicals (Peralta-Hernández et al. 2012; Alimirzaeva et al. 2019; He et al. 2019; Karim et al. 2021).

### Photo-/solar photo-electro-Fenton

Photo-electro-Fenton process consists of light (UV or visible) irradiation of electro-Fenton reactor. This process implemented first by Brillas' team allows for increasing mineralization efficiency of electro-Fenton process. The short-chain carboxylic acids formed during electro-Fenton oxidations are complexed by  $\text{Fe}^{3+}$  present in the medium and become recalcitrant to  $\cdot\text{OH}$ , resulting in low mineralization rates. On the other hand, UV or visible light irradiation can destroy this complex and thus facilitate the mineralization of carboxylic acids. For example, Eq. (16) shows the destruction of  $\text{Fe(III)}$ -carboxylic acid complex with the regeneration of  $\text{Fe}^{2+}$  (catalyst). The photo-generated  $\text{Fe}^{2+}$  ion can subsequently catalyze the Fenton reaction, which results in the formation of  $\text{Fe}^{3+}$  and ring closure [Eq. (11)]. Additionally, photo-reduction of  $\text{Fe}^{3+}$  generated in Fenton reaction allows the formation of additional  $\cdot\text{OH}$  [Eq. (17)] (Brillas et al. 2009; Oturan and Aaron 2014; Ganiyu et al. 2018; Divyapriya et al. 2021).



Although the photo-electro-Fenton in practice provides high oxidation/mineralization power, the use of artificial

light makes the process costly. Therefore, solar photo-electro-Fenton process have been developed to remediate this inconvenient (Bedolla-Guzman et al. 2016; Salazar et al. 2019; Brillas 2020; Wang et al. 2021). This process is effective for completely mineralizing synthetic azo dyes and real wastewater (Brillas 2022) with higher mineralization power and lower energy consumption than conventional electro-Fenton processes.

### Electrochemical oxidation of various azo dyes

Various electrochemical processes are used to remove azo dyes from wastewater: direct and indirect electrochemical oxidation, electro-Fenton, photoelectrocatalysis, photo-electro-Fenton, solar photo-electro-Fenton, and a combination of electrochemical processes with other physical–chemical or biological treatments. The combination of electro-oxidation with various types of physical and chemical treatment increases the efficiency of color and chemical oxygen demand removal. For example, this enhancement has been demonstrated during oxidative degradation of Reactive Black 5 by ultrasonic treatment coupled with electrochemical oxidation (Johin et al. 2019), sono-electro-Fenton in the presence of electrochemically generated hydrogen peroxide (Şahinkaya 2013), and photo-electro-Fenton with UV or sunlight irradiation in the presence of electrochemically generated hydrogen peroxide and semiconductor materials (Wang et al. 2008b; Sala et al. 2016). Electro-catalytic oxidation of Methyl Orange in a hybrid self-powered electrochemical cell has also been reported to be a variant of creating an energy-independent technology for wastewater treatment from azo dyes (Yang et al. 2013).

Electrochemical generation of Fenton's reagent is used as an effective and potentially practical method for removing azo dyes from wastewater (Isarain-Chávez et al. 2013). The rate of Methyl Orange oxidation is higher for electro-Fenton process as compared to anodic oxidation with electro-generated hydrogen peroxide (do Vale-Júnior et al. 2018). The addition of heterogeneous catalysts, such as magnetically separable nano- $\text{Fe}_3\text{O}_4$  (Sasidharan Pillai and Gupta 2016) and  $\text{Fe}_2(\text{MoO}_4)_3$ -kaolin-based iron molybdate (He et al. 2014) to Methyl Orange solution for hydrogen peroxide decomposition, leads to an increase in the rate of  $\cdot\text{OH}$  generation and, accordingly, an increase in the rate of decolorization and chemical oxygen demand removal (Jiang et al. 2016).

Among acid azo dyes, electrochemical oxidation of Methyl Orange was extensively studied by several researchers. Methyl Orange is used as a model compound for studying the activity of various electrode materials and in determining the effectiveness of new electrochemical methods.

Direct anodic oxidation of Methyl Orange and its indirect electrochemical oxidation are also studied with the generation of active chlorine on the anode or hydrogen peroxide on the cathode (Zhang et al. 2015) in solutions with a high NaCl concentration (Yu et al. 2015). These authors showed that a high current density, an acid environment, and an increase in the concentration of NaCl have a positive effect on the electro-oxidation rate of Methyl Orange. It should be noted that the electrochemical oxidation of Methyl Orange in chloride-containing solutions does not lead to the formation of intermediate organochlorine compounds (Pillai et al. 2015).

Acid Orange 7 is mainly used in printing and textile industries and hardly degrades by biological and other wastewater treatment methods. When dissolved in water, Acid Orange 7 can form three types of molecules with different charges depending on the solution pH (Chou et al. 2011). AO7 electrochemical oxidation in various electrolytes and using various approaches have been studied in sufficient detail (Chou et al. 2011; Qiao et al. 2015; Wu et al. 2016). An increase in the efficiency of electrochemical oxidation for complete removal Acid Orange 7 can be achieved by combining electrochemical oxidation with other treatment methods. Acid Orange 7 electrochemical oxidation results in the accumulation of toxic aromatic fragments, which can be removed using subsequent sorption (Li et al. 2015). The overall efficiency of Acid Orange 7 electrochemical oxidation using granular activated carbon as electrodes and in combination with coagulation reduces chemical oxygen demand and color to 99% and 87%, respectively (Xiong et al. 2001). Bio-electrochemical treatment of the solutions containing Acid Orange 7 azo dye has also been reported, which leads to complete decolorization of the solution with an additional mineralization of toxic products formed during azo dye oxidation (Pan et al. 2017).

During the Acid Orange 7 indirect electrochemical oxidation through the generation of hydrogen peroxide, the cathode material plays an important role. The cathode material was subjected to various modifications to increase the efficiency of hydrogen peroxide production yield. Modifying a carbon air-diffusion cathode with nanoparticles of tungsten oxide resulted in increased hydrogen peroxide yield and azo dye oxidation (Paz et al. 2018). In a polypyrrole framework, lignin-based composites deposited on graphite felt was also used as the cathode in Acid Orange 7 electrochemical oxidation (Sun et al. 2015). When the powdered sludge carbon resulted from pyrolysis reaction at 800 °C was used as the cathode, the Acid Orange 7 removal from the solutions occurred efficiently due to simultaneous adsorption and electro-oxidation (Sun et al. 2015). Besides, when an electrochemically active tubular carbon-graphite membrane was used as the cathode, Acid Orange 7 electro-oxidation was supplemented with dynamic filtration technology (Liang et al. 2016). The electrochemical oxidation of Acid Orange

7 took place rapidly in anodic oxidation with PbO<sub>2</sub>-coated RVC composite cathode (RVC/PbO<sub>2</sub>/TiNT) and an industrial stainless steel mesh anode (Ramírez et al. 2016). Combining the processes of ozonation and electrolysis with the formation of H<sub>2</sub>O<sub>2</sub> on the cathode led to an increase in the efficiency of the azo dye oxidation process. In this case, complete decolorization and total organic carbon removal at the level of 95.7% were obtained after 4 and 45 min of treatment, respectively (Bakheet et al. 2013).

The use of the electro-Fenton process also refers to Acid Orange 7 indirect electrochemical oxidation. Acid Orange 7 oxidation in the electro-Fenton process occurs with the formation of electro-generated ·OH, leading to the complete oxidative degradation of the dye up to its complete mineralization. H<sub>2</sub>O<sub>2</sub> and Fe<sup>2+</sup> ions are catalytically electro-generated on a carbon felt cathode (Özcan et al. 2009). The new cathode for electro-Fenton based on reduced graphene oxide deposited on the carbon felt surface makes it possible to decolorize the Acid Orange 7 solution after 5 min of electrolysis (Le et al. 2015). Electro-Fenton is the most efficient method for Acid Orange 7 removal. A comparison of two cathode materials, unidirectional carbon fiber and reticulated vitreous carbon, showed that the former electrode was more efficient in generating hydrogen peroxide and subsequent oxidation of Acid Orange 7 (Ramírez-Pereda et al. 2018).

According to the literature data, the efficiency of anodic oxidation and electro-Fenton processes of Acid Red 27 depends on the electrolyzer configuration, current density, electrolyte type, and electrodes used (Zhang et al. 2012). The solutions of food azo dye were processed using different anode materials at different temperatures and solution flow rates, which ensured the color and chemical oxygen demand removal of more than 75% (Elaiassaoui et al. 2019). When Ir-Sn-Sb mixed-oxide anode was used in the electro-Fenton and photo-electro-Fenton processes, the efficiency of Acid Yellow 36 oxidation increased compared to anodic oxidation. Oxidation of the dye occurred mainly by heterogeneous M(OH) and generated active chlorine species (Aguilar et al. 2017). In situ electrochemical generation of H<sub>2</sub>O<sub>2</sub> has also been used to oxidize the Acid Yellow 36 azo dye (Cruz-González et al. 2010). In this case, H<sub>2</sub>O<sub>2</sub> continuously formed in the dye solution from electro-reduction of dissolved molecular oxygen (Isaev and Aliev 2012; Rodríguez De León et al. 2019).

Using other physicochemical methods combined with electrochemical oxidation increases the efficiency of Acid Red 14 removal. The electro-Fenton process promotes about 60–70% of Acid Red 14 mineralization, while photo-electro-Fenton can mineralize Acid Red 14 more efficiently (total organic carbon removal of more than 94%) even at low current densities, due mainly to the contribution of UV light irradiation (Wang et al. 2008a). The addition of TiO<sub>2</sub> to the Acid Red 14 solution significantly enhances the dye

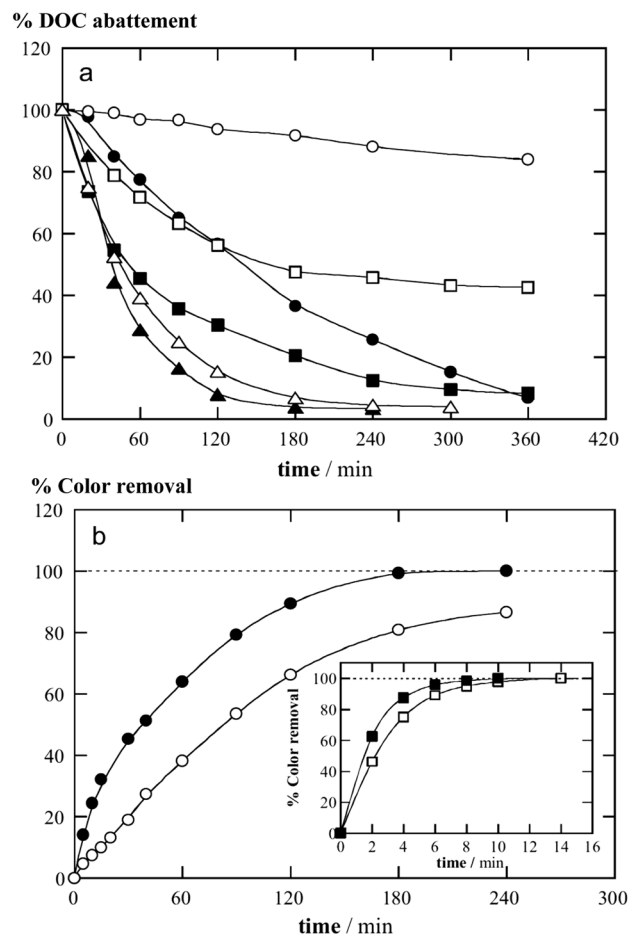
degradation (Shen et al. 2002), and the addition of  $\text{Fe}_3\text{O}_4$  nanoparticles leads to heterogeneous Fenton-like processes of dye oxidation on the catalyst surface (Es'haghzade et al. 2017). Acid Red 14 electrochemical degradation in a plasma flow (Barrera et al. 2020) is also more efficient than anodic oxidation (Wang et al. 2010). In the case of a plasma-stimulated oxidation process, the formation of hydrogen peroxide occurs in a plasma discharge, which enhances dye degradation, and the introduction of iron ions ( $\text{Fe}^{2+}/\text{Fe}^{3+}$ ) into the solution leads to the formation of an enormous amount of  $\cdot\text{OH}$  through Fenton reaction (Barrera et al. 2020).

The combination of electrochemical oxidation of Methyl Orange with the subsequent adsorption of degradation products increased the process efficiency due to the synergistic effect between electrolysis and adsorption (Liu et al. 2022). The combination of the AO16 electro-oxidation process with the subsequent adsorption process has also been reported, resulting in an increase in chemical oxygen demand removal efficiency (Zakaria et al. 2015). Comparatively treated the Acid Red 1 solutions by anodic oxidation with electro-generated  $\text{H}_2\text{O}_2$  (anodic oxidation- $\text{H}_2\text{O}_2$ ), electro-Fenton and photo-electro-Fenton processes at constant current density and oxidation power was found in the following sequence: anodic oxidation- $\text{H}_2\text{O}_2$  < electro-Fenton < photo-electro-Fenton. Faster and similar decolorization efficiency was achieved in electro-Fenton and photo-electro-Fenton owing to the quicker destruction of aromatics with hydroxyl radicals produced in bulk (Fig. 2).

The highest efficiency of dye oxidation by electro-oxidation process was reported in the case of the use of high oxygen over-potential anodes in combination with other oxidation processes, such as oxidation with electro-generated hydrogen peroxide (Vahid and Khataee 2013), electro-generated sodium hypochlorite (Akrouit and Bousselmi 2013), electro-Fenton (El-Desoky et al. 2010b; Rahmani et al. 2016; Zhang et al. 2019a, b), photo-electro-Fenton (Almeida et al. 2012, 2014; Pacheco-Álvarez et al. 2019), heterogeneous photo-catalysis (Santos et al. 2015; Morales et al. 2018), addition of persulfates (dos Santos et al. 2020b, a), and biological oxidation (Cui et al. 2020). Color removal ranges from 80% to complete decolorization, chemical oxygen demand from 60% to over 90% and total organic carbon from 50 to 80%. Table 3 shows comparative data on electrochemical oxidation of various azo dyes.

### Effect of electrode materials on the electrochemical degradation of azo dyes

Various electrode materials have been used to remove azo dyes from water using electrochemical oxidation. Using electrode materials with high oxygen over-potential makes



**Fig. 2** Dissolved organic carbon (DOC) abatement: **a** and color removal vs. electrolysis time for the degradation of Acid Red 1 (AR1) solutions, **b** using a Pt/air-diffusion cell (open symbols) or a boron-doped diamond (BDD)/air-diffusion cell (solid symbols). Method: (○,●) Anodic oxidation with formation  $\text{H}_2\text{O}_2$  (AO- $\text{H}_2\text{O}_2$ ), (□,■) electro-Fenton (EF) with 0.5 mM  $\text{Fe}^{2+}$  and (△,▲) photo-electro-Fenton (PEF) with 0.5 mM  $\text{Fe}^{2+}$  and 6 W ultraviolet light of  $\lambda_{\text{max}} = 360$  nm. Poor dissolved organic carbon (DOC) removal of the AR1 solution by AO- $\text{H}_2\text{O}_2$  with Pt, only reaching 16% mineralization at the end. The alternative use of a BDD anode causes a much faster DOC decay; up to attain 93% mineralization at 360 min. The slow DOC removal found for EF with Pt at long electrolysis time. The faster degradation process under the action of  $\cdot\text{OH}$  in the bulk can also be observed in EF with BDD, primordially during the first 180 min of treatment where 80% DOC reduction was already achieved. When the PEF process was applied, less influence of the anode material was found due to the potent action of UVA irradiation. PEF yielded a very fast mineralization of the AR1 solution to yield almost total mineralization (>96% DOC removal) after 300 min using Pt, and in a shorter time of 240 min for BDD. Reprinted by permission from Florenza et al. (2014a). Copyright 2014, Elsevier

it possible to treat azo dyes containing solutions effectively. On metal oxide electrodes, Methyl Orange oxidation proceeds mainly with the generation of hydroxyl radicals (Mais et al. 2020). When comparing the efficiency of the process of Methyl Orange electrochemical oxidation on

**Table 3** Parameters of electrochemical decolorization and chemical oxygen demand removal of acid dyes solutions

| Name of dye        | Electrode material  | Type of process   | Process parameters  | Color removal, %                                | Removal of COD, %            | References                  |
|--------------------|---|---|---|---|------------------------------|-----------------------------|
| Acid red 18        | Pb/PbO <sub>2</sub>   |   | Direct oxidation  | 99.9  | 80.0                         | Rahmani et al. 2015         |
| Acid red 1         | BDD or Pt   | Electro-Fenton  | [Dye] <sub>0</sub> = 236 mg/L, 0.05 M Na <sub>2</sub> SO <sub>4</sub> , pH = 3.0, 35 °C, j = 100 mA/cm <sup>2</sup>             | 100 in 10 min                                   | 100 in 240 min               | Florenza et al. 2014        |
| Acid red G         | Ti/PbO <sub>2</sub> and Fe <sub>3</sub> O <sub>4</sub> /Sb-SnO <sub>2</sub> particles | Direct oxidation  | [Dye] <sub>0</sub> = 100 mg/L, j = 50 mA/cm <sup>2</sup> , 25 °C, 0.1 M Na <sub>2</sub> SO <sub>4</sub>                         | 100   | 65.89                        | Yuan et al. 2019            |
| Acid blue 161      | Ti/Ru <sub>0.3</sub> Ti <sub>0.7</sub> O <sub>2</sub>                                 | Direct oxidation  | [Dye] <sub>0</sub> = 100 mg/L, j = 50 mA/cm <sup>2</sup> , 0.02 M Na <sub>2</sub> SO <sub>4</sub> , flow rate 10 mL/min, 60 min | 37  | –                            | de Almeida et al. 2019      |
| Acid orange 74     | Ru, IrO <sub>2</sub> , PbO <sub>2</sub> , BDD   | Direct and indirect oxidation                               | [Dye] <sub>0</sub> = 50 mg/L, j = 40 mA/cm <sup>2</sup> , 0.02 M Na <sub>2</sub> SO <sub>4</sub>                                | 65.7<br>73.8<br>85.1<br>100                     | 28.2<br>43.5<br>68.2<br>84.3 | Li et al. 2021              |
| Acid blue 92       | BDD   | Photo-stimulated electro-chemical oxidation                 | [Dye] <sub>0</sub> = 20 mg/L, applied current 0.1 A, flow rate 10 L/h, pH = 6   | 100 in 30 min                                   | –                            | Khataee et al. 2013         |
| Acid violet 1      | TiO <sub>2</sub> /RuO <sub>2</sub> (70%/30%)  | Electrochemical and photo-electrochemical oxidation         | j = 2.5 × 10 <sup>-2</sup> A/cm <sup>2</sup> , 60 °C, 180 min   | –   | 57                           | Socha et al. 2007           |
| Acid violet 7      | Si/BDD Nb/BDD   | Direct oxidation  | [Dye] <sub>0</sub> = 200 mg/L, 0.05 M Na <sub>2</sub> SO <sub>4</sub> , j = 60 mA/cm <sup>2</sup> , 120 min                     | 100 in 90 min<br>100 in 60 min                  | 85<br>83                     | Brito et al. 2018b          |
| Acid yellow 23     | Ti/IrO <sub>2</sub> -RuO <sub>2</sub>   | Electro-Fenton  | [Dye] <sub>0</sub> = 60 mg/L, pH = 3, modified Fe-C 160 g, flow rate 20 mL/min, applied current 200 mA                          | 80  | 30                           | Zhang et al. 2019a          |
| Eriochrome black T | BDD   | Electro-oxidation<br>Electro-Fenton<br>Photo-electro-Fenton | [Dye] <sub>0</sub> = 150 mg/L, 0.05 mM NaCl, pH = 3, j = 20 mA/cm <sup>2</sup>  | 100 in 60 min<br>100 in 45 min<br>100 in 35 min | 91<br>95<br>98               | Pacheco-Álvarez et al. 2019 |
| Acid blue 113      | RuO <sub>2</sub> /Ti  | Indirect oxidation  | [Dye] <sub>0</sub> = 160 mg/L, 0.03 M NaCl  | –   | 80.21                        | Mohan et al. 2001           |
| Acid black 194     | Ti/SnO <sub>2</sub> -Sb/PbO <sub>2</sub> -Pr  | Electro-Fenton  | [Dye] <sub>0</sub> = 100 mg/L, j = 30 mA/cm <sup>2</sup> , 0.1 M Na <sub>2</sub> SO <sub>4</sub>                                | –   | > 80                         | He et al. 2011              |
| Acid blue 29       | Sn-Cu-Sb anode  | Anodic oxidation  | [Dye] <sub>0</sub> = 60 mg/L, pH = 7.0, j = 10.0 mA/cm <sup>2</sup> , 0.05 M NaCl   | 100 in 300 min                                  | 100 in 600 min               | do Vale-Júnior et al. 2016  |
| Acid red 73        | Yttrium doped Ti/SnO <sub>2</sub> -Sb   | Anodic oxidation  | [Dye] <sub>0</sub> = 500 mg/L, j = 15 mA/cm <sup>2</sup> , 0.04 M NaCl, 60 min  | 100 in 40 min                                   | > 50 in 55 min               | Xu et al. 2013b             |

Table 3 (continued)

| Name of dye         | Electrode material  | Type of process                                | Process parameters  | Color removal, %       | Removal of COD, % | References                      |
|---------------------|---|--|---|------------------------|-------------------|---------------------------------|
| Sunset yellow FCF   | BDD   | Photo-electro-Fenton with sunlight irradiation | [Dye] <sub>0</sub> = 290 mg/L, pH = 3.0, <i>j</i> = 33.2–77.6 mA/cm <sup>2</sup>  | 100                    | 91–94             | Moreira et al. 2013             |
| Acid red 150        | BDD   | Photo-electro-Fenton                           | [Dye] <sub>0</sub> = 55 mg/L, 0.050 M, pH = 3.0, <i>j</i> = 100 mA/cm <sup>2</sup>  | 100 in 70 min          | in 300 min        | dos Santos et al. 2018          |
| Alizarin yellow R   | Carbon  | Bio-electro-catalytic oxidation                | Dye loading rate 205.9 ± 10.8 g/m <sup>3</sup> , 480 min  | 97.5                   | 93.8              | Cui et al. 2014                 |
| Allura red AC       | BDD   | Photo-electro-Fenton                           | [Dye] <sub>0</sub> = 230 mg/L, 0.05 M Na <sub>2</sub> SO <sub>4</sub> , pH = 3.0, <i>j</i> = 100 mA/cm <sup>2</sup>   | 100 in 30–35 min       | 96–97 in 360 min  | Thiam et al. 2015b              |
| Brown HT            | BDD   | Photo-electro-Fenton                           | [Dye] <sub>0</sub> = 50–80 mg/L, 0.05 M Na <sub>2</sub> SO <sub>4</sub> , pH = 2.8–3.0, <i>j</i> = 71 mA/cm <sup>2</sup>  | 100 in 40 min          | 80 in 60 min      | Corona-Bautista et al. 2021     |
| Acid black 1        | BDD   | Electro-Fenton                                 | [Dye] <sub>0</sub> = 62 mg/L, 0.05 M Na <sub>2</sub> SO <sub>4</sub> , pH = 3.0, 0.1 mM Fe <sup>2+</sup> , applied current 300 mA   | 100 in 10 min          | 98 in 120 min     | Afanga et al. 2021              |
| Acid yellow 25      | Ti/Ru <sub>0.3</sub> Ti <sub>0.7</sub> O <sub>2</sub>                           | Anodic oxidation                               | [Dye] <sub>0</sub> = 253 mg/L, pH = 7, 0.05 M NaCl, <i>j</i> = 80 mA/cm <sup>2</sup>  | 100 in 10 min          | 60 in 60 min      | Sandoval et al. 2019            |
| Cibacron® marine FG | Sb-SnO <sub>2</sub>   | Anodic oxidation                               | [Dye] <sub>0</sub> = 30 mg/L, <i>j</i> = 30 mA/cm <sup>2</sup> , flow rate 11.11 cm <sup>3</sup> /s, 900 cm <sup>3</sup> and 24 ± 2 °C  | 77.8 – 95.5 in 210 min | –                 | Da Silva et al. 2014            |
| Acid red 3R         | Ti/RuO <sub>2</sub> -IrO <sub>2</sub>   | Electro-Fenton                                 | applied voltage of 20.0 V, pH = 3.0, airflow of 0.24 m <sup>3</sup> /h  | 77.2 in 100 min        | –                 | Yue et al. 2014                 |
| Acid orange 7       | TiO <sub>2</sub> -RuO <sub>2</sub> /Ti electrodes modified with WO <sub>3</sub> | Photo-electro-catalytic                        | [Dye] <sub>0</sub> = 200 mg/L, 0.1 M Na <sub>2</sub> SO <sub>4</sub> , <i>j</i> = 0.01 A/cm <sup>2</sup> , ultraviolet and visible light irradiation  | –                      | 98.63 in 120 min  | Kusmierk and Chrzescjanska 2015 |
| Methyl orange       | TiO <sub>2</sub> nanotubes  | Photo-electro-catalytic                        | [Dye] <sub>0</sub> = 20 mg/L, 0.1 M Na <sub>2</sub> SO <sub>4</sub> , light intensity = 2.0 mW/cm <sup>2</sup> , applying bias potential of 0.6 V (vs. SCE), 200 W high-pressure mercury lamp | 90.6 in 300 min        | –                 | Zhao et al. 2009                |

BDD–boron-doped diamond; COD–chemical oxygen demand; [Dye]<sub>0</sub>–initial dye concentration; *j*–current density

various electrode materials, complete removal of color and chemical oxygen demand has been achieved only using the BDD anode, while residual chemical oxygen demand was in the solution treated with PbO<sub>2</sub> anode, and TiRuSnO<sub>2</sub> anode allows only partial oxidation (Labiadh et al. 2015). The use of heterostructures of various metal oxides as electrodes with additional treatment using ultrasound and UV light makes it possible to increase the efficiency of Methyl Orange oxidation due to the synergistic effect of various processes (He et al. 2010; Peng et al. 2013). Methyl Orange electrochemical oxidation on PbO<sub>2</sub> deposited on Ti/SnO<sub>2</sub>-Sb substrate and doped with P25-TiO<sub>2</sub> has been studied (Xu et al. 2013a). In this case, a synergistic effect was observed between electrochemical oxidation and photo-catalysis on P25-TiO<sub>2</sub> under UV light irradiation. The same synergistic effect was also observed for the composite electrode based on TiO<sub>2</sub> and BDD (Pacheco-Álvarez et al. 2018). PbO<sub>2</sub> nanospheres deposited on SnO<sub>2</sub> nanowires and deposited on a titanium substrate (PbO<sub>2</sub> nanospheres @ SnO<sub>2</sub> nanowires/Ti) also indicated high efficiency of Methyl Orange oxidation. During 60 min of electrolysis, chemical oxygen demand decreased by 92.7% at 25 °C and pH 5.0 under a current density of 15 mA/cm<sup>2</sup> (Li et al. 2014b).

The anode material plays a vital role in Acid Orange 7 electrochemical oxidation. When BDD is used as the anode, complete decolorization of the Acid Orange 7 solution and chemical oxygen demand removal by more than 90% were observed (Fernandes et al. 2004). When comparing the activity of platinum and BDD anodes, BDD shows a higher rate of Acid Orange 7 mineralization with the formation of end oxidation products such as CO<sub>2</sub> and inorganic ions such as sulfate, nitrate, and ammonium (Hammami et al. 2008; Zhang et al. 2014a). At the same time, it can be noted that Acid Orange 7 oxidation on BDD leads to the formation of polymer intermediates at low pH values (Chen and Chen 2006). The formation of inorganic compounds as end products of Acid Orange 7 oxidation also occurs when PbO<sub>2</sub> is used as the anode. The PbO<sub>2</sub> anode modified with neodymium and cerium also shows a high efficiency upon Acid Orange 7 oxidation (Qiao et al. 2018).

Comparison of SnO<sub>2</sub>-Sb, PbO<sub>2</sub>-F, and BDD anodes showed that a higher decolorization rate was obtained using the SnO<sub>2</sub>-Sb and PbO<sub>2</sub>-F anodes in dilute Acid Orange 7 solutions, while a higher rate of chemical oxygen demand removal from concentrated Acid Orange 7 solutions was obtained using BDD and SnO<sub>2</sub>-Sb electrodes (Mao et al. 2008). Ti/SnO<sub>2</sub>-Sb doped with titanium nitride (TiN) nanoparticles also had a higher Acid Orange 7 decolorization efficiency than Ti/Sb-SnO<sub>2</sub> (Duan et al. 2014). It was found that BDD was much more active than Ti/Sb<sub>2</sub>O<sub>5</sub>-SnO<sub>2</sub> electrodes during Acid Orange 7 oxidation (Chen et al. 2003). Ta<sub>2</sub>O<sub>5</sub> coating is an effective method for improving surface morphology and electrochemical characteristics of Ti/TiO<sub>2</sub>/

PbO<sub>2</sub> nanotubes. The degradation efficiency of Acid Orange 7 and total organic carbon removal using the Ti/TiO<sub>2</sub> NT/Ta<sub>2</sub>O<sub>5</sub>-PbO<sub>2</sub> anode was almost 100 and 98.3%, respectively, compared to the Ti/PbO<sub>2</sub> anode at the same electrical charge consumption 3 A·h/L (Gui et al. 2019). When TiO<sub>2</sub>-modified β-PbO<sub>2</sub> was used as the anode material in photo-electrocatalysis, the maximum efficiency of Acid Orange 7 removal was reached at pH of 2.29 (Li et al. 2006a). In this case, Acid Orange 7 was oxidized due to the formation of hydroxyl radicals and direct electron transfer, as well as the hole generation on TiO<sub>2</sub> upon UV light irradiation (Li et al. 2006b, 2014a).

The use of spent activated carbon (resulted from adsorption of wastewater with heavy metals) for electrochemical decolorization of the Acid Orange 7 solution in the presence of peroxydisulfate is reported by Li et al. (2016). Granular activated carbon electrode is able to decompose peroxy-monosulfate and peroxydisulfate, which leads to the formation of sulfate radicals (SO<sub>4</sub><sup>·-</sup>) and ·OH (Li et al. 2017a). Catalysts based on iron and cobalt supported by mesoporous silica lead to an increase in electrochemical activation of peroxydisulfate with the formation of SO<sub>4</sub><sup>·-</sup>, which leads to effective chemical oxygen demand and total organic carbon removals from the solution of Orange II (Cai et al. 2014). The same effect on Acid Orange 7 electrochemical oxidation by peroxydisulfate is also observed in the presence of Fe<sub>3</sub>O<sub>4</sub> (Lin et al. 2014). Activated carbon fiber can be used as an in situ regenerated cathode-adsorbent during Acid Orange 7 electrochemical oxidation in the presence of Fe<sup>3+</sup> ions and peroxy-monosulfate. The azo dye adsorbed on the cathode surface is able to completely degrade and mineralize the dye, leading to an in situ regeneration of the adsorbent (Sun et al. 2020).

Acid Orange 7 electrochemical oxidation is promoted by the presence of chlorides in the solution. The formation of active chlorine contributes to faster indirect oxidation of the dye molecules. The degree of total organic carbon removal using Ti/RuO<sub>2</sub>-Pt electrode was 79.48% with complete decolorization of the solution (Zhang et al. 2014b). In chloride-containing solutions, decolorization proceeds faster upon increasing chloride concentration, but complete mineralization of Acid Orange 7 is not achieved when anodes with low oxygen over-potential are used (Scialdone et al. 2014). A more considerable chemical oxygen demand decrease for Acid Orange 7 solutions is observed using BDD (Scialdone et al. 2014).

Acid Orange 10 electrochemical oxidation has been studied using various electrode materials and approaches (Radha et al. 2012; Lounis et al. 2016; Hamous et al. 2020, 2021). In particular, Acid Orange 10 degradation on a platinum electrode was studied in detail by Hamous et al. (2020). The mechanism of Acid Orange 10 oxidation in chloride and sulfate electrolytes differs. The presence of chlorides in the



solution leads to accelerated oxidation of Acid Orange 10 molecules, just as for other azo dyes, which is associated with the formation of hypochlorite ions and indirect oxidation of the azo dye. Non-active electrodes, such as Ti/SnO<sub>2</sub>-Sb (Sarafraz et al. 2015) and Ti/PbO<sub>2</sub> (Bonyadinejad et al. 2016), are able to produce hydroxyl radicals through water oxidation. Under optimal electrolysis conditions, complete decolorization of the dye solution was achieved, and chemical oxygen demand/total organic carbon removal was 61.3/43.9% for Ti/SnO<sub>2</sub>-Sb and 63/60% for Ti/PbO<sub>2</sub>, respectively (Sarafraz et al. 2015; Bonyadinejad et al. 2016). Modification of the Ti/SnO<sub>2</sub>-Sb<sub>2</sub>O<sub>5</sub>-RuO<sub>2</sub> anode with tantalum improves electro-catalytic properties during Acid Orange 10 oxidation due to an increase in the ability to generate ·OH (Zhao et al. 2022). Only partial Acid Orange 10 oxidation was observed on a titanium anode coated with IrO<sub>2</sub>/TaO<sub>2</sub>/RuO<sub>2</sub> (Muthukumar et al. 2007). Ti/TiO<sub>2</sub>-based semiconductor anodes enable the oxidation of Acid Orange 10 upon UV light irradiation (Xie and Li 2006). In this case, the dye oxidation can occur through photo-electro-catalysis, electro-oxidation, and electro-Fenton processes.

Among the studied anode materials, BDD was proved to be the most potent anode for Acid Red 27 oxidation because of high oxygen over-potential and the formation of hydroxyl radicals slightly adsorbed on its surface, as compared to Pt (Jain et al. 2009) and PbO<sub>2</sub> (Elaissaoui et al. 2016, 2019). On the other side, anode materials such as Ti/IrO<sub>2</sub>-Ta<sub>2</sub>O<sub>5</sub> (Fajardo et al. 2016), IrO<sub>2</sub>-Ru<sub>2</sub>O-SnO<sub>2</sub>-TiO<sub>2</sub>/Ti, Ru<sub>2</sub>O-SnO<sub>2</sub>-TiO<sub>2</sub>/Ti (Salazar-Gastélum et al. 2013) and Ti/Pt-SnSb (Fajardo et al. 2017) are preferred as anodes in Acid Red 27 oxidation due to their relatively low cost, even though the dye oxidation efficiency is lower as compared to BDD (Fajardo et al. 2016).

Methyl Red electrochemical oxidation was studied by different groups (Panizza and Cerisola 2007; Santos et al. 2020a, b). It was noted that the degree of chemical oxygen demand removal depended on the anode material and decreased in the following order: Si/BDD > Ti/PbO<sub>2</sub> > Pt > Ti/Ti<sub>0.50</sub>Ru<sub>0.45</sub>Sn<sub>0.05</sub>O<sub>2</sub> (Panizza and Cerisola 2007). Under the optimal conditions, the electro-Fenton process (Zhou et al. 2008) led to decolorization of the solution with a concentration of 20 mg/L in 20 min, while at a higher dye concentration (100 mg/L) only 74% decolorization was achieved. In addition, Methyl Red electrochemical oxidation was studied using other anode materials such as PbO<sub>2</sub> and BDD (Panizza and Cerisola 2008), Ti/Ru<sub>0.34</sub>Ti<sub>0.66</sub>O<sub>2</sub> (Morais et al. 2013), RuO<sub>2</sub>-IrO<sub>2</sub>-TiO<sub>2</sub> (Sathishkumar et al. 2017), Zn(OH)<sub>2</sub> and ZnO thin films (Ahmad et al. 2022). Its oxidative degradation was also carried out by electro-Fenton process oxidation along with the generation of active chlorine species (Ma and Zhou 2009; Sathishkumar et al. 2017). Finally, Tavares et al. (2012) reported the electro-catalytic activity of two anode materials, Ti/Ru<sub>0.3</sub>Ti<sub>0.7</sub>O<sub>2</sub> and

Ti/Pt, during direct and indirect electrochemical oxidation of Methyl Red with the determination of the resulting oxidation products.

Under optimal conditions, when PbO<sub>2</sub> is used as anode, continuous oxidation of the Acid Red 18 dye occurs, leading to the removal of 99.9% of the dye and 80.0% of chemical oxygen demand after 180 min of electrolysis (Rahmani et al. 2015). The electro-Fenton process is a relatively fast and efficient method for Acid Red 18 removal from industrial wastewater (Malakootian and Moridi 2017). Complete mineralization is achieved after 15 min of electrolysis using heterogeneous catalysts such as magnetite (Fe<sub>3</sub>O<sub>4</sub>) and hematite (Fe<sub>2</sub>O<sub>3</sub>) (Ben Hafaiedh et al. 2020). Simultaneous ozone exposure and electrochemical oxidation synergistically affect Acid Red 18 removal from aqueous solutions (Parsa et al. 2014). Table 4 shows the results of processing Reactive Black 5 solutions using various electrode materials.

Electrochemical oxidation of Reactive Orange 16 azo dye was mainly carried out using BDD. A systematic study on the influence of various supporting electrolytes and various current densities on simultaneous ozone exposure and electrochemical oxidation synergistically affects Acid Red 18 removal from aqueous solutions of Reactive Orange 16 dye with BDD was made by Lanzoni Migliorini et al. (2017). A higher rate of Reactive Orange 16 oxidation was observed in the K<sub>2</sub>SO<sub>4</sub> solution at pH 10, which was associated with the effect of deprotonation of the dye molecule, which contributed to the destruction of the dye molecule, in particular, of the azo bond. In addition, a higher concentration of hydroxyl ions promoted the generation of hydroxyl radicals on BDD (Migliorini et al. 2011). Comparison of the efficiency of Reactive Orange 16 oxidation on Ti-Pt/β-PbO<sub>2</sub> and BDD using a filter-press reactor showed that BDD was more effective in decolorizing the solution than Ti-Pt/β-PbO<sub>2</sub>; complete decolorization was achieved by passing 1.0 Ah/L and 2.0 Ah/L, respectively. The presence of NaCl led to a decrease in the time for complete decolorization due to the electro-generation of active chlorine (Andrade et al. 2009).

The use of a platinum wire as an anode in Reactive Orange 16 oxidation showed lesser efficiency. After 4 h of electrolysis by chronoamperometry, the degree of decolorization of the dye solution was only 40% in an acidic medium and 18% in an alkaline medium (Aggadi et al. 2021). At the same time, 93% decolorization of the Reactive Orange 16 solution was achieved in a flow cell on a Pt electrode after 60 min at 2.2 V/SHE using 1.00 g/L NaCl as electrolyte (Gomes et al. 2011). A thin Pt film on a titanium substrate (Pt/Ti) (Gomes et al. 2009) and an anode based on platinum oxide (Mijin et al. 2015) also showed good efficiency in Reactive Orange 16 oxidation. For Pt electrode, a 93% decolorization was obtained after 60 min at 2.2 V/SHE using 0.017 M NaCl solution and 0.5 M H<sub>2</sub>SO<sub>4</sub> solution as an electrolyte. For Pt/Ti electrode, the color removal was 98%

**Table 4** Decolorization and chemical oxygen demand removal of Reactive Black 5 solution using various electrodes

| Anode material  | Type of process                           | Initial concentration | Current density               | Process parameters   | Color removal, % | COD TOC* removal, % | Reference                |
|---|---|-----------------------|-------------------------------|--|------------------|---------------------|--------------------------|
| Boron-doped diamond   | Anodic oxidation                          | 40 mg/L               | 1 mA/cm <sup>2</sup>          | 0.02 M Na <sub>2</sub> SO <sub>4</sub> , natural pH<br>100 mL/min, 40 min  | 97               | 51                  | Yavuz and Shahbazi 2012  |
| Reticulated vitreous carbon   | Electro-Fenton                            | 200 mg/L              | 20.6 mA/cm <sup>2</sup>       | 0.5 M Na <sub>2</sub> SO <sub>4</sub> , 23 °C,<br>flow rate 100 dm <sup>3</sup> /h,<br>90 min<br>[Fe <sup>2+</sup> ] ≥ 0.05 × 10 <sup>-3</sup> M | > 98             | 82                  | Vasconcelos et al. 2016a |
| RuO <sub>2</sub> /IrO <sub>2</sub> /TiO <sub>2</sub>                                    | Anodic oxidation                          | 300 mg/L              | 100 A/m <sup>2</sup>          | 0.008 M NaCl, 60 min   | 99               | 33<br>18*           | Jager et al. 2018        |
| Ti/RuO <sub>2</sub>   | Anodic oxidation in NaCl medium           | 40 mg/L               | 2.5 A/dm <sup>2</sup>         | 10 L/h, 0.1 M NaCl,<br>pH 10.6   | 100              | 74,05               | Raghu and Basha 2007     |
| Graphite  | Anodic oxidation                          | 70 mg/L               | –                             | 0.1 M Na <sub>2</sub> SO <sub>4</sub> , 3 h<br>0.4 L   | 100              | 95*                 | Rivera et al. 2011       |
| Ti/(RuO <sub>2</sub> ) <sub>0.8</sub> .(Sb <sub>2</sub> O <sub>3</sub> ) <sub>0.2</sub> | Anodic oxidation                          | 26.4–93.6 mg/L        | 0.62–12.38 mA/cm <sup>2</sup> | 0.0062–0.1238 M NaCl, 180 min  | 100              | 73.77               | Viana et al. 2018        |
| Ti/TiO <sub>2</sub> -RuO <sub>2</sub> -IrO <sub>2</sub>                                 | Three-dimensional electrochemical reactor | 25 mg/L               | 15 mA/cm <sup>2</sup>         | pH = 3, 60 min,<br>100 mg/L particle electrode   | 98.9             | 85.96               | Mengelizadeh et al. 2019 |
| Ti/Pt   | Indirect oxidation                        | 4 mg/L                | 571 A/m <sup>2</sup>          | pH 4.0,<br>[Ce(IV)] = 50 μM,<br>0.05 M Na <sub>2</sub> SO <sub>4</sub>   | 91.6             | 83.3*               | Feng et al. 2022         |

COD—chemical oxygen demand; TOC—total organic carbon

under the same conditions (Gomes et al. 2009). The use of thin-film TiO<sub>2</sub> electrodes led to the complete decolorization of the Reactive Orange 16 solution after 20 min of photoelectro-catalysis (Carneiro et al. 2004). The efficiency of Reactive Orange 7 oxidation in the flow mode was 90.91% (Basiri Parsa et al. 2015). Reactive Orange 7 oxidation was also studied using the C/PbO<sub>2</sub>, Pb + Sn/PbO<sub>2</sub> + SnO<sub>2</sub>, Pb/PbO<sub>2</sub> electrodes. At 25 °C and in the presence of 4 g/L NaCl, almost complete Reactive Orange 7 oxidation was achieved using these electrodes after 15 min (97.66%, 95.33, and 94.60% for C/PbO<sub>2</sub>, Pb + Sn/PbO<sub>2</sub> + SnO<sub>2</sub> and Pb/PbO<sub>2</sub> electrodes, respectively) at pH of 2.54 and current density of 25 mA/cm<sup>2</sup> (Ghalwa et al. 2012).

Using a titanium electrode modified with ZnO and carbon nanotubes, the maximum efficiency of Reactive Orange 7 oxidation for the dye mixture removal was only 25.9% (Mahmoudian et al. 2021), while using Ti/nano ZnO–CuO under optimal conditions, the color decreased by 99.16% and chemical oxygen demand by 66.66% after 60 min of electrolysis (Akbari et al. 2022). Complete oxidation of Reactive Orange 107 (RO107) azo dye using composite electrode materials Ce<sub>0.8</sub>Gd<sub>0.2</sub>O<sub>2</sub>, Ce<sub>0.8</sub>Nd<sub>0.2</sub>O<sub>2</sub> and Ce<sub>0.8</sub>Sm<sub>0.2</sub>O<sub>2</sub> was also reported (Rajkumar et al. (2015). Results obtained for

the electrochemical oxidation of some reactive azo dyes are given in Table 5.

Electrochemical oxidation of Congo Red was studied using BDD (Jalife-Jacobo et al. 2016), Pb/PbO<sub>2</sub> (Chen et al. 2021), graphite (Kaur and Kaur 2016), Ti/RuO<sub>2</sub>-IrO<sub>2</sub> (Sathishkumar et al. 2019), multiwalled carbon nanotubes—MnO<sub>2</sub>/Ni (Zhu and Chen 2021) and polyaniline-/graphene-modified anode (Li et al. 2022). Complete removal of total organic carbon during oxidation of direct azo dyes requires long electrolysis time, which is associated with the formation of a larger number of aromatic fragments produced upon breaking the –N=N– bond (Faouzi et al. 2006; Shetti et al. 2019). During Congo Red oxidation using BDD, a qualitative analysis by spectrophotometry showed different behaviors of Congo Red molecules during ozonation and electrochemical degradation. During ozonation, a rapid decolorization of the solution was observed, while the color remained until the end of the galvanostatic electrolysis. This is due to the difference in the oxidation mechanisms of the two processes. Simultaneous degradation of azo groups and subsequent degradation during electrochemical oxidation using BDD with complete removal of chemical oxygen

**Table 5** Parameters of electrochemical decolorization and chemical oxygen demand removal of some azo dyes solutions

| Name of the dye     | Electrode material  | Type of process   | Processing parameters  | Color removal, % | COD, TOC*, % | References                   |
|---------------------|---|---|--|------------------|--------------|------------------------------|
| Reactive yellow HF  | BDD   | Electro-Fenton  | [Dye] <sub>0</sub> = 300 mg/L, 0.05 M Na <sub>2</sub> SO <sub>4</sub> , pH 3, flow rate 4 L/min, <i>j</i> = 80 mA/cm <sup>2</sup> , 100 min      | 98               | –            | Bedolla-Guzman et al. 2017   |
| Reactive yellow 186 | Graphite  | Anodic oxidation  | pH = 3.9, 0.11 M NaCl, 18 min  | 99               | 73           | Rajkumar and Muthukumar 2017 |
| Procion black 5B    | Ti/RuO <sub>2</sub>   | Indirect oxidation with the generation of active chlorine | [COD] <sub>0</sub> = 1264, <i>j</i> = 2.5 A/dm <sup>2</sup> , flow rate 10 L/h, 0.017–0.068 M NaCl   | 100              | 74.05        | Raghu and Basha 2007         |
| Procion blue X      | Ti/RuO <sub>2</sub>   | Photo-electrochemical oxidation                           | [Dye] <sub>0</sub> = 50 mg/L, pH 2.3, 20 mL/min, <i>j</i> = 2.0 A/dm <sup>2</sup> , [TiO <sub>2</sub> ] = 40 mg/L                                | 100              | 96           | Neelavannan et al. 2007      |
| Reactive red 9      | Ti/RuO <sub>x</sub> -TiO <sub>x</sub>                       | Bio-electrochemical oxidation                             | [Dye] <sub>0</sub> = 100 mg/L, 0.08 M NaCl, pH = 12–13, <i>j</i> = 7.6 A/dm <sup>2</sup> , 3 h   | 97.9             | 80           | Senthilkumar et al. 2012     |
| Procion red MX-5B   | BDD   | Anodic oxidation  | [Dye] <sub>0</sub> = 100 mg/L, 0.035 M Na <sub>2</sub> SO <sub>4</sub> , <i>j</i> = 60 mA/cm <sup>2</sup> , 240 min                              | 100              | 100          | Cotillas et al. 2018         |
| Levafix blue CA     | Pt grid   | Electro-Fenton  | [Dye] <sub>0</sub> = 200 mg/L, 0.05 M Na <sub>2</sub> SO <sub>4</sub> , pH = 3.0, 0.5 mM Fe <sup>2+</sup> or Fe <sup>3+</sup>                    | 99               | 90           | El-Desoky et al. 2010a       |
| Reactive yellow 3   | Graphite  | Anodic oxidation  | [Dye] <sub>0</sub> = 50 mg/L, 0.05 M NaCl, <i>j</i> = 10 mA/cm <sup>2</sup>  | 99               | 88           | Majjaei et al. 2009          |
| Ruby F-2B           | Si/BDD  | Anodic oxidation  | [Dye] <sub>0</sub> = 20 mg/L, 0.12 M NaCl and 0.05 M Na <sub>2</sub> SO <sub>4</sub> , pH <sub>initial</sub> 6.2, 20 ± 2 °C, 15 min              | 100              | –            | Bogdanowicz et al. 2013      |
| Reactive black 8    | Ti/RuO <sub>2</sub> -IrO <sub>2</sub>                       | Sono-electrochemical oxidation                            | [Dye] <sub>0</sub> = 100 mg/L, 0.1 M NaCl, <i>j</i> = 31.7 mA/cm <sup>2</sup> , pH 5.4, ultrasound power 100 W/L, 90 min                         | 62.9             | 32.4         | Wu et al. 2012               |
| Reactive blue 194   | TiO <sub>2</sub> -NTs/Sb-SnO <sub>2</sub> /PbO <sub>2</sub> | Electro-catalytic oxidation                               | [Dye] <sub>0</sub> = 30 mg/L; 0.5 M Na <sub>2</sub> SO <sub>4</sub> , pH = 6.8; <i>j</i> = 100 mA/cm <sup>2</sup> , 30 min                       | 90               | 60*          | An et al. 2012               |
| Direct black 22     | Ti/TiO <sub>2</sub> /RuO <sub>2</sub>                       | Photo-stimulated electrochemical oxidation                | [Dye] <sub>0</sub> = 20 mg/L, 0.1 M Na <sub>2</sub> SO <sub>4</sub> , pressure 0.4 MPa   | 98               | –            | Isaev et al. 2012            |
|                     | TiO <sub>2</sub> nanotubes                                  | Photo-electrochemical oxidation                           | [Dye] <sub>0</sub> = 120 mg/L, 0.1 M Na <sub>2</sub> SO <sub>4</sub> , pH 6.9–7.3, <i>j</i> = 7.1 × 10 <sup>-3</sup> mA/cm <sup>2</sup> , 60 min | 74               | –            | Isaev et al. 2018            |

BDD—boron-doped diamond; COD—chemical oxygen demand; TOC—total organic carbon; [Dye]<sub>0</sub>—initial dye concentration; *j*—current density

demand and total organic carbon are assumed during ozonation (Faouzi Elahmadi et al. 2009). The better ability of  $\beta$ -PbO<sub>2</sub> to generate  $\cdot$ OH contributed to the Congo Red removal (68.62%) from its initial concentration of 20 mg/L and at current density of 8 mA cm<sup>-2</sup> for 20 min (Chen et al. 2021).

A comparative study of Direct Red 23 oxidation in aqueous solutions by electro-Fenton process using various anodes: carbon-graphite, Ti<sub>4</sub>O<sub>7</sub> Magneli phase, BDD and DSA, was reported by Titchou et al. (2021b). The highest total organic carbon removal efficiency was achieved using BDD anode at a current density of 5 mA/cm<sup>2</sup>. When treating a Direct Red 23 solution with an initial concentration of 60 mg/L, total organic carbon removal was about 86% at 6 h electrolysis and in the presence of NaCl and Na<sub>2</sub>SO<sub>4</sub> electrolytes. Using BDD anode led to the complete decolorization and 50.2% mineralization during electrochemical degradation of Direct Blue 71 dye operated in flow mode and under galvanostatic conditions, at a current density of 7.75 mA/cm<sup>2</sup> and a flow rate of 600 mL/min (Xu et al. 2022). The presence of chloride ions accelerated the oxidation of direct azo dyes (Kupferle et al. 2006; Jalife-Jacobo et al. 2016) including Congo Red (Jalife-Jacobo et al. 2016) and Direct Red 83 (Kupferle et al. 2006). Complete decolorization of the Direct Blue 71 triazo dye solution was achieved after 90 min of electrolysis with Pt anode, and complete mineralization occurred after 120 min in a laboratory electrochemical reactor (Parsa et al. 2009).

Electrochemical treatment is able to achieve almost complete chemical oxygen demand removal from wastewater with high current yield (Vaghela et al. 2005). When treating wastewater containing a mixture of active azo dyes by electrocoagulation in combination with electrochemical oxidation processes, in particular electro-Fenton process, complete removal of turbidity and color and 97% removal of total organic carbon were achieved. In this case, energy consumption for decolorization of wastewater was 0.45–1.5 kWh/kg of removed total organic carbon depending on the current density (Zazou et al. 2019).

Studies on the treatment of wastewater containing azo dyes have been carried out using various anode materials such as Ti/Pt (Wang et al. 2009), RuO<sub>2</sub>/IrO<sub>2</sub>/TaO<sub>2</sub> (Bhaskar Raju et al. 2009), graphite (Bhatnagar et al. 2014), Ti–Pt/ $\beta$ -PbO<sub>2</sub> and Ti/Ti<sub>0.7</sub>–Ru<sub>0.3</sub>O<sub>2</sub> (Aquino et al. 2014), BDD (Zhu et al. 2011), and Ti/RuO<sub>2</sub>/IrO<sub>2</sub> (Raghu et al. 2009). Notably, higher efficiency in chemical oxygen demand and total organic carbon removals were observed for metal oxide electrodes and BDD. The use of electrochemical process for oxidative degradation of organic azo dyes made it possible to bring the indices of wastewater to the standard level for its discharge into the environment without further treatment (Gallios et al. 2012).

## Factors controlling the performance of the electrochemical oxidation of azo dyes

Various factors, including pH, applied current or voltage, hydrogen peroxide generation rate (in the case of electro-Fenton process), electrode material, initial dye concentration, electrolyte type and concentration, electrode spacing and electrolysis time, affect the removal of azo dyes by electrochemical oxidation processes (Vasudevan and Oturan 2014; Nidheesh et al. 2018; Rodríguez-Narváez et al. 2021; Qiao and Xiong 2021; Sun et al. 2022). The transition to a more complex structure of the dye molecule led to a decrease in the rate of electrochemical decolorization. It was shown (Chen et al. 2020) that the degradation rate changed downward in the following series: fuchsine acid–Reactive Red 2–Acid Orange G–Alizarin Red–Acid Blue 92–Reactive Orange X–GN–Orange II–Reactive Blue 19. The use of the electro-Fenton process led to a significant acceleration of oxidation yield of reactive azine azo dyes. For example, the decrease in total organic carbon for Acid Red 2 during 3 h of electrolysis was 87% (Lei et al. 2015). The use of ultrasound also significantly enhanced electro-oxidation of reactive azo dyes (Somayajula et al. 2012).

Among reactive dyes, electrochemical oxidation of Reactive Orange 7 attracted the most attention of researchers. The effect of the initial dye concentration, solution pH, electrolyte concentration, and current density on the efficiency of Reactive Orange 7 removal using Ti/Sb–SnO<sub>2</sub> anode has been studied. Under the optimal conditions, complete decolorization was achieved after 5 min; chemical oxygen demand reduction was up to 70.3% after 90 min (Basiri Parsa et al. 2013). Depending on the type of anode and cathode materials, the type of process and the electrolyte, acid azo dye Acid Red 18 can be degraded due to a single or combined action: direct anodic oxidation, indirect (mediated) oxidation near the anode or in the bulk of the solution by the homogeneously generated  $\cdot$ OH and by indirect oxidation with active chlorine (Thiam et al. 2015a, 2016).

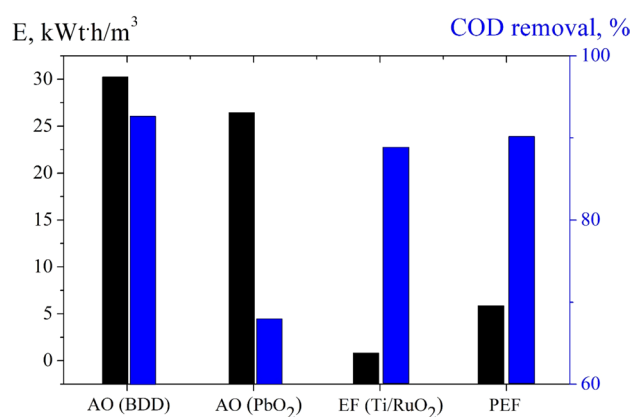
The efficiency of Methyl Orange removal from solutions by electrolysis is affected by current density, electrolyte concentration and solution pH (Oukili and Loukili 2019). Aeration of Methyl Orange solutions during electrochemical oxidation increases the process efficiency, which is associated with the formation of hydrogen peroxide on the cathode (Li et al. 2013b; Zhang et al. 2015). The introduction of halogen salts to the solution increased the rate of Methyl Red mineralization as follows: control < NaCl < NaBr < NaF. The use of a titanium plate anode led to the formation of an anatase film on its surface, which enhanced the Methyl Red oxidation due to the synergistic effect resulting from the combination of electrochemical oxidation and photo-catalysis on a titanium anode (Martín de Vidales et al. 2020).

Acid Orange 7 electrochemical degradation combined with a photo-catalytic process led to a higher dye conversion (Kusmieriek and Chrzescijanska 2015). The use of a  $\text{TiO}_2$  coating consisting of 29% rutile, 9% anatase and 62%  $\text{Ti}_7\text{O}_{13}$  on a stainless steel substrate as a photo-anode and an air-diffusion cathode to produce  $\text{H}_2\text{O}_2$  in a photo-electrochemical cell under sunlight irradiation resulted in the complete decolorization of the solution after 120 min under optimal conditions. The photo-anode made by immobilizing a  $\text{TiO}_2$  film on activated carbon fibers ( $\text{TiO}_2/\text{AC}$ ) was also used to remove Orange II (Hou et al. 2009). Good results were obtained during AO7 photo-electrochemical oxidation using a composite electrode made of exfoliated graphite and bismuth vanadate ( $\text{EG-BiVO}_4$ ) (Orimolade and Arotiba 2019).

Using different anode materials and different electrochemical cell design options, the effect of different operating parameters, such as the anode material (Oliver-Tolentino et al. 2014; Popli and Patel 2015; Sowmiya et al. 2016; Soni et al. 2017), solution pH (Yavuz and Shahbazi 2012; Radi et al. 2012), nature of the electrolyte (Sakalis et al. 2005; Rivera et al. 2011; Vasconcelos et al. 2016b), initial dye concentration (Navarro et al. 2010; Li et al. 2019), cathode material (Méndez-Martínez et al. 2012; Aveiro et al. 2018), current density (Singh et al. 2017; Koulini et al. 2022), electrode potential (Cerón-Rivera et al. 2004) and applied voltage (Jović et al. 2013), on the efficiency of Reactive Black 5 removal was optimized. Several authors noted that color removal, current efficiency, chemical oxygen demand and/or total organic carbon decrease, and specific energy consumption are mainly depend on the above parameters (Rao et al. 2006; Bansal et al. 2013; Jager et al. 2018; Mengelizadeh et al. 2019; Saxena and Ruparelia 2019). In addition, the structure of the reactive azo dye can also affect the oxidation efficiency, as reported during electrochemical oxidation of four reactive azo dyes (Reactive Orange 91, Reactive Red 184, Reactive Blue 182, and Reactive Black 5) using a Ti/Pt electrode (Sakalis et al. 2005).

Examples of reactive azo dyes containing azine rings are Reactive Orange 4 and Reactive Orange 13, which differ only in one substituent:  $-\text{OH}$  (Reactive Orange 4) or  $-\text{NH}_2$  (Reactive Orange 13). During oxidation using a Ti/Pt anode in a chloride-containing electrolyte, it was found that the active group had an effect on the solution decolorization efficiency. The presence of the  $-\text{NH}_2$  substituent ensured a higher decolorization rate than that of the  $-\text{OH}$  substituent (Gutiérrez-Bouzán and Pepió 2014). In this case, the dye concentration was the most significant factor in electrochemical oxidation of the both reactive dyes, Reactive Orange 4 and Reactive Orange 13 (Nordin et al. 2015; López-Grimau et al. 2018).

High energy consumption of the electrochemical method is one of the disadvantages, which prevents its large-scale application for wastewater treatment. Therefore, most studies



**Fig. 3** Energy consumption (E) and chemical oxygen demand (COD) removal of wastewater from textile industries at anodic oxidation on boron-doped diamond (AO (BDD)); anodic oxidation on  $\text{PbO}_2$  (AO ( $\text{PbO}_2$ )); by electro-Fenton process oxidation with use of  $\text{Ti/RuO}_2$  anode (EF ( $\text{Ti/RuO}_2$ )) and photo-electro-Fenton (PEF) process. The AO (BDD) process is the most effective for the COD removal, but this is accompanied by increased energy consumption. The most preferred type of electrochemical oxidation of azo dyes with efficiency of COD removal and low power consumption is PEF. The diagram is made according to the data given in Aquino et al. (2011), Hmani et al. (2012) Kaur et al. (2019) and Salazar et al. (2019)

on electrochemical oxidation of azo dyes have been carried out in laboratory conditions using individual dyes as model pollutants. However, it is essential to test the treatment of real wastewater from the textile industry, which is a complex system containing not only azo dyes, but also other related pollutants, as well as a large amount of suspended solid particles, pH varying over wide ranges, high temperature, chemical oxygen demand and various mineral salts (Chatzisyneon et al. 2006; Solís et al. 2012).

The efficiency of electrochemical treatment of real wastewater from the textile industry was evaluated in several works to determine the optimal process conditions (Fig. 3). For example, effluents from ink manufacturing contain a wide variety of pollutants such as dyes, surface-active materials, and solvents (Mukimin et al. 2017). Electrochemical oxidation of a mixture of dyes (Methylene Blue and Rhodamine B), solvents (monoethylene glycol, diethylene glycol, and glycerol), and surface-active materials (sodium dodecyl benzenesulfonate) has been studied using a single-chamber electrochemical flow cell with BDD as the anode and stainless steel as the cathode (Cañizares et al. 2007).

## Degradation products and their toxicity evolution during electrochemical oxidation

Toxicity reduction of dye solutions during the application of electrochemical technologies for removing azo dyes is of great importance. Degradation products of azo dyes such as

aromatic amines can be mutagenic and carcinogenic (Selvaraj et al. 2021). Evaluating the toxicity of azo dye solutions after treatment using an electrochemical approach is vital for their subsequent discharge into water bodies or its use for other purposes. Incomplete oxidation of the azo dyes or their intermediates may cause the toxicity of the solution to change slightly, and sometimes may increase it because of the formation of more toxic intermediate products (Xia et al. 2020).

The possibility of toxic chlorinated organic intermediates production during the indirect electrochemical oxidation (Jager et al. 2018), which are more harmful than the original azo dyes, is a drawback of the system. Evaluation of the phytotoxicity using *Vigna radiata* of the initial wastewater containing azo dyes and solutions after anodic oxidation with generation active chlorine species on Ti/IrO<sub>2</sub>-RuO<sub>2</sub>-TiO<sub>2</sub> anode with subsequent biological treatment led to the decrease of toxicity (Aravind et al. 2016). At the beginning of electrochemical oxidation on Fe-doped PbO<sub>2</sub>, toxicity of the treated Acid Orange 7 solution towards *Vibrio fischeri* slightly increases and then rapidly decreases to non-toxicity upon increasing electrolysis time (Xia et al. 2020). In the initial period of treatment of azo dyes by electrochemical oxidation, an increase in the toxicity of the solution was observed (Le et al. 2016). When Acid Orange 7 was oxidized by the electro-Fenton process, an increase in the toxicity up to 100% was noted, which was measured by observing the inhibition of marine bacteria *Vibrio fischeri*. This is due to the formation of intermediates like 1,4-benzoquinone and 1,2-naphthoquinone, which are more toxic than the initial dye. Further electrochemical treatment leads to complete mineralization and a decrease the toxicity (Le et al. 2016).

During electrochemical oxidation of azo dyes, first of all, the azo bond breaks and then benzene and naphthalene rings are gradually destroyed forming anthraquinone structures (Yang et al. 2014), which leads to the decolorization of the solution. Subsequently, the aromatic ring opening reaction results in the formation of aliphatic compounds (Fajardo et al. 2016). Sulfur in the diazo dye turned into SO<sub>4</sub><sup>2-</sup>, and nitrogen to NO<sub>3</sub><sup>-</sup> and/or NH<sub>4</sub><sup>+</sup> ions, and a part of N is removed from the solution as in the form of nitrogen-containing gaseous products (Antonin et al. 2015). The oxidation of azo dyes leads to the formation of various intermediates. For example, a total of 21 aromatic intermediates and 13 hydroxylated derivatives, including diazo, monoazo, biphenyl, benzene, naphthalene and phthalic acid, were identified as intermediate products formed during the electrochemical oxidation of Congo Red dye (Solano et al. 2015). Tartaric, tartronic, acetic, oxalic and oxamic acids were identified as end-products. Like in the case of Congo Red oxidation, electrochemical oxidations of Evans blue diazo dye led to the formation of 19 aromatic intermediates and 16 hydroxylated derivatives, including diazo, monoazo,

biphenyl, benzene, naphthalic, and phthalic acids (Antonin et al. 2015).

Both aromatic fragments and nontoxic carboxylic acids, such as maleic, fumaric, formic, and oxalic ones, were identified as products of electrochemical oxidation of the Methyl Orange using various methods (Márquez et al. 2020). The detection of ascorbic, benzoic, and citric acids, as well as hydroquinone and 1,4-benzoquinone, was also reported upon Methyl Orange oxidation using BDD as an anode (Guivarch et al. 2003; Isarain-Chávez et al. 2013). Various aromatic compounds and carboxylic acids are the primary intermediates during Acid Orange 7 dye oxidation (Table 6). Carboxylic acids such as maleic, tartronic, acetic, formic, oxalic, and oxamic were identified as products of Acid Orange 10 electrochemical oxidation, while ammonium and sulfate were the main inorganic ions (El-Ghenymy et al. 2014).

Up to 15 aromatic structures and carboxylic acids, including oxalic and formic acids, were identified as end products of Acid Red 14 electrochemical oxidation. Nitrates and sulfates were the main ions formed during carmoisine mineralization (Thiam et al. 2015c). Analysis of the products of Acid Red 27 oxidation by high-performance liquid chromatography coupled with mass spectroscopy showed the presence of naphthalenediol isomers in the solution of primary amines (Zhang et al. 2009). The resulting amines underwent further degradation, and phthalic acid, phthalic anhydride, benzoic acid, and phenol were found in the solution (Fig. 4). The next step involved OH electrophilic addition to the aromatic ring to form phenolic hydroxyl derivatives, which could be converted to aliphatic intermediates by opening the aromatic ring (Zhang et al. 2009).

During Acid Yellow 36 electrochemical degradation, oxalic, maleic, formic, fumaric and other carboxylic acids form as main end-products before mineralization (Ruiz et al. 2011). In another work, maleic and acetic acids were reported as the end-products of electrochemical oxidation, and the accumulation of SO<sub>4</sub><sup>2-</sup>, NO<sub>3</sub><sup>-</sup> and NH<sub>4</sub><sup>+</sup> ions has also been revealed (Aguilar et al. 2017). It was reported that Methyl Red solution decolorization and carboxylic acid degradation occur on Si/BDD and Pb/PbO<sub>2</sub> anodes (Santos et al. 2020b, a). Two intermediate compounds, 2-aminobenzoic acid and N,N'-dimethyl-p-phenylenediamine, are the main intermediate products of the first stage of Methyl Red oxidation due to breaking of the azo bond. Both aromatic compounds are colorless, upon subsequent degradation by hydroxylation and ring opening; they form aliphatic primary and secondary amines (Santos et al. 2020b, a). An analysis of inorganic ions that form during Methyl Red electrochemical oxidation shows that NO<sub>3</sub><sup>-</sup> and NO<sub>2</sub><sup>-</sup> ions are resulted from the splitting of the chromophore group (Morais et al. 2013). Evaluation of phyto-toxicity of the Methyl Red solution after electro-oxidation for 10 min shows 100% germination of *Vigna radiata* samples (Sathishkumar et al. 2017).

**Table 6** Intermediates of Acid Orange 7 degradation products formed during electrochemical processes and identified by various analytical methods

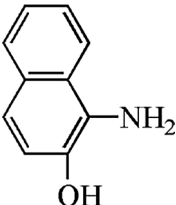

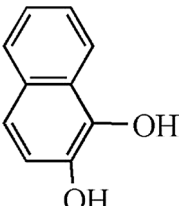
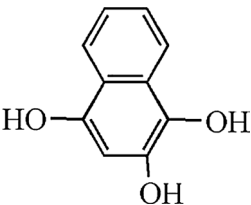
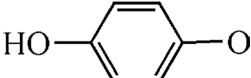
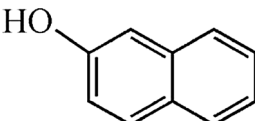
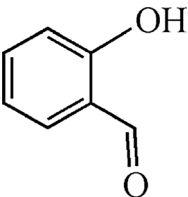
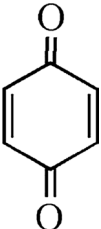
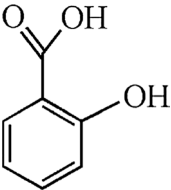
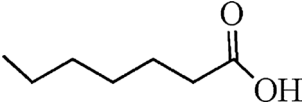
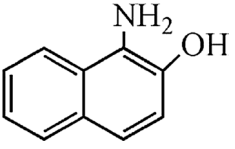
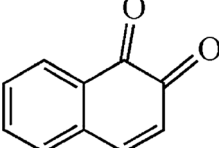
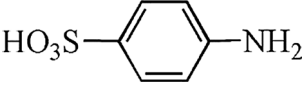
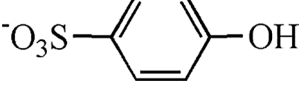
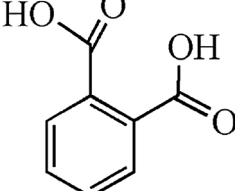
| Molecular formula                               | Name                        | Structure   | Electrolysis time | Electrolysis characteristics   | Detection method                     | References       |
|---|-----------------------------|---|-------------------|--|--------------------------------------|------------------|
| C <sub>10</sub> H <sub>9</sub> NO               | 1-Amino-2-naphthol          |    |                   |  |                                      |                  |
| C <sub>6</sub> H <sub>7</sub> NO <sub>3</sub> S | 4-Aminobenzenesulfonic acid |    | 10–30             | Fe-PbO <sub>2</sub> electrode<br>[Dye] <sub>0</sub> = 25–200 mg/L,<br>0.02–0.3 M<br>Na <sub>2</sub> SO <sub>4</sub> , pH = 3–11,<br>j = 10–40 mA/cm <sup>2</sup> | Gas chromatography–mass spectrometry | Xia et al. 2020  |
| C <sub>10</sub> H <sub>8</sub> O <sub>2</sub>   | Naphthalene-1,3-diol        |    |                   |  |                                      |                  |
| C <sub>10</sub> H <sub>8</sub> O <sub>3</sub>   | Naphthalene-1,2,4-triol     |   |                   |  |                                      |                  |
| C <sub>6</sub> H <sub>6</sub> O <sub>2</sub>    | <i>p</i> -Dihydroxybenzene  |  |                   |  |                                      |                  |
| C <sub>10</sub> H <sub>7</sub> OH               | 2-Naphthalenol              |  | 30                | Granular activated carbon electrode<br>[Dye] <sub>0</sub> = 300 mg/L,<br>0.02 M  | Gas chromatography–mass spectrometry | Zhao et al. 2010 |
| C <sub>7</sub> H <sub>6</sub> O <sub>2</sub>    | 2-Hydroxybenzaldehyde       |  | 30                |  |                                      |                  |
| C <sub>6</sub> H <sub>4</sub> O <sub>2</sub>    | <i>p</i> -Benzoquinone      |  | 60                | Na <sub>2</sub> SO <sub>4</sub> , pH = 3.0   |                                      |                  |

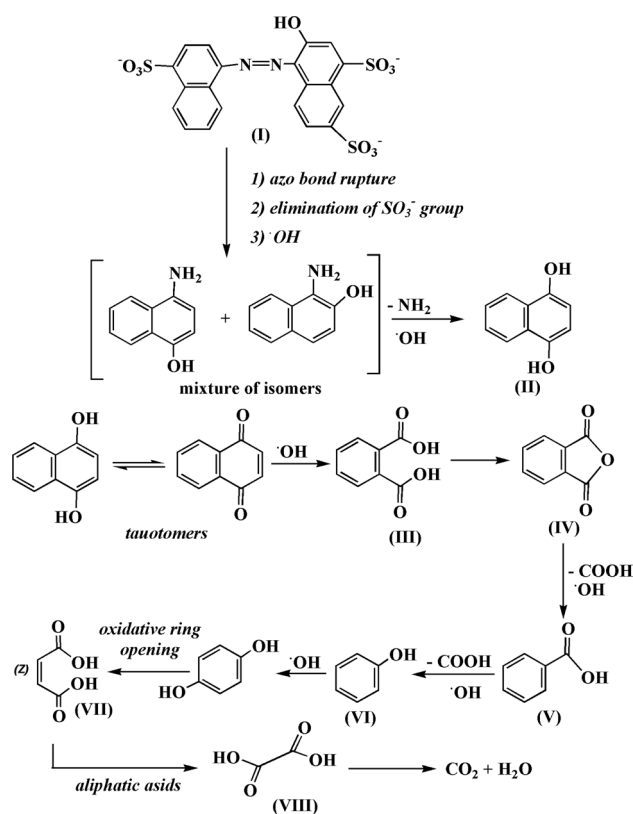
Table 6 (continued)

| Molecular formula                                 | Name                      | Structure   | Electrolysis time | Electrolysis characteristics   | Detection method                       | References          |
|---|---------------------------|---|-------------------|--|--|---------------------|
| C <sub>7</sub> H <sub>6</sub> O <sub>3</sub>      | Salicylic acid            |    | 120               |  |  |                     |
| C <sub>7</sub> H <sub>14</sub> O <sub>2</sub>     | Enanthic acid             |    | 180               |  |  |                     |
| C <sub>6</sub> H <sub>12</sub> O <sub>2</sub>     | Hexanoic acid             | CH <sub>3</sub> (CH <sub>2</sub> ) <sub>4</sub> COOH                                | 180               |  |  |                     |
| H <sub>2</sub> NC <sub>10</sub> H <sub>6</sub> OH | 1-Amino 2-naphthol        |    | 60                |  |  |                     |
| C <sub>10</sub> H <sub>6</sub> O <sub>2</sub>     | 1,2-naphthoquinone        |    | 30                | Boron-doped diamond anode<br>[Dye] <sub>0</sub> = 175 mg/L,<br>0.05 M Na <sub>2</sub> SO <sub>4</sub> ,<br>0.10 mM Fe <sup>2+</sup> ,<br>pH = 3.0, I = 60 mA | High-performance liquid chromatography | Hammami et al. 2008 |
| C <sub>6</sub> H <sub>7</sub> NO <sub>3</sub> S   | Sulfanilic acid           |   | 10                |  |  |                     |
| HOC <sub>6</sub> H <sub>4</sub> SO <sub>3</sub> H | 4-hydroxybenzenesulfonate |  | 5–10              |  |  |                     |
| C <sub>8</sub> H <sub>6</sub> O <sub>4</sub>      | Phthalic acid             |  | 50                |  |  |                     |

The presence of residual total organic carbon in acid azo dye solutions after electrolysis is associated with the formation of low molecular weight carboxylic acids, such as maleic, and amber acids, as intermediate and end oxidation products (Li et al. 2013a). Besides maleic acids, various aromatic compounds form as intermediate products of oxidation of acid azo dyes, which undergo degradation during further electrolysis. For example, 11 aromatic intermediates, 15 hydroxylated compounds, 13 desulfonated derivatives and 7 short linear carboxylic acids were identified as intermediates in AR1 oxidation using anodic oxidation-H<sub>2</sub>O<sub>2</sub>, electro-Fenton, and photo-electro-Fenton processes on Pt and BDD (Florenza et al. 2014). Ultimately, the complete mineralization of acid dyes led

to the formation of various inorganic ions such as NH<sub>4</sub><sup>+</sup>, NO<sub>3</sub><sup>-</sup>, NO<sub>2</sub><sup>-</sup>, and SO<sub>4</sub><sup>2-</sup> (Moreira et al. 2013; Thiam et al. 2015b; Afanga et al. 2021). Reactive Black 5 azo dye is resistant to biochemical oxidation under aerobic conditions, but can be removed under anaerobic conditions. However, Reactive Black 5 splitting leads to the formation of aromatic amines, which can be more toxic than the initial dye molecules (Yavuz and Shahbazi 2012). The Reactive Black 5 oxidation products are mainly identified using high-performance liquid chromatography and mass spectrometry. Electrochemical oxidation of this azo dye results in its gradual transformation into simpler molecules such as alkylsulfonylphenol derivatives. Electrochemical reduction and oxidation pathways of the Reactive Black 5





**Fig. 4** The proposed decomposition pathway for the electrochemical oxidation of amaranth dye (from solutions containing 100 mg/L analyte in 0.05 M  $K_2SO_4$  and adjusted to pH 12), using a boron-doped diamond anode and under 35 mA/cm<sup>2</sup> current density for 5 h: (I) amaranth dye,  $m/z=535$ ; (II) naphthalenediol,  $m/z=160$ ; (III) phthalic acid,  $m/z=166$ ; (IV) phthalic anhydride,  $m/z=158$ ; (V) benzoic acid,  $m/z=122$ ; (VI) phenol,  $m/z=94$ ; (VII) fumaric acid,  $m/z=116$ ; and (VIII) oxalic acid,  $m/z=90$ . Initially, the cleavage of the azo bond occurs with formation aromatic amines. In the next step, there is the elimination of sulfonic acid groups, followed by insertion of hydroxyl radical ( $\cdot OH$ ), forming a mixture of isomers (1,4 and/or 1,2-aminonaphthol). At this point occurs the  $NH_2$  elimination followed by insertion of  $\cdot OH$ , undergoes the naphthalenediol (II), this intermediate is in equilibrium keto-enolic (tautomers), and after addition of  $\cdot OH$  radical's phthalic acid is formed (III). The phthalic acid (III) converted into phthalic anhydride (IV) (internal cyclization) and subsequently into the benzoic acid (V), after decarboxylation and hydroxylation processes, and phenol (VI) is formed as a reactive intermediate, and after the addition of  $\cdot OH$  radicals, the fumaric acid (VII) is identified. At the last stage, the aromatic ring opening occurs and aliphatic acids, i.e., oxalic acid (VIII) is formation. Reprinted by permission from Barros et al. (2014). Copyright 2014, Elsevier

dye are described in the previous work (Méndez-Martínez et al. 2012).

Reactive azo dyes can contain azine rings, including triazines, which can lead to the formation of oxidation-resistant compounds during azo group destruction, in particular, cyanuric acid (2,4,6-tri-hydroxy-1,3,5-triazine), which is the end product of s-triazine oxidation (Goutailler et al. 2001). A product with a chemical structure close to

2-amino-1,5-naphthalenedisulfonic acid formed as an intermediate during the Reactive Orange 4 oxidation using Ti/SnO<sub>2</sub>-Sb-Pt (del Río et al. 2009, 2011). Electrochemical oxidation of chlorotriazine azo dyes Reactive Red 2 and Reactive Blue 81 using Ti/TiO<sub>2</sub>(70%)-RuO<sub>2</sub>(30%) anode under galvanostatic conditions led to the formation of substituted benzene rings, carboxylic acids, and hydrocarbons (Kusmieriek et al. 2011). 1-(3,6,8-Trihydroxy-1-naphthyl) urea, nitrobenzene, 1,4-benzoquinone, (3,6,8-trihydroxy-1-naphthyl) carbamic acid and phthalic acid were identified as intermediate products of Reactive Red 195 oxidation using Ti/SnO<sub>2</sub>-Sb/PbO<sub>2</sub> (Song et al. 2010).

The mechanism of oxidation of reactive azo dyes, as well as acid azo dyes, primarily involves breaking of the azo bond that leads to the decolorization of solution and the formation of the dye aromatic fragments. BDD can be singled out among the anode materials, which demonstrate good efficiency in the oxidation of reactive azo dyes (Bedolla-Guzman et al. 2017). During oxidation of Brilliant Yellow X-6G using BDD, the total organic carbon decreases by 72.8% after 2 h of electrolysis (Tang et al. 2020). Carboxylic acids are the main end products. For example, during the oxidation of Reactive Yellow 160 by anodic oxidation with generation of H<sub>2</sub>O<sub>2</sub>, electro-Fenton and photo-electro-Fenton processes, formation of maleic, fumaric, tartaric, acetic, oxalic, oxamic and formic acids was identified. These carboxylic acids were then completely oxidized until mineralization along with the formation of chloride, sulfate ions, ammonium ions, and, to a lesser extent, nitrate ions (Bedolla-Guzman et al. 2016).

## Reactors used for dye degradation

The electrochemical oxidation of azo dyes was carried out in various types of reactors and under various operating conditions. Details about the design of reactors for the electrochemical oxidation of organic compounds, particularly azo dyes, using a BDD anode are given in the review article authored by Cornejo et al. (2021). For electrochemical oxidation of Acid Red 27, reactors with a wide range of designs are used. Reactor design constitutes one of the aspects of increasing the performance of electrochemical processes (Fu et al. 2010; Pogacean et al. 2018; Chang et al. 2020). The use of traditional single-chamber electrolysis requires significant energy consumption, which depends on the anode material, current density and wastewater pH (Radha et al. 2009; Aquino et al. 2011). The use of BDD as the anode in electrochemical reactors for treating wastewater containing azo dyes leads to the maximum chemical oxygen demand removal. However, energy consumption for this electrode is higher, which is due to the oxidation of azo dyes at high anode potentials.

Reducing the inter-electrode space to 50  $\mu\text{m}$  can improve the operating costs (about 1  $\text{€}/\text{m}^3$ ) and total organic carbon removal during wastewater treatment without adding a background electrode when BDD is used as the anode (Ma et al. 2018). The presence of chloride ions in the solution and the formation of hydroxyl radicals during the electro-Fenton process can lead to a decrease in energy consumption with the same efficiency of chemical oxygen demand reduction (Kaur et al. 2019). Energy consumption for textile industry wastewater treatment was reduced by 25–40% by carrying out the process in a two-chamber electrolyzer and oxidizing dyes using the anode and cathode chambers (Raghu et al. 2009). In this type of reactors, hypochlorite ions forms in the anode chambers, and hydrogen peroxide forms in the cathode chamber (Bhaskar Raju et al. 2009).

In the case of indirect (mediated) oxidation, the azo dye removal occurs due to the formation of active chlorine (Szpyrkowicz et al. 2000). Research results showed that the solar photo-electro-Fenton process is the most economical for wastewater treatment (Salazar et al. 2019). Combining methods also makes it possible to reduce energy consumption for wastewater treatment. The electrochemical reactors type for photo-stimulation electrochemical oxidation has been reported in various works (Zainal et al. 2007; Aravind et al. 2018). Energy consumption in this case was about 29.8 and 39.5  $\text{Wh/g}$  of chemical oxygen demand removed during photo-stimulated electrochemical oxidation and electrochemical oxidation, respectively (Aravind et al. 2018). Different research groups (Zhu et al. 2011; Basha et al. 2011) have carried out experimental studies on wastewater containing azo dyes by combining electrochemical and biological methods using bio-electrochemical reactor. Biochemical oxidation can be used either as pretreatment or post-treatment of the electrochemical processing. The use of additional treatment, such as biological, with electrochemical oxidation provides a more complete mineralization and removal of toxicity for the treatment of azo dyes wastewater. An up-flow membrane-less bio-electrochemical system integrated with bio-contact oxidation was developed for degradation and/or mineralization of the Acid Orange 7 in wastewater (Pan et al. 2017). The schematic diagram of bio-electrochemical system integrated with bio-contact oxidation reactor is given in Fig. 5A.

Reactors for anodic oxidation processes with an electrochemical generation of  $\text{H}_2\text{O}_2$  (anodic oxidation- $\text{H}_2\text{O}_2$ ) were used for the oxidation of azo dyes (Peralta-Hernández and Godínez 2014; Ramírez-Pereda et al. 2019). Xu et al. (Xu et al. 2008) studied the oxidation of AO7 with electro-generation of hydrogen peroxide in a three-dimensional reactor (Fig. 5B). Granular activated carbon was used as the anode, and activated carbon fiber was used as the cathode in electrochemical reactors, which contributed to a higher hydrogen

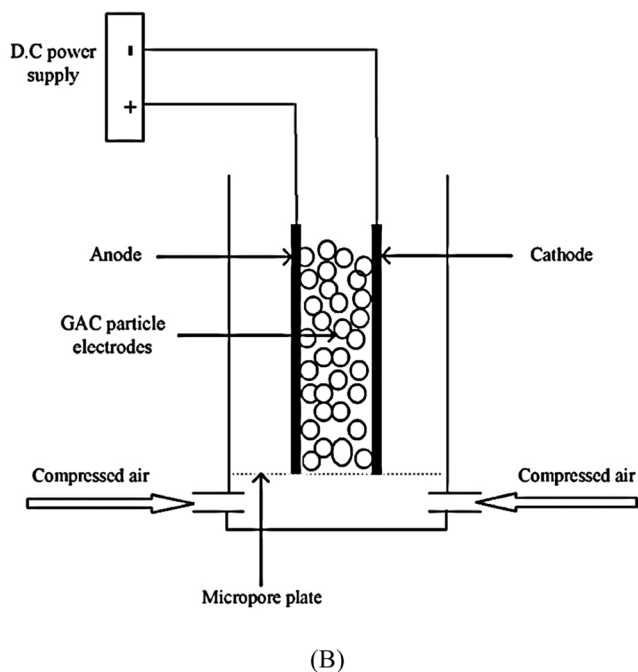
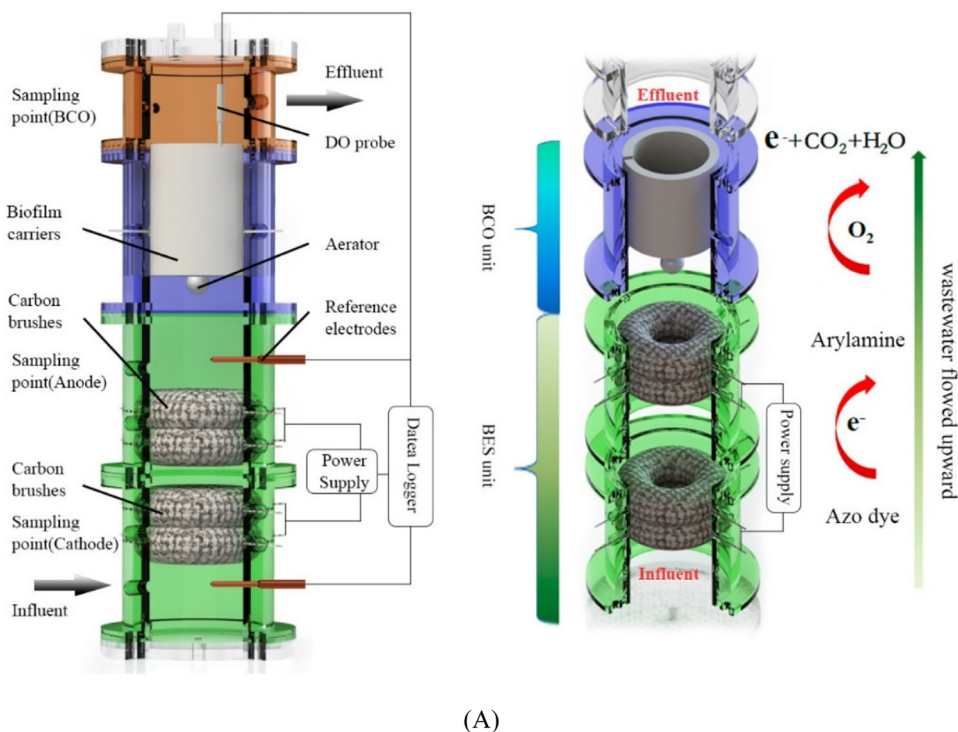
peroxide production yield. In the same way, Ramírez et al. (2016) used a carbon fabric cathode in the electrochemical reactor for the generation of  $\text{H}_2\text{O}_2$ . In reactors of this type, chemical oxygen demand removal up to 80%, total organic carbon removal up to 72%, and almost complete decolorization of the dye were achieved after 180 min of electrolysis. The use of granular activated carbon as the electrode led to the formation of aromatic intermediates at the initial stage of electrolysis. Then, these intermediates undertake ring-opening reactions and finally mineralized to  $\text{CO}_2$ ,  $\text{H}_2\text{O}$  and inorganic ions (Zhao et al. 2010; Li et al. 2017b).

Comparative degradation of the industrial azo dye Blue BR has been studied by the anodic oxidation, electro-Fenton and photo-electro-Fenton process using BDD anode in a laboratory stirred tank reactor. Based on chemical oxygen demand removal rate, an increasing relative oxidation power was established as follows: anodic oxidation < electro-Fenton < photo-electro-Fenton in agreement with their decolorization trend (Alcocer et al. 2018). The electrochemical oxidation of azo dye Acid Violet 7 was investigated using planar disk electrodes placed in an inlet–outlet (I–O) cylindrical reaction chamber. Two different I–O configurations were studied, one parallel and the other perpendicular to the electrodes. The effect of cell design on the hydrodynamic characteristics and efficiency of the reactors in terms of color and chemical oxygen demand removal was studied. The degradation results indicated that the color elimination was quite efficient regardless of the type of reactor used and its complete removal could be reached in less than 80 min at an applied current density of 30  $\text{mA}/\text{cm}^2$  and above. However, higher chemical oxygen demand removal efficiency was always achieved in the parallel I–O flow cell compared to perpendicular I–O flow reactor at all of the current densities studied, which can be attributed to the possibility of some stagnation in the lateral regions of the electrodes (Brito et al. 2018a).

## Conclusion

The use of electrochemical oxidation makes it possible to completely mineralize azo dyes of various classes. Efficient removal of azo dyes using electrochemical oxidation is achieved in many cases due to the formation of highly reactive hydroxyl radicals. Boron-doped diamond and  $\text{PbO}_2$  can be noted as non-active anode materials with high oxygen over-potential and high rate of the formation of heterogeneous hydroxyl radicals. In this aspect, preparation and study of new highly efficient anode materials for azo dye removal from wastewater are directions for future research. The use of indirect electrochemical oxidation due to the generation of hypochlorite ion,  $\text{O}_3$ ,  $\text{H}_2\text{O}_2$ , and other oxidizing agents

**Fig. 5** **A** Up-flow membrane-less bio-electrochemical system integrated with bio-contact oxidation reactor. The integrated bio-electrochemical system integrated with bio-contact oxidation reactor consists of two units, a bio-electrochemical system (BES) in the lower part and a bio-contact oxidation (BCO) unit in the upper part. The bio-cathodes and the bio-anodes fixed on the lower portion and upper portion of BES, respectively. Biofilm carriers made up of porous plastic fiber are used for supporting microbial growth in the aerobic reactor. Biofilm carriers tied to a ring-shaped frame installed in the upper BCO unit. Aerator was placed at the bottom of the ring-shaped frame in bio-contact oxidation unit to supply the oxygen for the growth of microbes on bio-carriers. The bio-electrochemical system integrated with bio-contact oxidation reactor was operated in a continuous mode. Reprinted with permission from Pan et al. (2017). **B** The three-dimensional electrode reactor is a cylindrical tank with the microporous plate attached to the lower part of the tank and used to support the particle electrode. Through the particle electrode dispersed the bubbles that arose formed the compressed air. The granular activated carbon packed between the cathode and anode to form a three-dimensional electrode. Three-dimensional electrode reactor, Xu et al. (2008). Copyright 2008, Elsevier. Copyright 2017, Elsevier



also attracts several researchers. The most promising processes for the degradation of azo dyes are electro-Fenton and photoelectro-Fenton processes, which can be implemented at relatively low energy consumption and have a high rate of COD and TOC removal efficiencies. In most cases, during electrochemical oxidation of azo dyes, low molecular weight organic compounds, particularly short-chain carboxylic acids, form as end-products. In some cases, complete

mineralization to inorganic compounds occurs depending on the anode materials and the method of electrochemical oxidation. The combination of the methods of electrochemical oxidation with other methods for removing azo dyes, such as biological treatment, adsorption, membrane filtration, photocatalysis, constitutes one of the promising research areas in the field of removing azo dyes from wastewater. Unfortunately, most of the studies on the electrochemical oxidation

of azo dyes were carried out in laboratory conditions using various azo dyes as model compounds. The effect of the azo dye structure on the efficiency of electrochemical oxidation using various approaches remains unclear. Therefore, the study on the mechanism of electrochemical oxidation of azo dyes depending on their structures is a challenging task. The combination of electrochemical oxidation with the generation of electric power is also one of the directions for further research, as this will allow to create an energy-independent technologies for wastewater treatment.

**Authors' contributions** A. B. Isaev, A. G. Magomedova contributed to conceptualization, methodology, validation, formal analysis, investigation, writing—original draft, visualization, data curation; N. S. Shabanov did conceptualization, methodology, validation, writing—review; P. V. Nidheesh done conceptualization, methodology, validation, writing—review and editing, supervision; M. A. Oturan performed conceptualization, methodology, validation, writing—review and editing, supervision.

**Funding** There is no funding received for this research.

**Availability of data and material** Availability of data and material is not applicable to this article as no new data were created or analyzed in this study.

## Declarations

**Conflicts of interest** The authors declare they have no financial interests.

**Ethics approval** This study does not require ethics approval.

**Consent to participate** Informed consents were obtained from all participants.

**Consent for publication** Consents were obtained from all authors for publication.

## References

- Abdessamad NEH, Akrouit H, Bousselmi L (2014) Comparative anodic oxidation on boron-doped diamond electrode of two different dyes: separately and mixed. *Desalin Water Treat* 52:1735–1744. <https://doi.org/10.1080/19443994.2013.812950>
- Afanga H, Zazou H, Titchou FE, El Gaayda J, Sopaj F, Akbour RA, Hamdani M (2021) Electrochemical oxidation of naphthol blue black with different supporting electrolytes using a BDD/carbon felt cell. *J Environ Chem Eng* 9:104498. <https://doi.org/10.1016/J.JECE.2020.104498>
- Aguilar ZG, Brillas E, Salazar M, Nava JL, Sirés I (2017) Evidence of fenton-like reaction with active chlorine during the electrocatalytic oxidation of acid yellow 36 azo dye with Ir-Sn-Sb oxide anode in the presence of iron ion. *Appl Catal B Environ* 206:44–52. <https://doi.org/10.1016/J.APCATB.2017.01.006>
- Ahmad AA, Al-Bataineh QM, Aljarrah IA, Telfah AD (2022) Electrochemical degradation of methyl red in zinc hydroxide and zinc oxide thin films, physical and chemical activation. *Mater Chem Phys* 280:125793. <https://doi.org/10.1016/j.matchemphys.2022.125793>
- Akbari N, Nabizadeh Chianeh F, Arab A (2022) Efficient electrochemical oxidation of reactive dye using a novel Ti/nanoZnO–CuO anode: electrode characterization, modeling, and operational parameters optimization. *J Appl Electrochem* 52:189–202. <https://doi.org/10.1007/S10800-021-01634-1>
- Akrouit H, Bousselmi L (2013) Water treatment for color and COD removal by electrochemical oxidation on boron-doped diamond anode. *Arab J Geosci* 6:5033–5041. <https://doi.org/10.1007/S12517-012-0706-3>
- Alagesan J, Jaisankar MS, Muthuramalingam S, Mousset E, Chellam PV (2021) Influence of number of azo bonds and mass transport limitations towards the elimination capacity of continuous electrochemical process for the removal of textile industrial dyes. *Chemosphere* 262:128381. <https://doi.org/10.1016/J.CHEMOSPHERE.2020.128381>
- Alcocer S, Picos A, Uribe AR, Pérez T, Peralta-Hernández JM (2018) Comparative study for degradation of industrial dyes by electrochemical advanced oxidation processes with BDD anode in a laboratory stirred tank reactor. *Chemosphere* 205:682–689. <https://doi.org/10.1016/J.CHEMOSPHERE.2018.04.155>
- Al-Degs Y, Khraisheh MAM, Allen SJ, Ahmad MN (2000) Effect of carbon surface chemistry on the removal of reactive dyes from textile effluent. *Water Res* 34:927–935. [https://doi.org/10.1016/S0043-1354\(99\)00200-6](https://doi.org/10.1016/S0043-1354(99)00200-6)
- Alimirzaeva ZM, Isaev AB, Shabanov NS, Magomedova AG, Kadiev MV, Kaviyarasu K (2019) Photoelectrocatalytic activity PbO<sub>2</sub> loaded highly oriented TiO<sub>2</sub> nanotubes arrays. *Mater Today Proc* 36:325–327. <https://doi.org/10.1016/j.matpr.2020.04.111>
- Almeida LC, Garcia-Segura S, Arias C, Bocchi N, Brillas E (2012) Electrochemical mineralization of the azo dye acid red 29 (Chromotrope 2R) by photoelectro-fenton process. *Chemosphere* 89:751–758. <https://doi.org/10.1016/J.CHEMOSPHERE.2012.07.007>
- Almeida LC, Silva BF, Zanoni MVB (2014) Combined photoelectrocatalytic/electro-Fenton process using a Pt/TiO<sub>2</sub> NTs photoanode for enhanced degradation of an azo dye: a mechanistic study. *J Electroanal Chem* 734:43–52. <https://doi.org/10.1016/J.JELECHEM.2014.09.035>
- Almomani F, Baranova EA (2012) Electro-oxidation of two reactive azo dyes on boron-doped diamond electrode. *Water Sci Technol* 66:465–471. <https://doi.org/10.2166/WST.2012.180>
- Almomani F, Baranova EA (2013) Kinetic study of electro-Fenton oxidation of azo dyes on boron-doped diamond electrode. *Environ Technol (United Kingdom)* 34:1473–1479. <https://doi.org/10.1080/09593330.2012.758644>
- Alsantali RI, Raja QA, Alzahrani AYA et al (2022) Miscellaneous azo dyes: a comprehensive review on recent advancements in biological and industrial applications. *Dye Pigment* 199:110050. <https://doi.org/10.1016/J.DYEPIG.2021.110050>
- An H, Cui H, Zhang W, Zhai J, Qian Y, Xie X, Li Q (2012) Fabrication and electrochemical treatment application of a microstructured TiO<sub>2</sub>-NTs/Sb–SnO<sub>2</sub>/PbO<sub>2</sub> anode in the degradation of C.I. Reactive Blue 194 (RB 194). *Chem Eng J* 209:86–93. <https://doi.org/10.1016/J.CEJ.2012.07.089>
- Andrade LS, Tasso TT, da Silva DL, Rocha-Filho RC, Bocchi N, Biaggio SR (2009) On the performances of lead dioxide and boron-doped diamond electrodes in the anodic oxidation of simulated wastewater containing the Reactive Orange 16 dye. *Electrochim Acta* 54:2024–2030. <https://doi.org/10.1016/j.electacta.2008.08.026>
- Antonin VS, Garcia-Segura S, Santos MC, Brillas E (2015) Degradation of Evans blue diazo dye by electrochemical processes based on Fenton's reaction chemistry. *J Electroanal Chem* 747:1–11. <https://doi.org/10.1016/j.jelechem.2015.03.032>

- Aquino JM, Pereira GF, Rocha-Filho RC, Bocchi N, Biaggio SR (2011) Electrochemical degradation of a real textile effluent using boron-doped diamond or  $\beta$ -PbO<sub>2</sub> as anode. *J Hazard Mater* 192:1275–1282. <https://doi.org/10.1016/j.jhazmat.2011.06.039>
- Aquino JM, Rocha-Filho RC, Ruotolo LAM, Bocchi N, Biaggio SR (2014) Electrochemical degradation of a real textile wastewater using  $\beta$ -PbO<sub>2</sub> and DSA® anodes. *Chem Eng J* 251:138–145. <https://doi.org/10.1016/j.cej.2014.04.032>
- Araújo KC, Oliveira GR, Fernandes NS, Zanta CL, Castro SSL, da Silva DR, Martínez-Huitle CA (2014) Electrochemical removal of synthetic textile dyes from aqueous solutions using Ti/Pt anode: role of dye structure. *Environ Sci Pollut Res* 21:9777–9784. <https://doi.org/10.1007/S11356-014-2918-4>
- Araújo KC, dos Santos EV, Nidheesh PV, Martínez-Huitle CA (2022) Fundamentals and advances on the mechanisms of electrochemical generation of persulfate and sulfate radicals in aqueous medium. *Curr Opin Chem Eng* 38:100870. <https://doi.org/10.1016/j.coche.2022.100870>
- Aravind P, Selvaraj H, Ferro S, Sundaram M (2016) An integrated (electro-and bio-oxidation) approach for remediation of industrial wastewater containing azo-dyes: understanding the degradation mechanism and toxicity assessment. *J Hazard Mater* 318:203–215. <https://doi.org/10.1016/J.JHAZMAT.2016.07.028>
- Aravind P, Selvaraj H, Ferro S, Neelavannan GM, Sundaram M (2018) A one-pot approach: oxychloride radicals enhanced electrochemical oxidation for the treatment of textile dye wastewater trailed by mixed salts recycling. *J Clean Prod* 182:246–258. <https://doi.org/10.1016/J.JCLEPRO.2018.02.064>
- Asghar A, Raman AAA, Daud WMAW (2015) Advanced oxidation processes for in-situ production of hydrogen peroxide/hydroxyl radical for textile wastewater treatment: a review. *J Clean Prod* 87:826–838
- Aveiro LR, Da Silva AGM, Candido EG et al (2018) Application and stability of cathodes with manganese dioxide nanoflowers supported on vulcan by fenton systems for the degradation of RB5 azo dye. *Chemosphere* 208:131–138. <https://doi.org/10.1016/J.CHEMOSPHERE.2018.05.107>
- Ayati A, Shahrak MN, Tanhaei B, Sillanpää M (2016) Emerging adsorptive removal of azo dye by metal–organic frameworks. *Chemosphere* 160:30–44. <https://doi.org/10.1016/j.chemosphere.2016.06.065>
- Bafana A, Devi SS, Chakrabarti T (2011) Azo dyes: past, present and the future. *Environ Rev* 19:350–370. <https://doi.org/10.1139/a11-018>
- Bakheet B, Yuan S, Li Z, Wang H, Zuo J, Komarneni S, Wang Y (2013) Electro-peroxone treatment of orange II dye wastewater. *Water Res* 47:6234–6243. <https://doi.org/10.1016/j.watres.2013.07.042>
- Bansal S, Kushwaha JP, Sangal VK (2013) Electrochemical treatment of reactive black 5 textile wastewater: optimization, kinetics, and disposal study. *Water Environ Res* 85:2294–2306. <https://doi.org/10.2175/106143013x13807328848414>
- Barrera H, Cruz-Olivares J, Frontana-Urbe BA, Gómez-Díaz A, Reyes-Romero PG, Barrera-Díaz CE (2020) Electro-oxidation–plasma treatment for azo dye carmoisine (Acid red 14) in an aqueous solution. *Materials* 13:1463. <https://doi.org/10.3390/MA13061463>
- Barros WRP, Steter JR, Lanza MRV, Motheo AJ (2014) Degradation of amaranth dye in alkaline medium by ultrasonic cavitation coupled with electrochemical oxidation using a boron-doped diamond anode. *Electrochim Acta* 143:180–187. <https://doi.org/10.1016/j.electacta.2014.07.141>
- Basha CA, Selvakumar KV, Prabhu HJ, Sivashanmugam P, Lee CW (2011) Degradation studies for textile reactive dye by combined electrochemical, microbial and photocatalytic methods. *Sep Purif Technol* 79:303–309. <https://doi.org/10.1016/J.SEPPUR.2011.02.036>
- Basiri Parsa J, Merati Z, Abbasi M (2013) Modeling and optimizing of electrochemical oxidation of C.I. Reactive orange 7 on the Ti/Sb–SnO<sub>2</sub> as anode via response surface methodology. *J Ind Eng Chem* 19:1350–1355. <https://doi.org/10.1016/J.JIEC.2012.12.039>
- Basiri Parsa J, Bahiraei M, Nabizadeh Chianeh F (2015) Application of response surface methodology for electrochemical oxidation of the C.I. reactive orange 7 using flow reactor with Ti/Sb–SnO<sub>2</sub> anode. *Desalin Water Treat* 57:20027–20036. <https://doi.org/10.1080/19443994.2015.1101712>
- Bassouini DG, Hamad HA, El-Ashtouky ESZ, Amin NK, Abd El-Latif MM (2017) Comparative performance of anodic oxidation and electrocoagulation as clean processes for electrocatalytic degradation of diazo dye acid brown 14 in aqueous medium. *J Hazard Mater* 335:178–187. <https://doi.org/10.1016/J.JHAZMAT.2017.04.045>
- Bedolla-Guzman A, Sirés I, Thiam A, Peralta-Hernández JM, Gutiérrez-Granados S, Brillas E (2016) Application of anodic oxidation, electro-fenton and UVA photoelectro-Fenton to decolorize and mineralize acidic solutions of reactive yellow 160 azo dye. *Electrochim Acta* 206:307–316. <https://doi.org/10.1016/J.ELECTACTA.2016.04.166>
- Bedolla-Guzman A, Feria-Reyes R, Gutierrez-Granados S, Peralta-Hernández JM (2017) Decolorization and degradation of reactive yellow HF aqueous solutions by electrochemical advanced oxidation processes. *Environ Sci Pollut Res* 24:12506–12514. <https://doi.org/10.1007/S11356-016-7286-9>
- Ben Hafaiedh N, Fourcade F, Bellakhal N, Amrane A (2020) Iron oxide nanoparticles as heterogeneous electro-fenton catalysts for the removal of AR18 azo dye. *Environ Technol* 41:2146–2153. <https://doi.org/10.1080/09593330.2018.1557258>
- Benkhaya S, El HS, El HA (2017) Classifications, properties and applications of textile dyes: a review. *Appl J Environ Eng Sci* 3:311–320
- Benkhaya S, M'rabet S, El Harfi A (2020) Classifications, properties, recent synthesis and applications of azo dyes. *Heliyon*. <https://doi.org/10.1016/j.heliyon.2020.e03271>
- Benkhaya S, M'rabet S, El Harfi A (2020) A review on classifications, recent synthesis and applications of textile dyes. *Inorg Chem Commun*. <https://doi.org/10.1016/j.inoche.2020.107891>
- Berradi M, Hsissou R, Khudhair M, Assouag M, Cherkaoui O, El Bachiri A, El Harfi A (2019) Textile finishing dyes and their impact on aquatic environs. *Heliyon*. <https://doi.org/10.1016/j.heliyon.2019.e02711>
- Bhaskar Raju G, Thalamadai Karuppiah M, Latha SS, Priya DL, Parvathy S, Prabhakar S (2009) Electrochemical pretreatment of textile effluents and effect of electrode materials on the removal of organics. *Desalination* 249:167–174. <https://doi.org/10.1016/j.desal.2008.08.012>
- Bhatia D, Sharma NR, Singh J, Kanwar RS (2017) Biological methods for textile dye removal from wastewater: a review. *Crit Rev Environ Sci Technol* 47:1836–1876. <https://doi.org/10.1080/10643389.2017.1393263>
- Bhatnagar R, Joshi H, Mall ID, Srivastava VC (2014) Electrochemical oxidation of textile industry wastewater by graphite electrodes. *J Environ Sci Heal Part A Toxic/hazardous Subst Environ Eng* 49:955–966. <https://doi.org/10.1080/10934529.2014.894320>
- Bogdanowicz R, Fabiańska A, Golunski L et al (2013) Influence of the boron doping level on the electrochemical oxidation of the azo dyes at Si/BDD thin film electrodes. *Diam Relat Mater* 39:122–127. <https://doi.org/10.1016/j.diamond.2013.08.004>
- Bokare AD, Choi W (2014) Review of iron-free Fenton-like systems for activating H<sub>2</sub>O<sub>2</sub> in advanced oxidation processes. *J Hazard*

- Mater 275:121–135. <https://doi.org/10.1016/j.jhazmat.2014.04.054>
- Bonyadinejad G, Sarafranz M, Khosravi M, Ebrahimi A, Taghavi-Shahri SM, Nateghi R, Rastaghi S (2016) Electrochemical degradation of the acid orange 10 dye on a Ti/PbO<sub>2</sub> anode assessed by response surface methodology. *Korean J Chem Eng* 33:189–196. <https://doi.org/10.1007/S11814-015-0115-X>
- Brillas E (2022) Fenton, photo-Fenton, electro-Fenton, and their combined treatments for the removal of insecticides from waters and soils A review. *Sep Purif Technol* 284:120290. <https://doi.org/10.1016/J.SEPPUR.2021.120290>
- Brillas E (2023) Solar photoelectro-Fenton: a very effective and cost-efficient electrochemical advanced oxidation process for the removal of organic pollutants from synthetic and real wastewaters. *Chemosphere* 327:138532. <https://doi.org/10.1016/J.CHEMOSPHERE.2023.138532>
- Brillas E, Garcia-Segura S (2023) Recent progress of applied TiO<sub>2</sub> photoelectrocatalysis for the degradation of organic pollutants in wastewaters. *J Environ Chem Eng* 11:109635. <https://doi.org/10.1016/j.jece.2023.109635>
- Brillas E, Martínez-Huitle CA (2015) Decontamination of wastewaters containing synthetic organic dyes by electrochemical methods. An updated review. *Appl Catal B Environ* 166:603–643. <https://doi.org/10.1016/j.apcatb.2014.11.016>
- Brillas E, Sirés I, Oturan MA (2009) Electro-Fenton process and related electrochemical technologies based on Fenton's reaction chemistry. *Chem Rev* 109:6570–6631. <https://doi.org/10.1021/cr900136g>
- Brito CN, Ferreira MB, de Moura Santos ECM, Léon JLL, Ganiyu SO, Martínez-Huitle CA (2018a) Electrochemical degradation of Azo-dye acid violet 7 using BDD anode: effect of flow reactor configuration on cell hydrodynamics and dye removal efficiency. *J Appl Electrochem* 48:1321–1330. <https://doi.org/10.1007/S10800-018-1257-4/FIGURES/8>
- Brito CN, Ferreira MB, de Oliveira Marcionilio SML, de Moura Santos ECM, Leon JLL, Ganiyu SO, Martínez-Huitle CA (2018) Electrochemical oxidation of acid violet 7 Dye by Using Si/BDD and Nb/BDD Electrodes. *J Electrochem Soc* 165:E250–E255. <https://doi.org/10.1149/2.1111805jes>
- Brüschweiler BJ, Küng S, Bürgi D, Muralt L, Nyfeler E (2014) Identification of non-regulated aromatic amines of toxicological concern which can be cleaved from azo dyes used in clothing textiles. *Regul Toxicol Pharmacol* 69:263–272. <https://doi.org/10.1016/j.yrtph.2014.04.011>
- Cai C, Zhang H, Zhong X, Hou L (2014) Electrochemical enhanced heterogeneous activation of peroxydisulfate by Fe–Co/SBA-15 catalyst for the degradation of orange II in water. *Water Res* 66:473–485. <https://doi.org/10.1016/j.watres.2014.08.039>
- Cañizares P, Louhichi B, Gadri A, Nasr B, Paz R, Rodrigo MA, Saez C (2007) Electrochemical treatment of the pollutants generated in an ink-manufacturing process. *J Hazard Mater* 146:552–557. <https://doi.org/10.1016/J.JHAZMAT.2007.04.085>
- Cao D, Wang Y, Zhao X (2017) Combination of photocatalytic and electrochemical degradation of organic pollutants from water. *Curr Opin Green Sustain Chem* 6:78–84. <https://doi.org/10.1016/J.COGSC.2017.05.007>
- Cao X, Wang H, Long X, Nishimura O, Li X (2021) Limitation of voltage reversal in the degradation of azo dye by a stacked double-anode microbial fuel cell and characterization of the microbial community structure. *Sci Total Environ* 754:142454. <https://doi.org/10.1016/J.SCITOTENV.2020.142454>
- Carneiro PA, Osugi ME, Sene JJ, Anderson M, Zanoni MVB (2004) Evaluation of color removal and degradation of a reactive textile azo dye on nanoporous TiO<sub>2</sub> thin-film electrodes. *Electrochim Acta* 49:3807–3820. <https://doi.org/10.1016/J.ELECTACTA.2003.12.057>
- Cerón-Rivera M, Dávila-Jiménez MM, Elizalde-González MP (2004) Degradation of the textile dyes basic yellow 28 and Reactive black 5 using diamond and metal alloys electrodes. *Chemosphere* 55:1–10. <https://doi.org/10.1016/J.CHEMOSPHERE.2003.10.060>
- Chatzisympson E, Xekoukoulotakis NP, Coz A, Kalogerakis N, Mantzavinos D (2006) Electrochemical treatment of textile dyes and dyehouse effluents. *J Hazard Mater* 137:998–1007. <https://doi.org/10.1016/J.JHAZMAT.2006.03.032>
- Chen X, Chen G (2006) Anodic oxidation of orange II on Ti/BDD electrode: variable effects. *Sep Purif Technol* 48:45–49. <https://doi.org/10.1016/J.SEPPUR.2005.07.024>
- Chen X, Chen G, Yue PL (2003) Anodic oxidation of dyes at novel Ti/B-diamond electrodes. *Chem Eng Sci* 58:995–1001. [https://doi.org/10.1016/S0009-2509\(02\)00640-1](https://doi.org/10.1016/S0009-2509(02)00640-1)
- Chen W, Li W, Liu F et al (2020) Microstructure of boron doped diamond electrodes and studies on its basic electrochemical characteristics and applicability of dye degradation. *J Environ Chem Eng* 8:104348. <https://doi.org/10.1016/J.JECE.2020.104348>
- Chen Z, Xie G, Pan Z, Zhou X, Lai W, Zheng L, Xu Y (2021) A novel Pb/PbO<sub>2</sub> electrodes prepared by the method of thermal oxidation-electrochemical oxidation: Characteristic and electrocatalytic oxidation performance. *J Alloys Compd* 851:156834. <https://doi.org/10.1016/J.JALLCOM.2020.156834>
- Chou WL, Wang CT, Chang CP (2011) Comparison of removal of acid orange 7 by electrooxidation using various anode materials. *Desalination* 266:201–207. <https://doi.org/10.1016/J.DESAL.2010.08.027>
- Chung KT (2016) Azo dyes and human health: a review. *J Environ Sci Heal Part C Environ Carcinog Ecotoxicol Rev* 34:233–261. <https://doi.org/10.1080/10590501.2016.1236602>
- Clematis D, Panizza M (2021) Application of boron-doped diamond electrodes for electrochemical oxidation of real wastewaters. *Curr Opin Electrochem* 30:100844. <https://doi.org/10.1016/J.COELEC.2021.100844>
- Comninellis C (1994) Electrocatalysis in the electrochemical conversion/combustion of organic pollutants for waste water treatment. *Electrochim Acta* 39:1857–1862. [https://doi.org/10.1016/0013-4686\(94\)85175-1](https://doi.org/10.1016/0013-4686(94)85175-1)
- Copaciu F, Opreș O, Coman V, Ristoiu D, Niinemets Ü, Copolovici L (2013) Diffuse water pollution by anthraquinone and azo dyes in environment importantly alters foliage volatiles, carotenoids and physiology in wheat (*Triticum aestivum*). *Water Air Soil Pollut*. <https://doi.org/10.1007/s11270-013-1478-4>
- Cornejo OM, Murrieta MF, Castañeda LF, Nava JL (2021) Electrochemical reactors equipped with BDD electrodes: Geometrical aspects and applications in water treatment. *Curr Opin Solid State Mater Sci* 25:100935. <https://doi.org/10.1016/J.COSSMS.2021.100935>
- Corona-Bautista M, Picos-Benítez A, Villaseñor-Basulto D, Bandala E, Peralta-Hernández JM (2021) Discoloration of azo dye Brown HT using different advanced oxidation processes. *Chemosphere* 267:129234. <https://doi.org/10.1016/J.CHEMOSPHERE.2020.129234>
- Costa CR, Montilla F, Morallón E, Olivi P (2009) Electrochemical oxidation of acid black 210 dye on the boron-doped diamond electrode in the presence of phosphate ions: effect of current density, pH, and chloride ions. *Electrochim Acta* 54:7048–7055. <https://doi.org/10.1016/J.ELECTACTA.2009.07.027>
- Cotillas S, Llanos J, Cañizares P, Clematis D, Cerisola G, Rodrigo MA, Panizza M (2018) Removal of procion red MX-5B dye from wastewater by conductive-diamond electrochemical oxidation. *Electrochim Acta* 263:1–7. <https://doi.org/10.1016/j.electacta.2018.01.052>

- Cruz-González K, Torres-López O, García-León A, Guzmán-Mar JL, Reyes LH, Hernández-Ramírez A, Peralta-Hernández JM (2010) Determination of optimum operating parameters for acid Yellow 36 decolorization by electro-Fenton process using BDD cathode. *Chem Eng J* 160:199–206. <https://doi.org/10.1016/j.cej.2010.03.043>
- Cui D, Guo YQ, Lee HS et al (2014) Efficient azo dye removal in bio-electrochemical system and post-aerobic bioreactor: optimization and characterization. *Chem Eng J* 243:355–363. <https://doi.org/10.1016/J.CEJ.2013.10.082>
- Cui D, Cui MH, Liang B, Liu WZ, Tang ZE, Wang AJ (2020) Mutual effect between electrochemically active bacteria (EAB) and azo dye in bio-electrochemical system (BES). *Chemosphere* 239:124787. <https://doi.org/10.1016/J.CHEMOSPHERE.2019.124787>
- Cui MH, Liu WZ, Tang ZE, Cui D (2021) Recent advancements in azo dye decolorization in bio-electrochemical systems (BESs): Insights into decolorization mechanism and practical application. *Water Res* 203:117512. <https://doi.org/10.1016/J.WATRES.2021.117512>
- da Costa Soares IC, da Silva DR, do Nascimento JHO, Garcia-Segura S, Martínez-Huitle CA (2017) Functional group influences on the reactive azo dye decolorization performance by electrochemical oxidation and electro-Fenton technologies. *Environ Sci Pollut Res* 24:24167–24176. <https://doi.org/10.1007/s11356-017-0041-z>
- Da Silva LM, Gonçalves IC, Teles JJS, Franco DV (2014) Application of oxide fine-mesh electrodes composed of Sb-SnO<sub>2</sub> for the electrochemical oxidation of cibacron marine FG using an SPE filter-press reactor. *Electrochim Acta* 146:714–732. <https://doi.org/10.1016/j.electacta.2014.09.070>
- de Almeida EJ, de Andrade AR, Corso CR (2019) Evaluation of the acid blue 161 dye degradation through electrochemical oxidation combined with microbiological systems. *Int J Environ Sci Technol* 16:8185–8196. <https://doi.org/10.1007/S13762-019-02377-5/FIGURES/4>
- de Moraes CC, da Silva AJC, Ferreira MB, de Araújo DM, Zanta CL, Castro SSL (2013) Electrochemical degradation of methyl red using Ti/Ru<sub>0.3</sub>Ti<sub>0.7</sub>O<sub>2</sub>: fragmentation of Azo group. *Electrocatalysis* 4:312–319. <https://doi.org/10.1007/S12678-013-0166-X>
- del Río AI, Molina J, Bonastre J, Cases F (2009) Study of the electrochemical oxidation and reduction of C.I. Reactive Orange 4 in sodium sulphate alkaline solutions. *J Hazard Mater* 172:187–195. <https://doi.org/10.1016/J.JHAZMAT.2009.06.147>
- del Río AI, Fernández J, Molina J, Bonastre J, Cases F (2011) Electrochemical treatment of a synthetic wastewater containing a sulphonated azo dye. Determination of naphthalenesulphonic compounds produced as main by-products. *Desalination* 273:428–435. <https://doi.org/10.1016/J.DESAL.2011.01.070>
- Deng F, Brillas E (2023) Advances in the decontamination of wastewaters with synthetic organic dyes by electrochemical Fenton-based processes. *Sep Purif Technol*. <https://doi.org/10.1016/J.SEPPUR.2023.123764>
- Deng D, Lamssali M, Aryal N, Ofori-Boadu A, Jha MK, Samuel RE (2020) Textiles wastewater treatment technology: a review. *Water Environ Res* 92:1805–1810. <https://doi.org/10.1002/WER.1437>
- Divyapriya G, Nidheesh PV (2020) Importance of graphene in the electro-fenton process. *ACS Omega* 5:4725–4732. <https://doi.org/10.1021/acsomega.9b04201>
- Divyapriya G, Nidheesh PV (2021) Electrochemically generated sulfate radicals by boron doped diamond and its environmental applications. *Curr Opin Solid State Mater Sci* 25:100921. <https://doi.org/10.1016/j.cossms.2021.100921>
- Divyapriya G, Singh S, Martínez-Huitle CA, Scaria J, Karim AV, Nidheesh PV (2021) Treatment of real wastewater by photoelectrochemical methods: An overview. *Chemosphere* 276:130188. <https://doi.org/10.1016/j.chemosphere.2021.130188>
- do Vale-Júnior E, Dosta S, Cano IG, Guilemany JM, Garcia-Segura S, Martínez-Huitle CA (2016) Acid blue 29 decolorization and mineralization by anodic oxidation with a cold gas spray synthesized Sn–Cu–Sb alloy anode. *Chemosphere* 148:47–54. <https://doi.org/10.1016/J.CHEMOSPHERE.2016.01.015>
- do Vale-Júnior E, da Silva DR, Fajardo AS, Martínez-Huitle CA (2018) Treatment of an azo dye effluent by peroxi-coagulation and its comparison to traditional electrochemical advanced processes. *Chemosphere* 204:548–555. <https://doi.org/10.1016/j.chemosphere.2018.04.007>
- dos Santos AJ, Martínez-Huitle CA, Sirés I, Brillas E (2018) Use of Pt and boron-doped diamond anodes in the electrochemical advanced oxidation of ponceau SS diazo dye in acidic sulfate medium. *ChemElectroChem* 5:685–693. <https://doi.org/10.1002/celec.201701238>
- dos Santos AJ, Brillas E, Cabot PL, Sirés I (2020) Simultaneous persulfate activation by electrogenerated H<sub>2</sub>O<sub>2</sub> and anodic oxidation at a boron-doped diamond anode for the treatment of dye solutions. *Sci Total Environ* 747:141541. <https://doi.org/10.1016/j.scitotenv.2020.141541>
- Duan Y, Wen Q, Chen Y, Guilemany JM, Garcia-Segura S, Martínez-Huitle CA (2014) Preparation and characterization of TiN-doped Ti/SnO<sub>2</sub>-Sb electrode by dip coating for Orange II decolorization. *Appl Surf Sci* 320:746–755. <https://doi.org/10.1016/J.APSUSC.2014.09.182>
- El Aggadi S, Kaichouh G, El Abbassi Z, Fekhaoui M, Hourch AE (2021) Electrode material in electrochemical decolorization of dyestuffs wastewater: a review. *E3S Web Conf* 234:00058. <https://doi.org/10.1051/e3sconf/202123400058>
- Elaissaoui I, Akrouit H, Grassini S, Fulginiti D, Bousselmi L (2016) Role of SiO<sub>x</sub> interlayer in the electrochemical degradation of Amaranth dye using SS/PbO<sub>2</sub> anodes. *Mater Des* 110:633–643. <https://doi.org/10.1016/J.MATDES.2016.08.044>
- Elaissaoui I, Akrouit H, Grassini S, Fulginiti D, Bousselmi L (2019) Effect of coating method on the structure and properties of a novel PbO<sub>2</sub> anode for electrochemical oxidation of Amaranth dye. *Chemosphere* 217:26–34. <https://doi.org/10.1016/J.CHEMOSPHERE.2018.10.161>
- El-Ashtoukhy ESZ, Amin NK, Abd El-Latif MM, Bassyouni DG, Hamad HA (2017) New insights into the anodic oxidation and electrocoagulation using a self-gas stirred reactor: a comparative study for synthetic C.I reactive violet 2 wastewater. *J Clean Prod* 167:432–446. <https://doi.org/10.1016/J.JCLEPRO.2017.08.174>
- El-Desoky HS, Ghoneim MM, El-Sheikh R, Zidan NM (2010a) Oxidation of Levafix CA reactive azo-dyes in industrial wastewater of textile dyeing by electro-generated Fenton's reagent. *J Hazard Mater* 175:858–865
- El-Desoky HS, Ghoneim MM, Zidan NM (2010b) Decolorization and degradation of Ponceau S azo-dye in aqueous solutions by the electrochemical advanced Fenton oxidation. *Desalination* 264:143–150. <https://doi.org/10.1016/J.DESAL.2010.07.018>
- El-Ghenymy A, Centellas F, Garrido JA, Rodríguez RM, Sirés I, Cabo PL, Brillas E (2014) Decolorization and mineralization of orange G azo dye solutions by anodic oxidation with a boron-doped diamond anode in divided and undivided tank reactors. *Electrochim Acta* 130:568–576. <https://doi.org/10.1016/J.ELECTACTA.2014.03.066>
- El-Kacemi S, Zazou H, Oturan N, Dietze M, Hamdani M, Es-Souni M, Oturan MA (2017) Nanostructured ZnO-TiO<sub>2</sub> thin film oxide as anode material in electrooxidation of organic pollutants. Application to the removal of dye amido black 10B from water. *Environ Sci Pollut Res* 24:1442–1449. <https://doi.org/10.1007/s11356-016-7920-6>

- Elkacmi R, Bennajah M (2019) Advanced oxidation technologies for the treatment and detoxification of olive mill wastewater: a general review. *J Water Reuse Desalin* 9:463–505. <https://doi.org/10.2166/wrd.2019.033>
- Eshaghzade Z, Pajootan E, Bahrami H, Arami M (2017) Facile synthesis of Fe<sub>3</sub>O<sub>4</sub> nanoparticles via aqueous based electro chemical route for heterogeneous electro-Fenton removal of azo dyes. *J Taiwan Inst Chem Eng* 71:91–105. <https://doi.org/10.1016/j.jtice.2016.11.015>
- Fajardo AS, Martins RC, Martínez-Huitle CA, Quinta-Ferreira RM (2016) Treatment of Amaranth dye in aqueous solution by using one cell or two cells in series with active and non-active anodes. *Electrochim Acta* 210:96–104. <https://doi.org/10.1016/J.ELECTACTA.2016.05.102>
- Fajardo AS, Martins RC, Silva DR, Quinta-Ferreira RM, Martinez-Huitle CA (2017) Electrochemical abatement of amaranth dye solutions using individual or an assembling of flow cells with Ti/Pt and Ti/Pt-SnSb anodes. *Sep Purif Technol* 179:194–203. <https://doi.org/10.1016/J.SEPPUR.2017.01.029>
- Fan L, Zhou Y, Yang W, Chen G, Yang F (2008) Electrochemical degradation of aqueous solution of Amaranth azo dye on ACF under potentiostatic model. *Dye Pigment* 76:440–446. <https://doi.org/10.1016/J.DYEPIG.2006.09.013>
- Fauzi M, Cañizares P, Gadri A et al (2006) Advanced oxidation processes for the treatment of wastes polluted with azoic dyes. *Electrochim Acta* 52:325–331. <https://doi.org/10.1016/J.ELECTACTA.2006.05.011>
- Fauzi Elahmadi M, Bensalah N, Gadri A (2009) Treatment of aqueous wastes contaminated with Congo Red dye by electrochemical oxidation and ozonation processes. *J Hazard Mater* 168:1163–1169. <https://doi.org/10.1016/J.JHAZMAT.2009.02.139>
- Feng J, Cerniglia CE, Chen H (2012) Toxicological significance of azo dye metabolism by human intestinal microbiota. *Front Biosci (elite Ed)* 4:568. <https://doi.org/10.2741/e400>
- Feng Z, Tian Q, Yang Q, Zhou Y, Zhao H, Zhao G (2021) Selectively photoelectrocatalytic reduction of oxygen to hydroxyl radical and singlet oxygen: mechanism and validation in coal wastewater. *Appl Catal B Environ* 286:119908. <https://doi.org/10.1016/J.APCATB.2021.119908>
- Feng L, Liu J, Guo Z et al (2022) Reactive black 5 dyeing wastewater treatment by electrolysis-Ce (IV) electrochemical oxidation technology: Influencing factors, synergy and enhancement mechanisms. *Sep Purif Technol* 285:120314. <https://doi.org/10.1016/J.SEPPUR.2021.120314>
- Fernandes A, Morao A, Magrinho M, Lopes A, Goncalves I (2004) Electrochemical degradation of C. I. acid orange 7. *Dye Pigment* 61:287–296. <https://doi.org/10.1016/J.DYEPIG.2003.11.008>
- Fidaleo M, Lavecchia R, Petrucci E, Zuurro A (2016) Application of a novel definitive screening design to decolorization of an azo dye on boron-doped diamond electrodes. *Int J Environ Sci Technol* 13:835–842. <https://doi.org/10.1007/S13762-016-0933-3>
- Florenza X, Solano AMS, Centellas F, Martínez-Huitle CA, Brillas E, Garcia-Segura S (2014) Degradation of the azo dye acid red 1 by anodic oxidation and indirect electrochemical processes based on Fenton's reaction chemistry. Relationship between decolorization, mineralization and products. *Electrochim Acta* 142:276–288. <https://doi.org/10.1016/J.ELECTACTA.2014.07.117>
- Fu L, You S-J, Zhang G, Yang FL, Fang XH (2010) Degradation of azo dyes using in-situ Fenton reaction incorporated into H<sub>2</sub>O<sub>2</sub>-producing microbial fuel cell. *Chem Eng J* 160:164–169. <https://doi.org/10.1016/j.cej.2010.03.032>
- Gallios G, Violintzis X, Voinovskii I, Voulgaropoulos A (2012) Electrochemical oxidation of synthetic dyes in simulated wastewaters. *NATO Sci Peace Secur Ser A Chem Biol*. [https://doi.org/10.1007/978-94-007-2488-4\\_31](https://doi.org/10.1007/978-94-007-2488-4_31)
- Ganiyu SO, Zhou M, Martínez-Huitle CA (2018) Heterogeneous electro-Fenton and photoelectro-Fenton processes: a critical review of fundamental principles and application for water/wastewater treatment. *Appl Catal B Environ* 235:103–129. <https://doi.org/10.1016/j.apcatb.2018.04.044>
- Ganzenko O, Huguenot D, van Hullebusch ED, Esposito G, Oturan MA (2014) Electrochemical advanced oxidation and biological processes for wastewater treatment: a review of the combined approaches. *Environ Sci Pollut Res*. <https://doi.org/10.1007/s11356-014-2770-6>
- Ganzoury MA, Ghasemian S, Zhang N, Yagar M, De Lannoy CF (2022) Mixed metal oxide anodes used for the electrochemical degradation of a real mixed industrial wastewater. *Chemosphere* 286:131600. <https://doi.org/10.1016/J.CHEMOSPHERE.2021.131600>
- Garcia-Segura S, Brillas E (2017) Applied photoelectrocatalysis on the degradation of organic pollutants in wastewaters. *J Photochem Photobiol C Photochem Rev* 31:1–35. <https://doi.org/10.1016/j.jphotochemrev.2017.01.005>
- Garcia-Segura S, Ocon JD, Chong MN (2018) Electrochemical oxidation remediation of real wastewater effluents—a review. *Process Saf Environ Prot* 113:48–67. <https://doi.org/10.1016/j.psep.2017.09.014>
- Ge MZ, Cao CY, Huang JY et al (2016) Synthesis, modification, and photo/photoelectrocatalytic degradation applications of TiO<sub>2</sub> nanotube arrays: a review. *Nanotechnol Rev* 5:75–112. <https://doi.org/10.1515/NTREV-2015-0049>
- Ghalwa NA, Gaber M, Khedr AM, Salem MF (2012) Comparative study of commercial oxide electrodes performance in electrochemical degradation of reactive orange 7 dye in aqueous solutions. *Int J Electrochem Sci* 7:6044–6058
- Ghime D, Ghosh P (2019) Removal of organic compounds found in the wastewater through electrochemical advanced oxidation processes: a review. *Russ J Electrochem* 55:591–620. <https://doi.org/10.1134/S1023193519050057>
- Golka K, Koppes S, Myslak ZW (2004) Carcinogenicity of azo colorants: influence of solubility and bioavailability. *Toxicol Lett* 151:203–210. <https://doi.org/10.1016/J.TOXLET.2003.11.016>
- Gomes L, Freitas RG, Malpass GRP, Pereira EC, Motheo ADJ (2009) Pt film electrodes prepared by the Pechini method for electrochemical decolourisation of Reactive Orange 16. *J Appl Electrochem* 39:117–121. <https://doi.org/10.1007/s10800-008-9649-5>
- Gomes L, Miwa DW, Malpass GRP, Motheo AJ (2011) Electrochemical degradation of the dye reactive orange 16 using electrochemical flow-cell. *J Braz Chem Soc* 22:1299–1306
- Gopinath A, Pisharody L, Popat A, Nidheesh PV (2022) Supported catalysts for heterogeneous electro-Fenton processes: Recent trends and future directions. *Curr Opin Solid State Mater Sci* 26:100981. <https://doi.org/10.1016/j.cossms.2022.100981>
- Gottlieb A, Shaw C, Smith A, Wheatley A, Forsythe S (2003) The toxicity of textile reactive azo dyes after hydrolysis and decolourisation. *J Biotechnol* 101:49–56. [https://doi.org/10.1016/S0168-1656\(02\)00302-4](https://doi.org/10.1016/S0168-1656(02)00302-4)
- Goutailler G, Valette JC, Guillard C, Passé O, Faure R (2001) Photocatalysed degradation of cyromazine in aqueous titanium dioxide suspensions: Comparison with photolysis. *J Photochem Photobiol A Chem* 141:79–84. [https://doi.org/10.1016/S1010-6030\(01\)00425-7](https://doi.org/10.1016/S1010-6030(01)00425-7)
- Gui L, Peng J, Li P, Peng R, Yu P, Luo Y (2019) Electrochemical degradation of dye on TiO<sub>2</sub> nanotube array constructed anode. *Chemosphere* 235:1189–1196. <https://doi.org/10.1016/j.chemosphere.2019.06.170>
- Guivarch E, Trevin S, Lahitte C, Oturan MA (2003) Degradation of azo dyes in water by electro-fenton process. *Environ Chem Lett* 1:38–44. <https://doi.org/10.1007/S10311-002-0017-0>



- Gürses A, Açıkyıldız M, Güneş K, Gürses M (2016) Dyes and Pigments
- Gutiérrez-Bouzán C, Pepió M (2014) Interaction between pH and conductivity in the indirect electro-oxidation of Azo dyes. *Ind Eng Chem Res* 53:18993–19000. <https://doi.org/10.1021/IE502460E>
- Hammami S, Bellakhal N, Oturan N, Oturan MA, Dachraoui M (2008) Degradation of acid orange 7 by electrochemically generated ·OH radicals in acidic aqueous medium using a boron-doped diamond or platinum anode: a mechanistic study. *Chemosphere* 73:678–684. <https://doi.org/10.1016/j.chemosphere.2008.07.010>
- Hamous H, Khenifi A, Bouberka Z, Derriche Z (2020) Electrochemical degradation of orange G in  $K_2SO_4$  and KCl medium. *Environ Eng Res* 25:571–578. <https://doi.org/10.4491/eer.2019.174>
- Hamous H, Khenifi A, Orts F, Bonastre J, Cases F (2021) Carbon textiles electrodes modified with RGO and Pt nanoparticles used for electrochemical treatment of azo dye. *J Electroanal Chem* 887:115154. <https://doi.org/10.1016/J.JELECHEM.2021.115154>
- Hashemi SH, Kaykhaii M (2022) Azo dyes: sources, occurrence, toxicity, sampling, analysis, and their removal methods. *Emerg Freshw Pollut*. <https://doi.org/10.1016/B978-0-12-822850-0.00013-2>
- He H, Zhou Z (2017) Electro-fenton process for water and wastewater treatment. *Crit Rev Environ Sci Technol* 47:2100–2131. <https://doi.org/10.1080/10643389.2017.1405673>
- He P, Wang L, Xue J, Cao Z (2010) Electrolytic treatment of methyl orange in aqueous solution using three-dimensional electrode reactor coupling ultrasonics. *Environ Technol* 31:417–422. <https://doi.org/10.1080/09593330903511413>
- He Z, Huang C, Wang Q, Jiang Z, Chen J, Song S (2011) Preparation of a praseodymium Modified  $Ti/SnO_2-Sb/PbO_2$  Electrode and its application in the anodic degradation of the Azo dye acid black 194. *Int J Electrochem Sci* 6:4341–4354
- He W, Ma Q, Wang J, Yu J, Bao W, Ma H, Amrane A (2014) Preparation of novel kaolin-based particle electrodes for treating methyl orange wastewater. *Appl Clay Sci* 99:178–186. <https://doi.org/10.1016/J.CLAY.2014.06.030>
- He Y, Lin H, Guo Z, Zhang W, Li H, Huang W (2019) Recent developments and advances in boron-doped diamond electrodes for electrochemical oxidation of organic pollutants. *Sep Purif Technol* 212:802–821. <https://doi.org/10.1016/J.SEPPUR.2018.11.056>
- Hernández-Zamora M, Martínez-Jerónimo F (2019a) Congo red dye diversely affects organisms of different trophic levels: a comparative study with microalgae, cladocerans, and zebrafish embryos. *Environ Sci Pollut Res* 26:11743–11755. <https://doi.org/10.1007/s11356-019-04589-1>
- Hernández-Zamora M, Martínez-Jerónimo F (2019b) Exposure to the azo dye direct blue 15 produces toxic effects on microalgae, cladocerans, and zebrafish embryos. *Ecotoxicology* 28:890–902. <https://doi.org/10.1007/s10646-019-02087-1>
- Hmani E, Samet Y, Abdelhédi R (2012) Electrochemical degradation of auramine-O dye at boron-doped diamond and lead dioxide electrodes. *Diam Relat Mater* 30:1–8. <https://doi.org/10.1016/j.diamond.2012.08.003>
- Hou Y, Qu J, Zhao X, Lei P, Wan D, Huang CP (2009) Electro-photocatalytic degradation of acid orange II using a novel  $TiO_2/ACF$  photoanode. *Sci Total Environ* 407:2431–2439. <https://doi.org/10.1016/J.SCITOTENV.2008.12.055>
- Isaev AB, Aliev ZM (2012) Effect of oxygen pressure on the electrochemical oxidation of chrome brown azo dye. *Russ J Appl Chem* 85:776–781. <https://doi.org/10.1134/S1070427212050163>
- Isaev AB, Magomedova AG (2022) Advanced oxidation processes based emerging technologies for dye wastewater treatment. *Moscow Univ Chem Bull* 77:181–196. <https://doi.org/10.3103/S0027131422040046>
- Isaev AB, Aliev ZM, Adamadzieva NA (2012) Photoelectrochemical oxidation of C.I. direct black 22 azo dye under elevated oxygen pressure. *Russ J Appl Chem* 85:765–769. <https://doi.org/10.1134/S107042721205014X>
- Isaev AB, Shabanov NS, Orudzhiev FF (2018) Influence of oxygen pressure to photoelectrochemical oxidation C.I. direct black 22 on  $TiO_2$  nanotube array photoanode. *Int J Environ Sci Technol* 15:1609–1618. <https://doi.org/10.1007/s13762-017-1523-8>
- Isarain-Chávez E, De La Rosa C, Martínez-Huitle CA, Peralta-Hernández JM (2013) On-site hydrogen peroxide production at pilot flow plant: application to electro-fenton process. *Int J Electrochem Sci* 8:3084–3094
- Jager D, Kupka D, Vaclavikova M, Ivanicova L, Gallios G (2018) Degradation of reactive black 5 by electrochemical oxidation. *Chemosphere* 190:405–416. <https://doi.org/10.1016/J.CHEMOSPHERE.2017.09.126>
- Jáger D, Kupka D, Václaviková M, Ivamčová L, Gallios G (2019) Electrochemical oxidation of reactive black 5 azo dye in chloride media. *Geosci Eng* 7:39–47
- Jain R, Sharma N, Radhapyari K (2009) Electrochemical treatment of pharmaceutical azo dye amaranth from waste water. *J Appl Electrochem* 39:577–582. <https://doi.org/10.1007/S10800-008-9695-Z>
- Jalife-Jacobo H, Feria-Reyes R, Serrano-Torres O, Gutiérrez-Granados S, Peralta-Hernández JM (2016) Diazo dye congo red degradation using a boron-doped diamond anode: an experimental study on the effect of supporting electrolytes. *J Hazard Mater* 319:78–83. <https://doi.org/10.1016/j.jhazmat.2016.02.056>
- Javid R, Qazi UY (2019) Catalytic oxidation process for the degradation of synthetic dyes: an overview. *Int J Environ Res Public Heal* 16:2066. <https://doi.org/10.3390/IJERPH16112066>
- Jiang H, Sun Y, Feng J, Wang J (2016) Heterogeneous electro-Fenton oxidation of azo dye methyl orange catalyzed by magnetic  $Fe_3O_4$  nanoparticles. *Water Sci Technol* 74:1116–1126. <https://doi.org/10.2166/wst.2016.300>
- Jiang Y, Zhao H, Liang J et al (2021) Anodic oxidation for the degradation of organic pollutants: Anode materials, operating conditions and mechanisms. A mini review. *Electrochem Commun* 123:106912. <https://doi.org/10.1016/j.elecom.2020.106912>
- Jiani L, Zhicheng X, Hao X, Dan Q, Zhengwei L, Wei Y, Yu W (2020) Pulsed electrochemical oxidation of acid Red G and crystal violet by  $PbO_2$  anode. *J Environ Chem Eng* 8:103773. <https://doi.org/10.1016/J.JECE.2020.103773>
- Jin XC, Liu GQ, Xu ZH, Tao WY (2007) Decolorization of a dye industry effluent by *aspergillus fumigatus* XC6. *Appl Microbiol Biotechnol* 74:239–243. <https://doi.org/10.1007/S00253-006-0658-1/FIGURES/3>
- Johin J, Nidheesh PV, Sivasankar T (2019) Sono-electro-chemical treatment of reactive black 5 dye and real textile effluent using  $MnSO_4/Na_2S_2O_8$  electrolytes. *Arab J Sci Eng* 44:9987–9996. <https://doi.org/10.1007/s13369-019-04159-0>
- Jović M, Stanković D, Manojlović D, Anđelković I, Milic A, Dojčinović B, Roglić G (2013) Study of the electrochemical oxidation of reactive textile dyes using platinum electrode. *Int J Electrochem Sci* 8:168–183
- Jović-Jovičić N, Milutinović-Nikolić A, Banković P, Mojović Z, Žunić M, Gržetić I, Jovanović D (2010) Organo-inorganic bentonite for simultaneous adsorption of acid orange 10 and lead ions. *Appl Clay Sci* 47:452–456. <https://doi.org/10.1016/J.CLAY.2009.11.005>
- Joy AC, Gandhimathi R, Niveditha SV, Ramesh ST, Nidheesh PV (2020) Photoelectro-peroxone process for the degradation of reactive azo dye in aqueous solution. *Sep Sci Technol* 55:2550–2559. <https://doi.org/10.1080/01496395.2019.1634732>
- Karim AV, Nidheesh PV, Oturan MA (2021) Boron-doped diamond electrodes for the mineralization of organic pollutants in the real

- wastewater. *Curr Opin Electrochem* 30:100855. <https://doi.org/10.1016/j.coelec.2021.100855>
- Katuri KP, Venkata Mohan S, Sridhar S, Pati BR, Sarma PN (2009) Laccase-membrane reactors for decolorization of an acid azo dye in aqueous phase: process optimization. *Water Res* 43:3647–3658. <https://doi.org/10.1016/j.watres.2009.05.028>
- Kaur R, Kaur H (2016) Electrochemical degradation of congo red from aqueous solution: role of graphite anode as electrode material. *Port Electrochim Acta* 34:185–196. <https://doi.org/10.4152/pea.201603185>
- Kaur P, Sangal VK, Kushwaha JP (2019) Parametric study of electro-Fenton treatment for real textile wastewater, disposal study and its cost analysis. *Int J Environ Sci Technol* 16:801–810. <https://doi.org/10.1007/s13762-018-1696-9>
- Kenova TA, Kornienko GV, Golubtsova OA, Kornienko VL, Maksimov NG (2018) Electrochemical degradation of mordant blue 13 azo dye using boron-doped diamond and dimensionally stable anodes: influence of experimental parameters and water matrix. *Environ Sci Pollut Res* 25:30425–30440. <https://doi.org/10.1007/S11356-018-2977-Z>
- Khan MD, Li D, Tabraiz S, Shamurad B, Scott K, Khan MZ, Yu EH (2021) Integrated air cathode microbial fuel cell-aerobic bioreactor set-up for enhanced bioelectrodegradation of azo dye acid blue 29. *Sci Total Environ* 756:143752. <https://doi.org/10.1016/J.SCITOTENV.2020.143752>
- Khan MD, Thimmappa R, Anwer AH et al (2021b) Redox mediator as cathode modifier for enhanced degradation of azo dye in a sequential dual chamber microbial fuel cell-aerobic treatment process. *Int J Hydrogen Energy* 46:39427–39437. <https://doi.org/10.1016/J.IJHYDENE.2021.09.151>
- Kharlamova TA, Aliev ZM (2016) Use of electrolysis under pressure for destructive oxidation of phenol and azo dyes. *Russ J Electrochem* 52:251–259. <https://doi.org/10.1134/S102319351603006X>
- Khataee A, Khataee A, Fathinia M, Vahid B, Joo SW (2013) Kinetic modeling of photoassisted-electrochemical process for degradation of an azo dye using boron-doped diamond anode and cathode with carbon nanotubes. *J Ind Eng Chem* 19:1890–1894. <https://doi.org/10.1016/J.JIEC.2013.02.037>
- Khataee A, Akbarpour A, Vahid B (2014) Photoassisted electrochemical degradation of an azo dye using Ti/RuO<sub>2</sub> anode and carbon nanotubes containing gas-diffusion cathode. *J Taiwan Inst Chem Eng* 45:930–936. <https://doi.org/10.1016/J.JTICE.2013.08.015>
- Khosravi R, Fazlzadehdavil M, Barikbin B, Hossini H (2015) Electro-decolorization of reactive red 198 from aqueous solutions using aluminum electrodes systems: modeling and optimization of operating parameters. *Desalin Water Treat* 54:37–41. <https://doi.org/10.1080/19443994.2014.913204>
- Kiernan J (2001) Classification and naming of dyes, stains and fluorochromes. *Biotech Histochem* 76:261–278. <https://doi.org/10.1080/bih.76.5-6.261.278>
- Koulini GV, Laiju AR, Ramesh ST, Gandhimathi R, Nidheesh PV (2022) Effective degradation of azo dye from textile wastewater by electro-peroxone process. *Chemosphere* 289:133152. <https://doi.org/10.1016/j.chemosphere.2021.133152>
- Krishnan S, Martínez-Huitle CA, Nidheesh PV (2022) An overview of chelate modified electro-Fenton processes. *J Environ Chem Eng* 10:107183. <https://doi.org/10.1016/j.jece.2022.107183>
- Kupferle MJ, Galal A, Bishop PL (2006) Electrolytic treatment of azo dye wastewaters: impact of matrix chloride content. *J Environ Eng* 132:514–518. [https://doi.org/10.1061/\(ASCE\)0733-9372\(2006\)132:5\(514\)](https://doi.org/10.1061/(ASCE)0733-9372(2006)132:5(514))
- Kusmieriek E, Chrzescijanska E (2015) Application of TiO<sub>2</sub>-RuO<sub>2</sub>/Ti electrodes modified with WO<sub>3</sub> in electro- and photoelectrochemical oxidation of Acid Orange 7 dye. *J Photochem Photobiol A Chem* 302:59–68. <https://doi.org/10.1016/J.JPHOTOCHEM.2015.01.009>
- Kusmieriek E, Chrzescijanska E, Szadkowska-Nicze M, Kaluzna-Czaplinska J (2011) Electrochemical discolouration and degradation of reactive dichlorotriazine dyes: reaction pathways. *J Appl Electrochem* 41:51–62. <https://doi.org/10.1007/S10800-010-0206-7/FIGURES/11>
- Labiadh L, Barbucci A, Cerisola G, Gadri A, Ammar S, Panizza M (2015) Role of anode material on the electrochemical oxidation of methyl orange. *J Solid State Electrochem* 19:3177–3183. <https://doi.org/10.1007/S10008-015-2928-2>
- Laghrib F, Bakasse M, Lahrach S, El Mhammedi MA (2020) Advanced oxidation processes: photo-electro-Fenton remediation process for wastewater contaminated by organic azo dyes. *Int J Environ Anal Chem*. <https://doi.org/10.1080/03067319.2020.1711892>
- Lahkimi A, Oturan MA, Oturan N, Chaouch M (2007) Removal of textile dyes from water by the electro-Fenton process. *Environ Chem Lett* 5:35–39. <https://doi.org/10.1007/s10311-006-0058-x>
- Lanzoni Migliorini F, Couto AB, Alves SA, Lanza MRDV, Ferreira NG (2017) Influence of supporting electrolytes on RO 16 dye electrochemical oxidation using boron doped diamond electrodes. *Mater Res* 20:584–591. <https://doi.org/10.1590/1980-5373-MR-2016-0153>
- Le TXH, Bechelany M, Lacour S, Oturan N, Oturan MA, Cretin M (2015) High removal efficiency of dye pollutants by electron-Fenton process using a graphene based cathode. *Carbon N Y* 94:1003–1011. <https://doi.org/10.1016/j.carbon.2015.07.086>
- Le TXH, Van NT, Yacouba ZA et al (2016) Toxicity removal assessments related to degradation pathways of azo dyes: toward an optimization of electro-fenton treatment. *Chemosphere* 161:308–318. <https://doi.org/10.1016/J.CHEMOSPHERE.2016.06.108>
- Lei Y, Liu H, Jiang C, Shen Z, Wang W (2015) A trickle bed electrochemical reactor for generation of hydrogen peroxide and degradation of an azo dye in water. *J Adv Oxid Technol* 18:47–56. <https://doi.org/10.1515/JAOTS-2015-0106>
- Li G, Qu J, Zhang X, Liu H, Liu H (2006a) Electrochemically assisted photocatalytic degradation of orange II: Influence of initial pH values. *J Mol Catal A Chem* 259:238–244. <https://doi.org/10.1016/J.MOLCATA.2006.06.038>
- Li G, Qu J, Zhang X, Ge J (2006b) Electrochemically assisted photocatalytic degradation of acid orange 7 with  $\beta$ -PbO<sub>2</sub> electrodes modified by TiO<sub>2</sub>. *Water Res* 40:213–220. <https://doi.org/10.1016/j.watres.2005.10.039>
- Li N, Dong SS, Lv WY, Huang S, Chen H, Yao Y, Chen W (2013a) Enhanced electrocatalytic oxidation of dyes in aqueous solution using cobalt phthalocyanine modified activated carbon fiber anode. *Sci China Chem* 56:1757–1764. <https://doi.org/10.1007/S11426-013-4942-5>
- Li X, Xu H, Yan W, Yang L (2013) Degradation of methyl orange waste water by electrochemical oxidation method. *J Phys Conf Ser* 418:012134. <https://doi.org/10.1088/1742-6596/418/1/012134>
- Li F, Li G, Zhang X (2014a) Mechanism of enhanced removal of quinonic intermediates during electrochemical oxidation of orange II under ultraviolet irradiation. *J Environ Sci* 26:708–715. [https://doi.org/10.1016/S1001-0742\(13\)60435-0](https://doi.org/10.1016/S1001-0742(13)60435-0)
- Li X, Li X, Yang W, Chen X, Li W, Luo B, Wang K (2014b) Preparation of 3D PbO<sub>2</sub> nanospheres@SnO<sub>2</sub> nanowires/Ti electrode and its application in methyl orange degradation. *Electrochim Acta* 146:15–22. <https://doi.org/10.1016/J.ELECTACTA.2014.08.150>
- Li G, Feng Y, Chai X, Yang Z, Zhang X (2015) Adsorption of cyclic organics generated during electrochemical oxidation of orange II by activated carbon fibres and toxicity test. *J Water Process Eng* 7:21–26. <https://doi.org/10.1016/J.JWPE.2015.04.012>
- Li J, Lin H, Yang L, Zhang H (2016) Copper-spent activated carbon as a heterogeneous peroxydisulfate catalyst for the degradation of

- acid orange 7 in an electrochemical reactor. *Water Sci Technol* 73:1802–1808. <https://doi.org/10.2166/WST.2016.027>
- Li J, Lin H, Zhu K, Zhang H (2017a) Degradation of acid orange 7 using peroxymonosulfate catalyzed by granulated activated carbon and enhanced by electrolysis. *Chemosphere* 188:139–147. <https://doi.org/10.1016/J.CHEMOSPHERE.2017.08.137>
- Li XY, Xu J, Cheng JP, Feng L, Shi YF, Ji J (2017b) TiO<sub>2</sub>-SiO<sub>2</sub>/GAC particles for enhanced electrocatalytic removal of acid orange 7 (AO7) dyeing wastewater in a three-dimensional electrochemical reactor. *Sep Purif Technol* 187:303–310. <https://doi.org/10.1016/J.SEPPUR.2017.06.058>
- Li J, Guan Q, Hong J, Chang CT (2019) Electrochemical oxidation of azo dye wastewater using graphene-based electrode materials. *J Nanosci Nanotechnol* 19:7308–7314. <https://doi.org/10.1166/JNN.2019.16656>
- Li A, Weng J, Yan X, Li H, Shi H, Wu X (2021) Electrochemical oxidation of acid orange 74 using Ru, IrO<sub>2</sub>, PbO<sub>2</sub>, and boron doped diamond anodes: direct and indirect oxidation. *J Electroanal Chem* 898:115622. <https://doi.org/10.1016/J.JELECHEM.2021.115622>
- Li R, Li T, Wan Y et al (2022) Efficient decolorization of azo dye wastewater with polyaniline/graphene modified anode in microbial electrochemical systems. *J Hazard Mater* 421:126740. <https://doi.org/10.1016/J.JHAZMAT.2021.126740>
- Liang P, Rivallin M, Cerneaux S, Lacour S, Petit E, Cretin M (2016) Coupling cathodic electro-fenton reaction to membrane filtration for AO7 dye degradation: a successful feasibility study. *J Memb Sci* 510:182–190. <https://doi.org/10.1016/J.MEMSCI.2016.02.071>
- Lin H, Zhang H, Hou L (2014) Degradation of C. I. acid orange 7 in aqueous solution by a novel electro/Fe<sub>3</sub>O<sub>4</sub>/PDS process. *J Hazard Mater* 276:182–191. <https://doi.org/10.1016/j.jhazmat.2014.05.021>
- Liu CF, Huang CP, Hu CC, Huang C (2019) A dual TiO<sub>2</sub>/Ti-stainless steel anode for the degradation of orange G in a coupling photoelectrochemical and photo-electro-Fenton system. *Sci Total Environ* 659:221–229. <https://doi.org/10.1016/j.scitotenv.2018.12.224>
- Liu X, Chen Z, Du W, Liu P, Zhang L, Shi F (2022) Treatment of wastewater containing methyl orange dye by fluidized three dimensional electrochemical oxidation process integrated with chemical oxidation and adsorption. *J Environ Manage* 311:114775. <https://doi.org/10.1016/J.JENVMAN.2022.114775>
- López-Grimau V, Pepió M, Gutiérrez-Bouzán C, Buscio V (2018) Kinetic models for the electrochemical decolouration of two reactive azo dyes. *Desalin Water Treat* 136:405–412. <https://doi.org/10.5004/DWT.2018.22901>
- Lounis M, Samar ME, Hamdaoui O (2016) Sono-electrochemical degradation of orange G in pure water, natural water, and seawater: effect of operating parameters. *Desalin Water Treat* 57:22533–22542. <https://doi.org/10.1080/19443994.2015.1129513>
- Luo X, Liang C, Hu Y (2019) Comparison of different enhanced coagulation methods for azo dye removal from wastewater. *Sustain* 11:1–14. <https://doi.org/10.3390/su11174760>
- Ma X, Zhou M (2009) A comparative study of azo dye decolorization by electro-Fenton in two common electrolytes. *J Chem Technol Biotechnol* 84:1544–1549. <https://doi.org/10.1002/JCTB.2218>
- Ma P, Ma H, Sabatino S, Galia A, Scialdone O (2018) Electrochemical treatment of real wastewater. Part 1: effluents with low conductivity. *Chem Eng J* 336:133–140. <https://doi.org/10.1016/j.cej.2017.11.046>
- Ma M, Huang Y, Liu J et al (2020) Engineering the photoelectrochemical behaviors of ZnO for efficient solar water splitting. *J Semicond*. <https://doi.org/10.1088/1674-4926/41/9/091702>
- Ma D, Yi H, Lai C et al (2021) Critical review of advanced oxidation processes in organic wastewater treatment. *Chemosphere* 275:130104. <https://doi.org/10.1016/j.chemosphere.2021.130104>
- Mahmoudian F, Nabizadeh Chianeh F, Sajjadi SM (2021) Simultaneous electrochemical decolorization of Acid Red 33, Reactive Orange 7, Acid Yellow 3 and Malachite Green dyes by electrochemically prepared Ti/nanoZnO-MWCNTs anode: Experimental design. *J Electroanal Chem* 884:115066. <https://doi.org/10.1016/J.JELECHEM.2021.115066>
- Mais L, Vacca A, Mascia M, Usai EM, Tronci S, Palmas S (2020) Experimental study on the optimisation of azo-dyes removal by photo-electrochemical oxidation with TiO<sub>2</sub> nanotubes. *Chemosphere* 248:125938. <https://doi.org/10.1016/J.CHEMOSPHERE.2020.125938>
- Malakootian M, Moridi A (2017) Efficiency of electro-Fenton process in removing Acid Red 18 dye from aqueous solutions. *Process Saf Environ Prot* 111:138–147. <https://doi.org/10.1016/j.psep.2017.06.008>
- Maljajei A, Arami M, Mahmoodi NM (2009) Decolorization and aromatic ring degradation of colored textile wastewater using indirect electrochemical oxidation method. *Desalination* 249:1074–1078. <https://doi.org/10.1016/J.DESAL.2009.05.016>
- Mao X, Tian F, Gan F, Lin A, Zhang X (2008) Comparison of the performances of Ti/SnO<sub>2</sub>-Sb, Ti/SnO<sub>2</sub>-Sb/PbO<sub>2</sub>, and Nb/BDD anodes on electrochemical degradation of azo dye. *Russ J Electrochem* 44:802–811. <https://doi.org/10.1134/S1023193508070069>
- Márquez AA, Sirés I, Brillas E, Nava JL (2020) Mineralization of methyl orange azo dye by processes based on H<sub>2</sub>O<sub>2</sub> electro-generation at a 3D-like air-diffusion cathode. *Chemosphere* 259:127466. <https://doi.org/10.1016/J.CHEMOSPHERE.2020.127466>
- Martín de Vidales MJ, Rua J, de Juan JLM, Fernández-Martínez F, Dos Santos-García AJ (2020) Degradation of contaminants of emerging concern by electrochemical oxidation: Coupling of ultraviolet and ultrasound radiations. *Materials* 13:1–12. <https://doi.org/10.3390/ma13235551>
- Martínez-Huitle CA (2021) Environment-friendly electrochemical processes. *Mater* 14:1548. <https://doi.org/10.3390/MA14061548>
- Martínez-Huitle CA, Brillas E (2009) Decontamination of wastewaters containing synthetic organic dyes by electrochemical methods: a general review. *Appl Catal B Environ* 87:105–145. <https://doi.org/10.1016/J.APCATB.2008.09.017>
- Martínez-Huitle CA, Rodrigo MA, Sirés I, Scialdone O (2015) Single and coupled electrochemical processes and reactors for the abatement of organic water pollutants: a critical review. *Chem Rev* 115:13362–13407. <https://doi.org/10.1021/acs.chemrev.5b00361>
- Méndez-Martínez AJ, Dávila-Jiménez MM, Ornelas-Dávila O, Elizalde-González MP, Arroyo-Abad U, Sirés I, Brillas E (2012) Electrochemical reduction and oxidation pathways for reactive black 5 dye using nickel electrodes in divided and undivided cells. *Electrochim Acta* 59:140–149. <https://doi.org/10.1016/J.ELECTACTA.2011.10.047>
- Mengelzadeh N, Pourzamani H, Saloot MK, Hajizadeh Y, Parseh I, Parastar S, Niknam N (2019) Electrochemical degradation of reactive black 5 using three-dimensional electrochemical system based on multivalued carbon nanotubes. *J Environ Eng* 145:04019021. [https://doi.org/10.1061/\(asce\)ee.1943-7870.0001517](https://doi.org/10.1061/(asce)ee.1943-7870.0001517)
- Migliorini FL, Braga NA, Alves SA, Lanza MRDV, Baldan MR, Ferreira NG (2011) Anodic oxidation of wastewater containing the reactive orange 16 dye using heavily boron-doped diamond electrodes. *J Hazard Mater* 192:1683–1689. <https://doi.org/10.1016/j.jhazmat.2011.07.007>

- Mijin D, Tomić VD, Grgur BN (2015) Electrochemical decolorization of the reactive orange 16 dye using a dimensionally stable Ti/PtOx anode. *J Serbian Chem Soc* 80:903–915. <https://doi.org/10.2298/JSC140917107M>
- Mohan N, Balasubramanian N, Subramanian V (2001) Electrochemical treatment of simulated textile effluent. *Chem Eng Technol* 24:749–753. <https://doi.org/10.1002/1521-4125>
- Morales U, Escudero CJ, Rivero MJ, Ortiz I, Rocha JM, Peralta-Hernández JM (2018) Coupling of the electrochemical oxidation (EO-BDD)/photocatalysis (TiO<sub>2</sub>-Fe-N) processes for degradation of acid blue BR dye. *J Electroanal Chem* 808:180–188. <https://doi.org/10.1016/J.JELECHEM.2017.12.014>
- Moreira FC, Garcia-Segura S, Vilar VJP, Boaventura RA, Brillas E (2013) Decolorization and mineralization of sunset yellow FCF azo dye by anodic oxidation, electro-Fenton, UVA photoelectro-Fenton and solar photoelectro-Fenton processes. *Appl Catal B Environ* 142–143:877–890. <https://doi.org/10.1016/j.apcatb.2013.03.023>
- Moreira FC, Boaventura RAR, Brillas E, Vilar VJP (2017) Electrochemical advanced oxidation processes: a review on their application to synthetic and real wastewaters. *Appl Catal B Environ* 202:217–261. <https://doi.org/10.1016/j.apcatb.2016.08.037>
- Mukimin A, Zen N, Purwanto A, Wicaksono KA, Vistanty H, Alfauzi AS (2017) Application of a full-scale electrocatalytic reactor as real batik printing wastewater treatment by indirect oxidation process. *J Environ Chem Eng* 5:5222–5232. <https://doi.org/10.1016/J.JECE.2017.09.053>
- Muthukumar M, Karuppiyah MT, Raju GB (2007) Electrochemical removal of CI acid orange 10 from aqueous solutions. *Sep Purif Technol* 55:198–205. <https://doi.org/10.1016/J.SEPPUR.2006.11.014>
- Nabizadeh Chianeh F, Basiri Parsa J (2015) Decolorization of azo dye C.I. Acid Red 33 from aqueous solutions by anodic oxidation on MWCNTs/Ti electrodes. *Desalin Water Treat* 57:20574–20581. <https://doi.org/10.1080/19443994.2015.1110716>
- Navarro HI, Alvarez A, Uruchurtu Chavarín J, León I (2010) Reactive black 5 treatment and hydrogen production by PEM electrolysis. *ECS Trans* 29:259–272. <https://doi.org/10.1149/1.3532323/XML>
- Neelavannan MG, Revathi M, Ahmed Basha C (2007) Photocatalytic and electrochemical combined treatment of textile wash water. *J Hazard Mater* 149:371–378. <https://doi.org/10.1016/J.JHAZM.AT.2007.04.025>
- Nidheesh PV, Gandhimathi R (2012) Trends in electro-Fenton process for water and wastewater treatment: an overview. *Desalination* 299:1–15. <https://doi.org/10.1016/j.desal.2012.05.011>
- Nidheesh PV, Gandhimathi R, Ramesh ST (2013) Degradation of dyes from aqueous solution by Fenton processes: a review. *Environ Sci Pollut Res* 20:2099–2132. <https://doi.org/10.1007/s11356-012-1385-z>
- Nidheesh PV, Zhou M, Oturan MA (2018) An overview on the removal of synthetic dyes from water by electrochemical advanced oxidation processes. *Chemosphere* 197:210–227. <https://doi.org/10.1016/j.chemosphere.2017.12.195>
- Nidheesh PV, Divyapriya G, Oturan N, Trellu C, Oturan MA (2019) Environmental applications of boron-doped diamond electrodes: I. Applications in water and wastewater treatment. *ChemElectroChem* 6:2124–2142. <https://doi.org/10.1002/celec.201801876>
- Nidheesh PV, Couras C, Karim AV, Nadais H (2022a) A review of integrated advanced oxidation processes and biological processes for organic pollutant removal. *Chem Eng Commun* 209:390–432. <https://doi.org/10.1080/00986445.2020.1864626>
- Nidheesh PV, Divyapriya G, Ezzahra Titchou F, Hamdani M (2022) Treatment of textile wastewater by sulfate radical based advanced oxidation processes. *Sep Purif Technol* 293:121115. <https://doi.org/10.1016/j.seppur.2022.121115>
- Nidheesh PV, Trellu C, Vargas HO, Mousset E, Ganiyu SO, Oturan MA (2023) Electro-Fenton process in combination with other advanced oxidation processes: challenges and opportunities. *Curr Opin Electrochem* 37:101171. <https://doi.org/10.1016/j.coelec.2022.101171>
- Nidheesh PV, Ganiyu SO, Martínez-Huitle CA et al (2023b) Recent advances in electro-Fenton process and its emerging applications. *Crit Rev Environ Sci Technol* 53:887–913. <https://doi.org/10.1080/10643389.2022.2093074>
- Nordin N, Amir SFM, Yusop MR, Othman MR (2015) Decolorization of C.I. reactive orange 4 and textile effluents by electrochemical oxidation technique using silver-carbon composite electrode. *Acta Chim Slov* 62:642–651. <https://doi.org/10.17344/ACSI.2014.1264>
- Oliveira FH, Osugi ME, Paschoal FMM, Profeti D, Olivi P, Zanoni MVB (2007) Electrochemical oxidation of an acid dye by active chlorine generated using Ti/Sn<sub>(1-x)</sub>Ir<sub>x</sub>O<sub>2</sub> electrodes. *J Appl Electrochem* 37:583–592. <https://doi.org/10.1007/S10800-006-9289-6>
- Oliver-Tolentino MA, Jiménez-Álvarez E, De Jesús M-O, García-Báez E, Franco-Hernández MO, Guzmán-Vargas A (2014) Effective electro-fenton degradation of reactive black 5 dye using modified electrode with Cu-zeolites. *J New Mater Electrochem Syst* 17:71–75. <https://doi.org/10.14447/jnmes.v17i2.426>
- Orimolade BO, Arotiba OA (2019) An exfoliated graphite-Bismuth vanadate composite photoanode for the photoelectrochemical degradation of acid orange 7 dye. *Electrocatalysis* 10:429–435. <https://doi.org/10.1007/S12678-019-00534-5>
- Oturan MA, Aaron JJ (2014) Advanced oxidation processes in water/wastewater treatment: principles and applications. a review. *Crit Rev Environ Sci Technol* 44:2577–2641. <https://doi.org/10.1080/10643389.2013.829765>
- Oturan N, Oturan MA (2018) Electro-fenton process: background, new developments, and applications. In: Martínez-Huitle CA, Rodrigo MA, Scialdone O (eds) *Electrochemical water and wastewater treatment*. Elsevier, Oxford (UK) and Cambridge (MA-USA), pp 193–221. <https://doi.org/10.1016/B978-0-12-813160-2.00008-0>
- Oukili K, Loukili M (2019) Optimization of textile azo dye degradation by electrochemical oxidation using box-behnken design. *Mediterr J Chem* 8:410–419. <https://doi.org/10.13171/MJC851907103KO>
- Özcan A, Oturan MA, Oturan N, Şahin Y (2009) Removal of acid orange 7 from water by electrochemically generated Fenton's reagent. *J Hazard Mater*. <https://doi.org/10.1016/j.jhazmat.2008.07.088>
- Pacheco-Álvarez MO, Rodríguez-Narváez OM, Wrobel K, Navarro-Mendoza R, Nava-Montes de Oca J, Peralta-Hernández J (2018) Improvement of the degradation of methyl orange using a TiO<sub>2</sub>/BDD composite electrode to promote electrochemical and photoelectro-oxidation processes. *Int J Electrochem Sci* 13:11549–11567. <https://doi.org/10.20964/2018.12.70>
- Pacheco-Álvarez MOA, Picos A, Pérez-Segura T, Peralta-Hernández JM (2019) Proposal for highly efficient electrochemical discoloration and degradation of azo dyes with parallel arrangement electrodes. *J Electroanal Chem* 838:195–203. <https://doi.org/10.1016/J.JELECHEM.2019.03.004>
- Pan Y, Wang Y, Zhou A et al (2017) Removal of azo dye in an up-flow membrane-less bioelectrochemical system integrated with bio-contact oxidation reactor. *Chem Eng J* 326:454–461. <https://doi.org/10.1016/J.CEJ.2017.05.146>
- Panizza M, Cerisola G (2007) Electrocatalytic materials for the electrochemical oxidation of synthetic dyes. *Appl Catal B Environ* 75:95–101. <https://doi.org/10.1016/J.APCATB.2007.04.001>

- Panizza M, Cerisola G (2008) Electrochemical degradation of methyl red using BDD and PbO<sub>2</sub> anodes. *Ind Eng Chem Res* 47:6816–6820. <https://doi.org/10.1021/IE8001292>
- Panizza M, Cerisola G (2009) Direct and mediated anodic oxidation of organic pollutants. *Chem Rev* 109:6541–6569. <https://doi.org/10.1021/cr9001319>
- Parsa JB, Rezaei M, Soleymani AR (2009) Electrochemical oxidation of an azo dye in aqueous media investigation of operational parameters and kinetics. *J Hazard Mater* 168:997–1003. <https://doi.org/10.1016/J.JHAZMAT.2009.02.134>
- Parsa JB, Golmirzaei M, Abbasi M (2014) Degradation of azo dye C.I. Acid red 18 in aqueous solution by ozone-electrolysis process. *J Ind Eng Chem* 20:689–694. <https://doi.org/10.1016/j.jiec.2013.05.034>
- Patidar R, Srivastava VC, Ritesh P, Srivastava VC (2020) Understanding of ultrasound enhanced electrochemical oxidation of persistent organic pollutants. *J Water Process Eng* 37:101378. <https://doi.org/10.1016/j.jwpe.2020.101378>
- Paz EC, Aveiro LR, Pinheiro VS et al (2018) Evaluation of H<sub>2</sub>O<sub>2</sub> electrogeneration and decolorization of Orange II azo dye using tungsten oxide nanoparticle-modified carbon. *Appl Catal B Environ* 232:436–445. <https://doi.org/10.1016/J.APCATB.2018.03.082>
- Paździor K, Bilińska L, Ledakowicz S (2019) A review of the existing and emerging technologies in the combination of AOPs and biological processes in industrial textile wastewater treatment. *Chem Eng J* 376:120597. <https://doi.org/10.1016/j.cej.2018.12.057>
- Pearce CI, Lloyd JR, Guthrie JT (2003) The removal of colour from textile wastewater using whole bacterial cells: a review. *Dye Pigment* 58:179–196. [https://doi.org/10.1016/S0143-7208\(03\)00064-0](https://doi.org/10.1016/S0143-7208(03)00064-0)
- Peng YP, Yeh YT, Wang PY, Huang CP (2013) A solar cell driven electrochemical process for the concurrent reduction of carbon dioxide and degradation of azo dye in dilute KHCO<sub>3</sub> electrolyte. *Sep Purif Technol* 117:3–11. <https://doi.org/10.1016/J.SEPPUR.2013.03.044>
- Peralta-Hernández JM, Godínez LA (2014) Electrochemical hydrogen peroxide production in acidic medium using a tubular photo-reactor: application in advanced oxidation processes. *J Mex Chem Soc* 58:348–355
- Peralta-Hernández JM, Méndez-Tovar M, Guerra-Sánchez R, Martínez-Huitle CA, Nava JL (2012) A brief review on environmental application of boron doped diamond electrodes as a new way for electrochemical incineration of synthetic dyes. *Int J Electrochem* 2012:1–18. <https://doi.org/10.1155/2012/154316>
- Petrucci E, Di Palma L, Lavecchia R, Zuorro A (2015a) Treatment of diazo dye reactive green 19 by anodic oxidation on a boron-doped diamond electrode. *J Ind Eng Chem* 26:116–121. <https://doi.org/10.1016/J.JIEC.2014.11.022>
- Petrucci E, Di Palma L, Lavecchia R, Zuorro A (2015b) Modeling and optimization of reactive green 19 oxidation on a BDD thin-film electrode. *J Taiwan Inst Chem Eng* 51:152–158. <https://doi.org/10.1016/J.JTICE.2015.01.005>
- Pillai IMS, Gupta AK, Tiwari MK (2015) Multivariate optimization for electrochemical oxidation of methyl orange: pathway identification and toxicity analysis. *J Environ Sci Health Part A* 50:301–310. <https://doi.org/10.1080/10934529.2015.981119>
- Pogacean F, Rosu M-C, Coros M et al (2018) Graphene/TiO<sub>2</sub>-Ag based composites used as sensitive electrode materials for amaranth electrochemical detection and degradation. *J Electrochem Soc* 165:B3054–B3059. <https://doi.org/10.1149/2.0101808JES/XML>
- Popli SA, Patel UD (2015) Electrochemical decolorization of Reactive Black 5 in an undivided cell using Ti and graphite anodes: effect of polypyrrole coating on anodes. *J Electrochem Sci Eng* 5:145–156. <https://doi.org/10.5599/JESE.164>
- Qiao J, Xiong Y (2021) Electrochemical oxidation technology: a review of its application in high-efficiency treatment of wastewater containing persistent organic pollutants. *J Water Process Eng* 44:102308. <https://doi.org/10.1016/J.JWPE.2021.102308>
- Qiao N, Chang J, Hu M, Ma H (2015) Novel bentonite particle electrodes based on Fenton catalyst and its application in orange II removal. *Desalin Water Treat* 57:17030–17038. <https://doi.org/10.1080/19443994.2015.1083889>
- Qiao Q, Singh S, Lo SL, Li Y, Jin J, Wang L (2018) Electrochemical oxidation of acid orange 7 dye with Ce, Nd, and Co-modified PbO<sub>2</sub> electrodes: preparation, characterization, optimization, and mineralization. *J Taiwan Inst Chem Eng* 84:110–122. <https://doi.org/10.1016/J.JTICE.2018.01.008>
- Radha KV, Sridevi V, Kalaivani K (2009) Electrochemical oxidation for the treatment of textile industry wastewater. *Bioresour Technol* 100:987–990. <https://doi.org/10.1016/J.BIORTECH.2008.06.048>
- Radha KV, Sridevi V, Kalaivani K, Raj M (2012) Electrochemical decolorization of the dye acid orange 10. *Desalin Water Treat* 7:6–11. <https://doi.org/10.5004/DWT.2009.309>
- Radi A, Mostafa MR, Hegazy TA, Elshafey RM (2012) Electrochemical study of vinylsulphone azo dye reactive black 5 and its determination at a glassy carbon electrode. *J Anal Chem* 67:890–894. <https://doi.org/10.1134/S1061934812110093>
- Raghu S, Basha CA (2007) Electrochemical treatment of procion Black 5B using cylindrical flow reactor—A pilot plant study. *J Hazard Mater* 139:381–390. <https://doi.org/10.1016/J.JHAZMAT.2006.06.082>
- Raghu S, Lee CW, Chellammal S, Palanichamy S, Basha CA (2009) Evaluation of electrochemical oxidation techniques for degradation of dye effluents—A comparative approach. *J Hazard Mater* 171:748–754. <https://doi.org/10.1016/j.jhazmat.2009.06.063>
- Rahmani AR, Godini K, Nematollahi D, Azarian G, Maleki S (2015) Degradation of azo dye C.I. Acid Red 18 using an eco-friendly and continuous electrochemical process. *Korean J Chem Eng* 33:532–538. <https://doi.org/10.1007/S11814-015-0175-Y>
- Rahmani AR, Shabanloo A, Fazlzadeh M, Poureshgh Y (2016) Investigation of operational parameters influencing in treatment of dye from water by electro-Fenton process. *Desalin Water Treat* 57:24387–24394. <https://doi.org/10.1080/19443994.2016.1146918>
- Rajkumar K, Muthukumar M (2017) Response surface optimization of electro-oxidation process for the treatment of C.I. Reactive yellow 186 dye: reaction pathways. *Appl Water Sci* 7:637–652. <https://doi.org/10.1007/S13201-015-0276-0>
- Rajkumar K, Muthukumar M, Mangalaraja RV (2015) Electrochemical degradation of C.I. Reactive orange 107 using gadolinium (Gd<sup>3+</sup>), neodymium (Nd<sup>3+</sup>) and Samarium (Sm<sup>3+</sup>) doped cerium oxide nanoparticles. *Int J Ind Chem* 6:285–295. <https://doi.org/10.1007/S40090-015-0051-Y/FIGURES/7>
- Ramírez C, Saldaña A, Hernández B et al (2013) Electrochemical oxidation of methyl orange azo dye at pilot flow plant using BDD technology. *J Ind Eng Chem* 19:571–579. <https://doi.org/10.1016/J.JIEC.2012.09.010>
- Ramírez B, Rondán V, Ortiz-Hernández L, Silva-Martínez S, Alvarez-Gallegos A (2016) Semi-empirical chemical model for indirect advanced oxidation of acid orange 7 using an unmodified carbon fabric cathode for H<sub>2</sub>O<sub>2</sub> production in an electrochemical reactor. *J Environ Manag* 171:29–34. <https://doi.org/10.1016/J.JENVMAN.2016.02.004>
- Ramírez-Pereda B, Álvarez-Gallegos A, Rangel-Peraza JG, Bustos-Terrones YA (2018) Kinetics of acid orange 7 oxidation by using carbon fiber and reticulated vitreous carbon in an electro-Fenton process. *J Environ Manag* 213:279–287. <https://doi.org/10.1016/j.jenvman.2018.01.022>

- Ramírez-Pereda B, Álvarez-Gallegos AA, Silva-Martínez S, Rangel-Peraza JG, Bustos-Terrones YA (2019) Evaluation of the simultaneous use of two compartments of an electrochemical reactor for the elimination of azo dyes. *J Electroanal Chem* 855:113593. <https://doi.org/10.1016/J.JELECHEM.2019.113593>
- Rao NN, Bose G, Khare P, Kaul SN (2006) Fenton and electro-fenton methods for oxidation of H-acid and reactive black 5. *J Environ Eng* 132:367–376. [https://doi.org/10.1061/\(asce\)0733-9372\(2006\)132:3\(367\)](https://doi.org/10.1061/(asce)0733-9372(2006)132:3(367))
- Raval NP, Shah PU, Shah NK (2016) Adsorptive amputation of hazardous azo dye congo red from wastewater: a critical review. *Environ Sci Pollut Res* 23:14810–14853. <https://doi.org/10.1007/s11356-016-6970-0>
- Rawat D, Mishra V, Sharma RS (2016) Detoxification of azo dyes in the context of environmental processes. *Chemosphere* 155:591–605. <https://doi.org/10.1016/J.CHEMOSPHERE.2016.04.068>
- Rivera M, Pazos M, Sanromán MÁ (2011) Development of an electrochemical cell for the removal of reactive black 5. *Desalination* 274:39–43. <https://doi.org/10.1016/j.desal.2011.01.074>
- Rodríguez De León N, Cruz-González K, Torres-López O, Ramírez AH, Guzmán-Mar J, Martínez-Huitle C, Peralta-Hernández JM (2019) Decolorization of synthetic azo dyes by electrochemically generated ·OH radicals in acidic medium using boron doped diamond (BDD) electrodes. *ECS Trans* 20:283–290. <https://doi.org/10.1149/1.3268396/XML>
- Rodríguez-Narváez OM, Picos AR, Bravo-Yumi N, Pacheco-Alvarez M, Martínez-Huitle CA, Peralta-Hernández JM (2021) Electrochemical oxidation technology to treat textile wastewaters. *Curr Opin Electrochem* 29:100806. <https://doi.org/10.1016/J.COELC.2021.100806>
- Rovina K, Siddiquee S, Shaarani SM (2017) Toxicology, extraction and analytical methods for determination of Amaranth in food and beverage products. *Trends Food Sci Technol* 65:68–79. <https://doi.org/10.1016/J.TIFS.2017.05.008>
- Ruan XC, Liu MY, Zeng QF, Ding YH (2010) Degradation and decolorization of reactive red X-3B aqueous solution by ozone integrated with internal micro-electrolysis. *Sep Purif Technol* 74:195–201. <https://doi.org/10.1016/J.SEPPUR.2010.06.005>
- Ruiz EJ, Arias C, Brillas E, Hernández-Ramírez A P-H (2011) Mineralization of acid yellow 36 azo dye by electro-Fenton and solar photoelectro-Fenton processes with a boron-doped diamond anode. *Chemosphere* 82:495–501. <https://doi.org/10.1016/j.chemosphere.2010.11.013>
- Şahinkaya S (2013) COD and color removal from synthetic textile wastewater by ultrasound assisted electro-Fenton oxidation process. *J Ind Eng Chem* 19:601–605. <https://doi.org/10.1016/j.jiec.2012.09.023>
- Sakalis A, Mpoulmpasakos K, Nickel U, Fytianos K, Voulgaropoulos A (2005) Evaluation of a novel electrochemical pilot plant process for azodyes removal from textile wastewater. *Chem Eng J* 111:63–70. <https://doi.org/10.1016/J.CEJ.2005.05.008>
- Sala M, López-Grimau V, Gutiérrez-Bouzán C (2016) Photoassisted Electrochemical Treatment of Azo and Phtalocyanine Reactive Dyes in the Presence of Surfactants. *Materials (Basel)* 9:211. <https://doi.org/10.3390/MA9030211>
- Salazar R, Ureta-Zañartu MS (2012) Degradation of acid violet 7 and reactive black 5 in water by electro-fenton and photo electro-fenton by. *J Chil Chem Soc* 57:999–1003. <https://doi.org/10.4067/S0717-97072012000100010>
- Salazar R, Gallardo-Arriaza J, Vidal J et al (2019) Treatment of industrial textile wastewater by the solar photoelectro-Fenton process: influence of solar radiation and applied current. *Sol Energy* 190:82–91. <https://doi.org/10.1016/j.solener.2019.07.072>
- Salazar-Gastélum MI, Reynoso-Soto EA, Lin SW, Perez-Sicairos S, Félix-Navarro RM (2013) Electrochemical and photoelectrochemical decoloration of amaranth dye azo using composited dimensional stable anodes. *J Environ Prot (Irvine, Calif)* 2013:136–143. <https://doi.org/10.4236/JEP.2013.41016>
- Sandoval MA, Zúñiga-Mallea N, Espinoza LC, Vidal J, Jara-Ulloa P, Salazar R (2019) Decolorization and degradation of a mixture of industrial azo dyes by anodic oxidation using a Ti/Ru<sub>0.3</sub>Ti<sub>0.7</sub>O<sub>2</sub> (DSA-Cl<sub>2</sub>) electrode. *ChemistrySelect* 4:13856–13866. <https://doi.org/10.1002/SLCT.201903150>
- Santana MHP, Da Silva LM, Freitas AC, Boodts JF, Fernandes KC, De Faria LA (2009) Application of electrochemically generated ozone to the discoloration and degradation of solutions containing the dye reactive orange 122. *J Hazard Mater* 164:10–17. <https://doi.org/10.1016/J.JHAZMAT.2008.07.108>
- Santos LM, De Amorim KP, Andrade LS, Batista PS, Trovó AG, Machado AE (2015) Dye degradation enhanced by coupling electrochemical process and heterogeneous photocatalysis. *J Braz Chem Soc* 26:1817–1823. <https://doi.org/10.5935/0103-5053.20150158>
- Santos JEL, Da Silva DR, Martínez-Huitle CA, Dos Santos EV, Quiroz MA (2020b) Cathodic hydrogen production by simultaneous oxidation of methyl red and 2,4-dichlorophenoxyacetate aqueous solutions using Pb/PbO<sub>2</sub>, Ti/Sb-doped SnO<sub>2</sub> and Si/BDD anodes. Part 1: electrochemical oxidation. *RSC Adv* 10:37695–37706. <https://doi.org/10.1039/d0ra03955a>
- Sarafraz M, Khosravi M, Bonyadinejad G, Ebrahimi A, Taghavi-Shahri SM, Nateghi R, Rastaghi S (2015) Electrochemical degradation of the acid orange 10 dye on a Ti/SnO<sub>2</sub>-Sb anode assessed by response surface methodology. *Int J Environ Health Eng* 4:31. <https://doi.org/10.4103/2277-9183.163975>
- Särkkä H, Bhatnagar A, Sillanpää M (2015) Recent developments of electro-oxidation in water treatment—a review. *J Electroanal Chem* 754:46–56. <https://doi.org/10.1016/J.JELECHEM.2015.06.016>
- Sasidharan Pillai IM, Gupta AK (2016) Effect of inorganic anions and oxidizing agents on electrochemical oxidation of methyl orange, malachite green and 2,4-dinitrophenol. *J Electroanal Chem* 762:66–72. <https://doi.org/10.1016/J.JELECHEM.2015.12.027>
- Sathishkumar K, Sathiyaraj S, Parthipan P, Akhil A, Murugan K, Rajasekar A (2017) Electrochemical decolorization of methyl red by RuO<sub>2</sub>-IrO<sub>2</sub>-TiO<sub>2</sub> electrode and biodegradation with *Pseudomonas stutzeri* MN1 and *Acinetobacter baumannii* MN3: an integrated approach. *Chemosphere* 183:204–211. <https://doi.org/10.1016/J.CHEMOSPHERE.2017.05.087>
- Sathishkumar K, AlSalhi MS, Sanganyado E, Devanesan S, Arulprakash A, Rajasekar A (2019) Sequential electrochemical oxidation and bio-treatment of the azo dye congo red and textile effluent. *J Photochem Photobiol B Biol* 200:111655. <https://doi.org/10.1016/j.jphotobiol.2019.111655>
- Saxena P, Ruparelia J (2019) Influence of supporting electrolytes on electrochemical treatability of reactive black 5 using dimensionally stable anode. *J Inst Eng Ser A* 100:299–310. <https://doi.org/10.1007/s40030-019-00360-4>
- Scialdone O (2009) Electrochemical oxidation of organic pollutants in water at metal oxide electrodes: a simple theoretical model including direct and indirect oxidation processes at the anodic surface. *Electrochim Acta* 54:6140–6147. <https://doi.org/10.1016/j.electacta.2009.05.066>
- Scialdone O, Galia A, Sabatino S (2014) Abatement of acid orange 7 in macro and micro reactors. Effect of the electrocatalytic route. *Appl Catal B Environ* 148–149:473–483. <https://doi.org/10.1016/J.APCATB.2013.11.005>
- Selvaraj V, Swarna Karthika T, Mansiya C, Alagar M (2021) An overview on recently developed techniques, mechanisms and intermediate involved in the advanced azo dye degradation for industrial applications. *J Mol Struct* 1224:129195. <https://doi.org/10.1016/J.MOLSTRUC.2020.129195>

- Senthil Rathi B, Senthil Kumar P (2022) Sustainable approach on the biodegradation of azo dyes: a short review. *Curr Opin Green Sustain Chem* 33:100578. <https://doi.org/10.1016/J.COAGSC.2021.100578>
- Senthilkumar S, Basha CA, Perumalsamy M, Prabhu HJ (2012) Electrochemical oxidation and aerobic biodegradation with isolated bacterial strains for dye wastewater: combined and integrated approach. *Electrochim Acta* 77:171–178. <https://doi.org/10.1016/J.ELECTACTA.2012.05.084>
- Shah MP (2019) Bioremediation of azo dye. *Microb Wastewater Treat*. <https://doi.org/10.1016/B978-0-12-816809-7.00006-3>
- Shen Z, Wang W, Jia J, Feng X, Hu W, Peng A (2002) Catalytically assisted electrochemical oxidation of dye acid red B. *Water Environ Res* 74:117–121. <https://doi.org/10.2175/106143002X139811>
- Shetti NP, Malode SJ, Malladi RS, Nargund SL, Shukla SS, Aminabhavi TM (2019) Electrochemical detection and degradation of textile dye congo red at graphene oxide modified electrode. *Microchem J* 146:387–392. <https://doi.org/10.1016/J.MICRO.2019.01.033>
- Shukla S, Oturan MA (2015) Dye removal using electrochemistry and semiconductor oxide nanotubes. *Environ Chem Lett* 13:157–172. <https://doi.org/10.1007/s10311-015-0501-y>
- Singh A, Verma A, Bansal P, Singla J (2017) Evaluation of the process parameters for electro fenton and electro chlorination treatment of reactive black 5 (RB5) Dye. *J Electrochem Soc* 164:E203–E212. <https://doi.org/10.1149/2.0471709JES/XML>
- Sirés I, Brillas E, Oturan MA, Rodrigo MA, Panizza M (2014) Electrochemical advanced oxidation processes: today and tomorrow. *A Review Environ Sci Pollut Res* 21:8336–8367. <https://doi.org/10.1007/s11356-014-2783-1>
- Socha A, Sochocka E, Podsiadły R, Sokołowska J (2006) Electrochemical and photoelectrochemical degradation of direct dyes. *Color Technol* 122:207–212. <https://doi.org/10.1111/J.1478-4408.2006.00027.X>
- Socha A, Sochocka E, Podsiadły R, Sokołowska J (2007) Electrochemical and photoelectrochemical treatment of C.I. Acid violet 1. *Dye Pigment* 73:390–393. <https://doi.org/10.1016/J.DYEPIG.2006.01.007>
- Solanki K, Subramanian S, Basu S (2013) Microbial fuel cells for azo dye treatment with electricity generation: a review. *Bioreour Technol* 131:564–571. <https://doi.org/10.1016/J.BIORTECH.2012.12.063>
- Solano AMS, Garcia-Segura S, Martínez-Huitle CA, Brillas E (2015) Degradation of acidic aqueous solutions of the diazo dye Congo Red by photo-assisted electrochemical processes based on Fenton's reaction chemistry. *Appl Catal B Environ* 168–169:559–571. <https://doi.org/10.1016/J.APCATB.2015.01.019>
- Solís M, Solís A, Pérez HI, Manjarrez N, Flores M (2012) Microbial decolouration of azo dyes: a review. *Process Biochem* 47:1723–1748. <https://doi.org/10.1016/J.PROCBIO.2012.08.014>
- Somayajula A, Asaithambi P, Susree M, Matheswaran M (2012) Sono-electrochemical oxidation for decolorization of reactive red 195. *Ultrason Sonochem* 19:803–811. <https://doi.org/10.1016/J.ULTSONCH.2011.12.019>
- Song S, Fan J, He Z, Zhan L, Liu Z, Chen J, Xu X (2010) Electrochemical degradation of azo dye C.I. Reactive red 195 by anodic oxidation on Ti/SnO<sub>2</sub>-Sb/PbO<sub>2</sub> electrodes. *Electrochim Acta* 55:3606–3613. <https://doi.org/10.1016/j.electacta.2010.01.101>
- Soni BD, Patel UD, Agrawal A, Ruparelia JP (2017) Application of BDD and DSA electrodes for the removal of RB 5 in batch and continuous operation. *J Water Process Eng* 17:11–21. <https://doi.org/10.1016/j.jwpe.2017.01.009>
- Sowmiya S, Gandhimathi R, Ramesh ST, Nidheesh PV (2016) Granular activated carbon as a particle electrode in three-dimensional electrochemical treatment of reactive black B from aqueous solution. *Environ Prog Sustain Energy* 35:1616–1622. <https://doi.org/10.1002/ep.12396>
- Srivastava V, Suresh Kumar M, Nidheesh PV, Martínez-Huitle CA (2021) Electro catalytic generation of reactive species at diamond electrodes and applications in microbial inactivation. *Curr Opin Electrochem* 30:100849. <https://doi.org/10.1016/j.coelec.2021.100849>
- Srivastava A, Rani RM, Patle DS, Kumar S (2022) Emerging bioremediation technologies for the treatment of textile wastewater containing synthetic dyes: a comprehensive review. *J Chem Technol Biotechnol* 97:26–41. <https://doi.org/10.1002/JCTB.6891>
- Steter JR, Barros WRP, Lanza MRV, Motheo AJ (2014) Electrochemical and sono-electrochemical processes applied to amaranth dye degradation. *Chemosphere* 117:200–207. <https://doi.org/10.1016/j.chemosphere.2014.06.085>
- Sun H, Chen T, Kong L, Cai Q, Xiong Y, Tian S (2015) Potential of sludge carbon as new granular electrodes for degradation of acid orange 7. *Ind Eng Chem Res* 54:5468–5474. <https://doi.org/10.1021/ACS.IECR.5B00780>
- Sun Z, Li S, Ding H et al (2020) Electrochemical/Fe<sup>3+</sup>/peroxymonosulfate system for the degradation of acid orange 7 adsorbed on activated carbon fiber cathode. *Chemosphere* 241:125125. <https://doi.org/10.1016/J.CHEMOSPHERE.2019.125125>
- Sun L, Mo Y, Zhang L (2022) A mini review on bio-electrochemical systems for the treatment of azo dye wastewater: State-of-the-art and future prospects. *Chemosphere* 294:133801. <https://doi.org/10.1016/J.CHEMOSPHERE.2022.133801>
- Syam Babu D, Nidheesh PV (2022) Treatment of arsenite contaminated water by electrochemically activated persulfate oxidation process. *Sep Purif Technol* 282:119999. <https://doi.org/10.1016/j.seppur.2021.119999>
- Szpyrkowicz L, Juzzolino C, Kaul SN, Daniele S, De Faveri MD (2000) Electrochemical oxidation of dyeing baths bearing disperse dyes. *Ind Eng Chem Res* 39:3241–3248. <https://doi.org/10.1021/ie9908480>
- Tang Y, He D, Guo Y et al (2020) Electrochemical oxidative degradation of X-6G dye by boron-doped diamond anodes: effect of operating parameters. *Chemosphere* 258:127368. <https://doi.org/10.1016/J.CHEMOSPHERE.2020.127368>
- Tarkwa J-B, Oturan N, Acayanka E et al (2019a) Photo-fenton oxidation of orange G azo dye: process optimization and mineralization mechanism. *Environ Chem Lett* 17:473–479. <https://doi.org/10.1007/s10311-018-0773-0>
- Tarkwa JB, Acayanka E, Jiang B, Oturan N, Kamgang GY, Laminsi S, Oturan MA (2019b) Highly efficient degradation of azo dye orange G using laterite soil as catalyst under irradiation of non-thermal plasma. *Appl Catal B Environ* 246:211–220. <https://doi.org/10.1016/j.apcatb.2019.01.066>
- Tavares MG, da Silva LVA, Sales Solano AM, Tonholo J, Martínez-Huitle CA, Zanta CL (2012) Electrochemical oxidation of methyl red using Ti/Ru<sub>0.3</sub>Ti<sub>0.7</sub>O<sub>2</sub> and Ti/Pt anodes. *Chem Eng J* 204–205:141–150. <https://doi.org/10.1016/j.cej.2012.07.056>
- Thiam A, Brillas E, Centellas F, Cabot PL, Sirés I (2015a) Electrochemical reactivity of Ponceau 4R (food additive E124) in different electrolytes and batch cells. *Electrochim Acta* 173:523–533. <https://doi.org/10.1016/J.ELECTACTA.2015.05.085>
- Thiam A, Sirés I, Garrido JA, Rodríguez RM, Brillas E (2015b) Decolorization and mineralization of allura red AC aqueous solutions by electrochemical advanced oxidation processes. *J Hazard Mater* 290:34–42. <https://doi.org/10.1016/J.JHAZMAT.2015.02.050>
- Thiam A, Sirés I, Garrido JA, Rodríguez RM, Brillas E (2015c) Effect of anions on electrochemical degradation of azo dye carmoisine (Acid Red 14) using a BDD anode and air-diffusion cathode.

- Sep Purif Technol 140:43–52. <https://doi.org/10.1016/j.seppur.2014.11.012>
- Thiam A, Brillas E, Garrido JA, Rodríguez RM, Sirés I (2016) Routes for the electrochemical degradation of the artificial food azo-colour Ponceau 4R by advanced oxidation processes. *Appl Catal B Environ* 180:227–236. <https://doi.org/10.1016/J.APCATB.2015.06.039>
- Titchou FE, Zazou H, Afanga H, El Gaayda J, Akbour RA, Nidheesh PV, Hamdani M (2021) An overview on the elimination of organic contaminants from aqueous systems using electrochemical advanced oxidation processes. *J Water Process Eng* 41:102040. <https://doi.org/10.1016/j.jwpe.2021.102040>
- Titchou FE, Zazou H, Afanga H et al (2021b) Electrochemical oxidation treatment of direct red 23 aqueous solutions: Influence of the operating conditions. *Sep Sci Technol*. <https://doi.org/10.1080/01496395.2021.1982978>
- Topaç FO, Dindar E, Uçaroğlu S, Başkaya HS (2009) Effect of a sulfonated azo dye and sulfanilic acid on nitrogen transformation processes in soil. *J Hazard Mater* 170:1006–1013. <https://doi.org/10.1016/J.JHAZMAT.2009.05.080>
- Trellu C, Rivallin M, Cerneaux S, Coetsier C, Causserand C, Oturan MA, Cretin M (2020) Integration of sub-stoichiometric titanium oxide reactive electrochemical membrane as anode in the electro-Fenton process. *Chem Eng J* 400:125936. <https://doi.org/10.1016/j.cej.2020.125936>
- Vaghela SS, Jethva AD, Mehta BB, Dave SP, Adimurthy S, Ramachandriah G (2005) Laboratory studies of electrochemical treatment of industrial azo dye effluent. *Environ Sci Technol* 39:2848–2855. <https://doi.org/10.1021/ES035370C>
- Vahid B, Khataee A (2013) Photoassisted electrochemical recirculation system with boron-doped diamond anode and carbon nanotubes containing cathode for degradation of a model azo dye. *Electrochim Acta* 88:614–620. <https://doi.org/10.1016/J.ELECTACTA.2012.10.069>
- Vasconcelos VM, Ponce-de-León C, Nava JL, Lanza MRV (2016a) Electrochemical degradation of RB-5 dye by anodic oxidation, electro-Fenton and by combining anodic oxidation–electro-Fenton in a filter-press flow cell. *J Electroanal Chem* 765:179–187. <https://doi.org/10.1016/j.jelechem.2015.07.040>
- Vasconcelos VM, de Souza L, Guaraldo TT, Migliorini FL, Baldan MR, Ferreira NG, Lanza MRDV (2016) Electrochemical oxidation of reactive black 5 and blue 19 dyes using a non commercial boron-doped diamond electrode. *Quim Nova* 39:1051–1058. <https://doi.org/10.5935/0100-4042.20160117>
- Vasudevan S, Oturan MA (2014) Electrochemistry: as cause and cure in water pollution-an overview. *Environ Chem Lett* 12:97–108. <https://doi.org/10.1007/s10311-013-0434-2>
- Viana DF, Salazar-Banda GR, Leite MS (2018) Electrochemical degradation of reactive black 5 with surface response and artificial neural networks optimization models. *Sep Sci Technol* 53:2647–2661. <https://doi.org/10.1080/01496395.2018.1463264>
- Vijayakumar V, Saravanathamizhan R, Balasubramanian N (2016) Electro oxidation of dye effluent in a tubular electrochemical reactor using TiO<sub>2</sub>/RuO<sub>2</sub> anode. *J Water Process Eng* 9:155–160. <https://doi.org/10.1016/J.JWPE.2015.12.006>
- Wang A, Qu J, Liu H, Ru J (2008) Mineralization of an azo dye acid red 14 by photoelectro-Fenton process using an activated carbon fiber cathode. *Appl Catal B Environ* 84:393–399. <https://doi.org/10.1016/J.APCATB.2008.04.016>
- Wang K, Chen HY, Huang LC, Su YC, Chang SH (2008) Degradation of reactive black 5 using combined electrochemical degradation-solar-light/immobilized TiO<sub>2</sub> film process and toxicity evaluation. *Chemosphere* 72:299–305. <https://doi.org/10.1016/J.CHEMOSPHERE.2008.02.012>
- Wang CT, Chou WL, Kuo YM, Chang FL (2009) Paired removal of color and COD from textile dyeing wastewater by simultaneous anodic and indirect cathodic oxidation. *J Hazard Mater* 169:16–22. <https://doi.org/10.1016/j.jhazmat.2009.03.054>
- Wang A, Li YY, Ru J (2010) The mechanism and application of the electro-Fenton process for azo dye Acid Red 14 degradation using an activated carbon fibre felt cathode. *J Chem Technol Biotechnol* 85:1463–1470. <https://doi.org/10.1002/JCTB.2450>
- Wang Z, Liu M, Xiao F, Postole G, Zhao H, Zhao G (2021) Recent advances and trends of heterogeneous electro-Fenton process for wastewater treatment-review. *Chinese Chem Lett*. <https://doi.org/10.1016/j.ccllet.2021.07.044>
- Wu J, Liu F, Zhang H, Zhang J, Li L (2012) Decolorization of CI reactive black 8 by electrochemical process with/without ultrasonic irradiation. *Desalin Water Treat* 44:36–43. <https://doi.org/10.1080/19443994.2012.691739>
- Wu J, He Z, Du X, Zhang C, Fu D (2016) Electrochemical degradation of acid orange II dye using mixed metal oxide anode: role of supporting electrolytes. *J Taiwan Inst Chem Eng* 59:303–310. <https://doi.org/10.1016/J.JTICE.2015.08.008>
- Xia Y, Wang G, Guo L, Dai Q, Ma X (2020) Electrochemical oxidation of Acid Orange 7 azo dye using a PbO<sub>2</sub> electrode: Parameter optimization, reaction mechanism and toxicity evaluation. *Chemosphere* 241:125010. <https://doi.org/10.1016/J.CHEMOSPHERE.2019.125010>
- Xie YB, Li XZ (2006) Interactive oxidation of photoelectrocatalysis and electro-Fenton for azo dye degradation using TiO<sub>2</sub>-Ti mesh and reticulated vitreous carbon electrodes. *Mater Chem Phys* 95:39–50. <https://doi.org/10.1016/j.matchemphys.2005.05.048>
- Xiong Y, Strunk PJ, Xia H, Zhu X, Karlsson HT (2001) Treatment of dye wastewater containing acid orange II using a cell with three-phase three-dimensional electrode. *Water Res* 35:4226–4230. [https://doi.org/10.1016/S0043-1354\(01\)00147-6](https://doi.org/10.1016/S0043-1354(01)00147-6)
- Xu L, Zhao H, Shi S, Zhang G, Ni J (2008) Electrolytic treatment of C.I. Acid orange 7 in aqueous solution using a three-dimensional electrode reactor. *Dye Pigment* 77:158–164. <https://doi.org/10.1016/J.DYEPIG.2007.04.004>
- Xu H, Zhang Q, Yan W, Chu W, Zhang L (2013a) Preparation and characterization of PbO<sub>2</sub> electrodes doped with TiO<sub>2</sub> and its degradation effect on azo dye wastewater. *Int J Electrochem Sci* 8:5382–5395
- Xu L, Guo Z, Du L (2013) Anodic oxidation of azo dye C.I. Acid Red 73 by the yttrium-doped Ti/SnO<sub>2</sub>-Sb electrodes. *Front Chem Sci Eng* 7:338–346. <https://doi.org/10.1007/S11705-013-1335-4>
- Xu L, Sun Y, Zhang L, Zhang J, Wang F (2015) Electrochemical oxidation of C.I. acid red 73 wastewater using Ti/SnO<sub>2</sub>-Sb electrodes modified by carbon nanotube. *Desalin Water Treat* 57:8815–8825. <https://doi.org/10.1080/19443994.2015.1025437>
- Xu J, Sun M, Zhang C, Wu M, Fu D (2022) Electrochemical mineralization of direct blue 71 with boron-doped diamond anodes: factor analysis and mechanisms study. *J Environ Chem Eng* 10:107031. <https://doi.org/10.1016/J.JECE.2021.107031>
- Yang Y, Zhang H, Lee S, Kim D, Hwang W, Wang ZL (2013) Hybrid energy cell for degradation of methyl orange by self-powered electrocatalytic oxidation. *Nano Lett* 13:803–808. <https://doi.org/10.1021/NL3046188>
- Yang B, Sun Y, Fu A, Du D (2014) Electrochemical oxidation rule of representative dye wastewater with Ti/SnO<sub>2</sub> as anode. *Chinese J Environ Eng* 8:1475–1481
- Yang B, Gao Y, Yan D, Xu H, Wang J (2018) Degradation characteristics of color index direct blue 15 dye using iron-carbon micro-electrolysis coupled with H<sub>2</sub>O<sub>2</sub>. *Int J Environ Res Public Health* 15:1523. <https://doi.org/10.3390/IJERPH15071523>



- Yavuz Y, Shahbazi R (2012) Anodic oxidation of reactive black 5 dye using boron doped diamond anodes in a bipolar trickle tower reactor. *Sep Purif Technol* 85:130–136. <https://doi.org/10.1016/j.seppur.2011.10.001>
- Yu H, Li Y, Zhao M, Dong H, Yu H, Zhan S, Zhang L (2015) Energy-saving removal of methyl orange in high salinity wastewater by electrochemical oxidation via a novel Ti/SnO<sub>2</sub>-Sb anode—Air diffusion cathode system. *Catal Today* 258:156–161. <https://doi.org/10.1016/J.CATTOD.2015.04.030>
- Yuan M, Salman NM, Guo H et al (2019) A 25D electrode system constructed of magnetic Sb–SnO<sub>2</sub> particles and a PbO<sub>2</sub> electrode and its electrocatalysis application on acid red G degradation. *Catalysts* 9:875. <https://doi.org/10.3390/CATAL9110875>
- Yue L, Wang K, Guo J, Yang J, Luo X, Lian J, Wang L (2014) Enhanced electrochemical oxidation of dye wastewater with Fe<sub>2</sub>O<sub>3</sub> supported catalyst. *J Ind Eng Chem* 20:725–731. <https://doi.org/10.1016/J.JIEC.2013.06.001>
- Zainal Z, Lee CY, Hussein MZ, Kassim A, Yusof NA (2007) Electrochemical-assisted photodegradation of mixed dye and textile effluents using TiO<sub>2</sub> thin films. *J Hazard Mater* 146:73–80. <https://doi.org/10.1016/J.JHAZMAT.2006.11.055>
- Zakaria Z, Ahmad WYW, Yusop MR, Othman MR (2015) COD and color removal of reactive orange 16 dye solution by electrochemical oxidation and adsorption method. *AIP Conf Proc* 1678:050007. <https://doi.org/10.1063/1.4931286>
- Zarei E, Ojani R (2016) Fundamentals and some applications of photoelectrocatalysis and effective factors on its efficiency: a review. *J Solid State Electrochem* 21:305–336. <https://doi.org/10.1007/S10008-016-3385-2>
- Zayed MA, Abo-Ayad ZA, Medany SS (2021) Catalytic efficient electro-oxidation degradation of DO26 textile dye via UV/VIS, COD, and GC/MS evaluation of by-products. *Electrocatalysis* 12:731–746. <https://doi.org/10.1007/S12678-021-00683-6>
- Zazou H, Afanga H, Akhouairi S et al (2019) Treatment of textile industry wastewater by electrocoagulation coupled with electrochemical advanced oxidation process. *J Water Process Eng* 28:214–221. <https://doi.org/10.1016/j.jwpe.2019.02.006>
- Zhang G, Yang F, Liu L (2009) Comparative study of Fe<sup>2+</sup>/H<sub>2</sub>O<sub>2</sub> and Fe<sup>3+</sup>/H<sub>2</sub>O<sub>2</sub> electro-oxidation systems in the degradation of amaranth using anthraquinone/polypyrrole composite film modified graphite cathode. *J Electroanal Chem* 632:154–161. <https://doi.org/10.1016/J.JELECHEM.2009.04.010>
- Zhang G, Wang S, Yang F (2012) Efficient adsorption and combined heterogeneous/homogeneous fenton oxidation of Amaranth using supported nano-FeOOH as cathodic catalysts. *J Phys Chem C* 116:3623–3634. <https://doi.org/10.1021/jp210167b>
- Zhang C, Liu L, Li W, Wu J, Rong F, Fu D (2014a) Electrochemical degradation of Acid Orange II dye with boron-doped diamond electrode: role of operating parameters in the absence and in the presence of NaCl. *J Electroanal Chem* 726:77–83. <https://doi.org/10.1016/J.JELECHEM.2014.05.015>
- Zhang F, Feng C, Li W, Cui J (2014b) Indirect electrochemical oxidation of dye wastewater containing acid orange 7 using Ti/RuO<sub>2</sub>-Pt electrode. *Int J Electrochem Sci* 9:943–954
- Zhang B, Wang Z, Zhou X, Shi C, Guo H, Feng C (2015) Electrochemical decolorization of methyl orange powered by bioelectricity from single-chamber microbial fuel cells. *Bioresour Technol* 181:360–362. <https://doi.org/10.1016/j.biortech.2015.01.076>
- Zhang C, Ren G, Wang W, Yu X, Yu F, Zhang Q, Zhou M (2019a) A new type of continuous-flow heterogeneous electro-Fenton reactor for tartrazine degradation. *Sep Purif Technol* 208:76–82. <https://doi.org/10.1016/J.SEPPUR.2018.05.016>
- Zhang X, Shao D, Lyu W, Tan G, Ren H (2019b) Utilizing discarded SiC heating rod to fabricate SiC/Sb-SnO<sub>2</sub> anode for electrochemical oxidation of wastewater. *Chem Eng J* 361:862–873. <https://doi.org/10.1016/J.CEJ.2018.12.085>
- Zhang X, Yu W, Guo Y, Li S, Chen Y, Wang H, Bian Z (2023) Recent advances in photoelectrocatalytic advanced oxidation processes: from mechanism understanding to catalyst design and actual applications. *Chem Eng J* 455:140801. <https://doi.org/10.1016/J.CEJ.2022.140801>
- Zhao Q, Li X, Wang N, Hou Y, Quan X, Chen G (2009) Facile fabrication, characterization, and enhanced photoelectrocatalytic degradation performance of highly oriented TiO<sub>2</sub> nanotube arrays. *J Nanoparticle Res* 11:2153–2162. <https://doi.org/10.1007/S11051-009-9685-Z>
- Zhao HZ, Sun Y, Xu LN, Ni JR (2010) Removal of acid orange 7 in simulated wastewater using a three-dimensional electrode reactor: removal mechanisms and dye degradation pathway. *Chemosphere* 78:46–51. <https://doi.org/10.1016/J.CHEMOSPHERE.2009.10.034>
- Zhao R, Wang YM, Li J, Meng W, Yang C, Sun C, Lan X (2022) Metal modified (Ni, Ce, Ta) Ti/SnO<sub>2</sub>-Sb<sub>2</sub>O<sub>5</sub>-RuO<sub>2</sub> electrodes for enhanced electrochemical degradation of Orange G. *J Appl Electrochem* 52:573–581. <https://doi.org/10.1007/S10800-021-01645-Y>
- Zhou M, Yu Q, Lei L (2008) The preparation and characterization of a graphite-PTFE cathode system for the decolorization of C.I. Acid red 2. *Dye Pigment* 77:129–136. <https://doi.org/10.1016/J.DYEPIG.2007.04.002>
- Zhu H, Chen Z (2021) Preparation of MWCNT-MnO<sub>2</sub>/Ni foam composite electrode for electrochemical degradation of Congo red wastewater. *Int J Electrochem Sci* 16:1–12. <https://doi.org/10.20964/2021.05.19>
- Zhu X, Ni J, Wei J, Xing X, Li H (2011) Destination of organic pollutants during electrochemical oxidation of biologically-pretreated dye wastewater using boron-doped diamond anode. *J Hazard Mater* 189:127–133. <https://doi.org/10.1016/J.JHAZMAT.2011.02.008>

**Publisher's Note** Springer Nature remains neutral with regard to jurisdictional claims in published maps and institutional affiliations.

Springer Nature or its licensor (e.g. a society or other partner) holds exclusive rights to this article under a publishing agreement with the author(s) or other rightsholder(s); author self-archiving of the accepted manuscript version of this article is solely governed by the terms of such publishing agreement and applicable law.